POLITECNICO DI MILANO

Master in Biomedical Engineering

Algorithmic Methodology for the Precise Localization of the Focus of Emission of a Standard X-ray System

DEIB
Dipartimento di Elettronica, Informazione e Bioingegneria del Politecnico di Milano

Supervisor: Prof. Pietro Cerveri

Master Thesis of:
Astor García Amor, number 897439

Academic Year 2017-2018

Abstract

Introduction

This research aims to demonstrate the validity and applicability of a new algorithmic methodology for the precise determination of the position in the space of the theoretical X-ray emitting focus of any clinical system. The proposed methodology requires the inclusion in the radiographed scene of a localizer object, of perfectly known geometry, on which no specific restrictions linked to the methodology that determines the position of the emitting focus are imposed. The methodology proposed is independent of any other method that requires the precise localization of the emitting focus of X-ray and, therefore, applicable in all those research or development scenarios in which it is only required to know the three-dimensional coordinates of the focus.

This research aims to establish and validate a theoretical methodology for localizing the X-ray emitting focus Therefore, the intention is to obtain the exact position of the mentioned focus in the space through its three reference cartesian coordinates (relative to a preestablished reference system). Although the precision shown by other existing techniques has been considered, in order to compare the performance of the one proposed here, a null theoretical error has been taken as a reference (that is, the error-free determination of the position of the X-ray emitting focus). The implementation in a practical system of the proposed methodology must consider the intrinsic errors of the identification of projected markers in the radiographic images. These errors are common to all related methods that use radiographic images as operational data.

In multiple biomedical applications, both in research and for the development of commercial technologies, the knowledge of the exact position of the X-ray emitter focus is required to determine aspects of the geometry of the radiographed scene (such as dimensions and position of objects of the scene). In clinical practice, commercial radiological systems constitute most of the equipment available, so it is very difficult, if not impossible, to obtain the exact spatial coordinates of the X-ray emitter focus with respect to an established known reference during a radiographic session in which patients are involved. Some commercial systems indicate the operator the approximate distance of the emitter focus to the radiographic plate with an accuracy of the order of centimetres, but that indication is not useful in most of the advanced biomedical applications.

The RSA systems (Röntgen Stereometric Analysis, Röntgen StereophotogrAmmetry o RadioAtereometric Analysis, according to different authors) and the focus calibration systems of the C-arm radiological equipment (which are discussed later in this text) determine, with some degree of precision, the spatial position of the X-ray emitting focus, but they are not systems specifically dedicated to this task. Additionally, their high acquisition and maintenance costs prevent from their use to work groups that need to know, only, the precise position of the X-ray emitter focus of a commercial system, with the intention of carrying out experimental or development work.

All the techniques referenced, intended to determine the spatial position of the X-ray emitting focus of a radiological system depend, to a large extent, on the well-known geometry of an object (usually denoted as *calibration object*) which must be placed on the radiographed scene. The laws of geometry force the use of this type of *localizer objects* to solve the uncertainty associated with the images obtained by the central projection. Usually, localizer objects are configured in a known spatial arrangement of quasi-punctual elements and named as *markers box*.

The localizer objects of the commercial systems available that determine the position of focus of X-ray, show complex dispositions of multiple markers to ensure that the purpose for which these systems are intended (RSA, calibration of C-arms…) can be achieved. Therefore, they are usually cumbersome to handle, difficult to build, have a very high cost and, moreover, it is not possible to acquire them without purchasing the complete system of which they are part. In addition to the mentioned aspects, the markers boxes are inextricably associated with a specific methodology (normally analytical) of determining the spatial coordinates of the X-ray emitting focus.

At present, the available commercial techniques are computer-implemented, which means that the software for calculating the position of the focus lacks flexibility and obliges the operator to follow a protocol for the identification of the radiographic markers, task on which the success of the analytical methodology used depends. These methodologies apply calculation algorithms linked, indissolubly, to the geometry and disposition of the markers in the localizers, which can represent a serious problem of application in the implementation of new experimental techniques or commercial developments.

In this research, it has been implemented a new algorithmic methodology that allows to determine, independently (that is, without being associated with any other technology) the precise position of the X-ray emitter focus of any commercial radiological system. The methodology proposed, dissociates the geometry of the localizer from the method for determining the focus position of X-ray object. It has also been possible to minimize the number of markers needed to accurately locate the focus of X–rays and to add flexibility to the requirements that characterize the localizer objects in terms of their geometry.

For practical purposes, the proposed methodology may be implemented for research purposes or to build commercial systems that require to precisely localize the emitting focus of an X-ray system, with a low cost of implementation and of construction of the localizer object.

Methods

The proposed methodology is based in the use of an algorithm, classified in the field of informatics as *brute force*. Thus, a wide range of positions of the localizer object and of the emitter focus of X-ray, virtually combined, are simulated. The coincidence of the virtual (simulated) projections of the localizer object with those of the real position of the object in the radiography, constitute the exploration stopping condition of the algorithm. In this research, in order to be able to validate the proposed methodology within the stablished time frame, the implementation of rotations in the simulation of the localizer object positions has not been addressed. There have only been considered displacements in the directions of a three-dimensional Cartesian reference system aligned with the radiographic plane. Far from reducing the practical applicability of the proposed methodology, the consideration of an aligned localizer object, in a plane, with the radiography, is present in multiple and related commercial technologies which determine the position of the X-ray emitting focus. The intrinsic scalability of the proposed methodology makes the future implementation of rotations in the simulation of the localizer object simple.

In order to statistically validate the convergence of the proposed positioning methodology, a *reference localizer* object has been defined and an experimental software, with which series of virtual cases have been simulated, has been implemented. It has been denoted as *convergence*, in the area of this research, to the methodology's capacity to narrow the positioning error of the emitter focus as a function of the control parameters of the algorithm. The *reference localizer* has been validated during the experimental stage of this research.

The experimental software developed has allowed, in addition, to determine the calculus times required for the direct application of the proposed localizing methodology. In this aspect, the direct application of the methodology has been proved unfeasible, already in the first round of tests, due to the unacceptable calculation times, even using high performance work stations. Because of this contingency, an application method for the original methodology of localizing is proposed, which allows the calculus times to be shortened by about 4 times. The proposed application method applies the original positioning methodology in four approximative stages, which obtain the precise position of the emitter focus by delimiting increasingly smaller intervals of exploration (ranges of simulated positions of the localizer and focus) until the eventual application of the direct positioning methodology, in the final stage, with a high degree of precision.

To validate both the positioning methodology and the proposed application method, tests have been carried out with a statistically significant number of simulated *cases*, starting from random positions of the X-ray emitter source sought and the localizer object. All the tests have been carried out with the experimental software implemented. In all the tests performed, the knowledge of the exact position of the X- ray emitting focus was compared with the position generated by the application of the proposed methodology. The only source of error is the necessary discretization of the simulated positions within the established exploration ranges.

Results

As a result of the application of the proposed positioning methodology, it has been possible to demonstrate, experimentally, its validity in any case of application (foreseeable real cases included) and that the positioning error generated can be limited by the variation of a single operational parameter. Likewise, it has been possible to validate the application method of the methodology, which makes its use in practice viable. With reduced times of application, of the order of minutes in a standard computer, it is possible to obtain the position of the X-ray emitter focus with theoretical errors of less than one tenth of a millimetre.

The software implemented has allowed, in addition, to study the influence of the characteristics of the localizer objects in the proposed localization methodology. It has been possible to determine the minimum number of markers needed and that only one additional geometric restriction must be met for their applicability. It has also been possible to establish the influence, in the accuracy of the position of the focus obtained, of the number of markers of the localizer objects used.

Conclusion

The research described in this report has demonstrated, experimentally, the possibility of accurately determining the spatial position of the X-ray emitting focus of any system used in clinical practice, without operative restrictions in the clinical practice. The accuracy of the obtained focus position equals or exceeds that of existent commercial systems for which information is available which, in addition, localize the focus position as an indirect task.

The proposed methodology can be easily implemented in a commercial computer and will allow any research or technological development group that needs it, to determine the position of the X-ray emitter focus economically, without having to resort to systems whose last purpose is not the determination of such position.

The direct application of the proposed localization methodology has shown not to be feasible in foreseeable practical applications. In order to overcome this difficulty, an application method has been developed, which has proved its validity, allowing the application of the methodology without hardly any temporal restrictions.

The proposed methodology does not impose requirements to the localizer object to be used, beyond having more than three markers and to have them distributed in more than one geometrical plane. Thus, the necessary localizers can be versatile and economical, both to build and operate, which puts them within the reach of working groups with limited resources.

Sommario

Introduzione

Questa ricerca ha lo scopo di dimostrare la validità e l'applicabilità di una nuova metodologia algoritmica per la determinazione precisa della posizione nello spazio del fuoco di emissione di raggi X teorico di qualsiasi sistema clinico. La metodologia proposta richiede l'inclusione nella scena radiografata di un oggetto localizzatore, di geometria perfettamente nota, su cui non esistono restrizioni specifiche legati alla metodologia di determinazione della posizione del fuoco di emissione. La metodologia proposta è indipendente da qualsiasi altro metodo che richiede la determinazione precisa del fuoco di emissione di raggi X e, quindi, applicabile in tutti quegli scenari di ricerca o sviluppo in cui sono richeste solo le coordinate tridimensionali di detto fuoco.

Questa ricerca mira a stabilire e convalidare una metodologia teorica di posizionamento dell fuoco emettitore di raggi X. Pertanto, si mira a ottenere l'esatta posizione di detto fuoco nello spazio (per mezzo delle sue tre coordinate cartesiane di riferimento) rispetto ad un sistema di riferimento pre-impostato. Sebbene sia stata considerata la precisione di altre tecniche esistenti, al fine di confrontare le prestazioni della soluzione proposta qui, lo studio della precisione di questa tecnica è stato fatto prendendo come riferimento un errore teorico nullo (questo è , la determinazione errore-libera della posizione del fuoco dei raggi X). L'attuazione in un sistema pratico della metodologia proposta, dovrà considerare gli errori intrinseci dei metodi di segnalazione nelle immagini radiografiche. Questi errori sono comuni a tutti i metodi correlati che utilizzano le immagini radiografiche come dati di funzionamento.

In molte applicazioni biomediche, sia la ricerca che lo sviluppo delle tecnologie commerciali, la conoscenza della posizione esatta del fuoco di emissione dei raggi X è richiesta per determinare gli aspetti della geometria della scena radiografata (proprio come dimensioni e posizione degli oggetti di la scena). Nella pratica clinica, i sistemi radiologici commerciali costituiscono la maggior parte delle attrezzature disponibili, così è molto difficile, se non impossibile, ottenere le coordinate spaziali esatte del fuoco di emissione di raggi X, rispetto ad un riferimento noto stabilito, durante una sessione radiografica che coinvolge i pazienti. Alcuni sistemi commerciali indicano all'operatore la distanza approssimativa del fuoco dell'emettitore alla piastra radiografica con una precisione dell'ordine di centimetro, ma tale indicazione non è utile nella maggior parte delle applicazioni biomediche avanzate.

Sistemi RSA (Röntegn Stereometric Analysis, Röntgen StereophotogrAmmetry oppure RadioAtereometric Analysis, secondo gli autori) e sistemi di calibrazioni per equipamenti radiologiche con C-arm (che sono discussi più avanti in questa relazione) determinano, con buona precisione, la posizione spaziale del fuoco di emissione di raggi X, ma non sono sistemi dedicati per la propria determinazione della posizione del fuoco. L'alto prezzo di acquisto e dell'operazione impedisce il loro uso a gruppi di lavoro che richiedono di conoscere solo la posizione precisa del fuoco di raggi X di un sistema commerciale con l'intenzione di svolgere un lavoro sperimentale o di sviluppo.

Tutte le tecniche, attualmente referenziate, destinate a determinare la posizione spaziale del fuoco di emissione di raggi X di un sistema radiologico dipendono, in misura maggiore o minore, della geometria, perfettamente nota, di un oggetto (di solito chiamato *Oggetto Localizzatore*) che deve essere posizionato sulla scena radiografata. Le leggi della geometria forzano l'uso di questo tipo di oggetti localizzati per risolvere l'incertezza associata alle immagini ottenute mediante proiezione centrale. In genere, gli oggetti localizzatori sono configurati in una disposizione spaziale nota di elementi quasi-puntuali, che sono chiamati marcatori.

Gli oggetti di localizzazione dei sistemi commerciali disponibili che sono in grado di determinare la posizzione del fuoco dei raggi X, presentano disposizioni complesse di marcatori multipli, per garantire che la missione a cui sono assegnati questi sistemi (RSA, calibrazione di C-arm...) è funzionale. Pertanto, sono ingombranti da maneggiare, difficili da costruire, hanno un costo molto elevato e, normalmente, non è possibile acquistarli senza farlo con il sistema completo di cui fanno parte. A parte gli aspetti citati, le scatole di marcatori sono indissolubilmente associati a una metodologia specifica (di solito analitica) di determinare le coordinate spaziali del fuoco dei raggi X.

Oggi, le tecniche commerciali disponibili sono implementate computazionalmente, che rende il software di calcolo della posizione del fuoco meno flessibile e obbliga l'operatore a seguire un protocollo di segnalazione di marcatori radiografati di cui dipende il successo della metodologia analitica di calcolo che usano. Queste metodologie applicano algoritmi di calcolo legati, indissolubilmente, alla geometria e alla disposizione dei marcatori nei localizzatori, che possono rappresentare un grave problema di applicazione nella implementazione di nuove tecniche sperimentali o nelli sviluppi commerciali.

In questa ricerca è stata implementata una nuova metodologia algoritmica che permette di determinare, indipendentemente (cioè, senza essere associato a nessun'altra tecnologia), la precisa posizione del fuoco di emissione di raggi X di qualsiasi sistema radiologico commerciale. La metodologia proposta, scollega la geometria dell'oggetto localizatore dal metodo di determinazione della posizione del fuoco dei raggi X. È stato anche minimizzato il numero di marcatori necessari per localizare accuratamente il fuoco di raggi X per diminuire le esigenze degli oggetti per quanto riguarda la loro geometria.

Per scopi pratici, la metodologia proposta può essere implementata per lo sviluppo di sistemi di ricerca o commerciali che richiedono la determinazione della posizione precisa del fuoco dell'emettitore di una fonte dei raggi X, con un basso costo di implementatzioine informatica e di costruzione dell'oggetto localizatore.

Metodo

La metodologia proposta è basata nell'uso di un algoritmo categorizzato, nel campo della informatica, come di "forza bruta". Così, una vasta gamma di posizioni di un oggetto localizzatore virtuale, combinati con tanti dei fuoco di raggi X sono matematicamente simulate. La coincidenza delle proiezioni virtuale (simulate) dell'oggetto di localizzazione con le proiezioni della posizione reale dell’oggetto sulla radiografia costituisce lo stato di arresto dell'esplorazione dell'algoritmo. In questa ricerca, al fine di convalidare la metodologia proposta entro il lasso di tempo stabilito, è stata dispensata l’implementazione delle rotazioni nella simulazione di localizzazione. E’ stato considerato solo lo spostamento, nelle direzioni di un sistema di riferimento cartesiano tridimensionale allineato con il piano radiografico. Lungi da sottrarre aplicabilità pratica alla metodologia proposta, la considerazione di un oggetto localizzatore allineato, in un piano, con la radiografia è considerata in più tecnologie commerciali correlati che determinano la posizione del fuoco di raggi X. La scalabilità intrinseca della metodologia proposta rende semplice l’implementazione futura di rotazioni nella simulazione della posizione dell'oggetto di localizzazione.

Per convalidare statisticamente la convergenza della metodologia di posizionamento proposta, è stato definito un oggetto localizzatore, chiamato di *riferimento*, ed è stato implementato un software sperimentale con cui sono stati provati sperimentalmente, virtualmente, una serie di casi simulati. E' stata chiamata convergenza, nel campo di questa ricerca, la capacità della metodologia proposta di limitare l'errore di posizionamento del fuoco emettitore a seconda dei parametri di controllo dell'algoritmo. L'oggetto *locatore di riferimento* è stato convalidato durante la fase sperimentale della ricerca.

Il software sperimentale sviluppato ha, inoltre, permesso di determinare i tempi di calcolo richiesti per applicare direttamente la metodologia di posizionamento che si propone. A questo proposito, l'applicazione diretta della metodologia si è dimostrata inattuabile già nei primi lotti di prove, a causa dei tempi di calcolo molto grandi, anche utilizzando workstation ad alte prestazioni. Come risultato di questa contingenza, si propone un *metodo di applicazione* della metodologia originale di localizzazione del fuoco emettitore che permette di accorciare i tempi di calcolo in circa di 4 volte. Il metodo di applicazione che è proposto, applica la metodologia di posizionamento originale in quattro fasi approssimative, ottiene la posizione precisa del fuoco, riducendo gli intervalli di esplorazione (gamme di posizioni simulati del localizzatore e il fuoco) fino ad applicare la metodologia diretta di posizionamento, nella fase finale, con un alto grado di precisione.

Per convalidare sia la metodologia di posizionamento che il metodo di applicazione proposto, lotti di prove sono stati condotti con un numero statisticamente significativo di casi simulati, a partire da posizioni casuali del fuoco dei raggi X cercato e dell'oggetto localizzatore. Tutte le prove sono state eseguite con il software sperimentale implementato. Le prove effettuate sono partite della conoscenza della posizione esatta del fuoco di raggi X, che è stata paragonata alla posizione generata dall'applicazione della metodologia proposta. L'unica fonte di errore è dovuta alla necessaria discretizzazione delle posizioni simulate all'interno della gamma di esplorazione stabilita.

Risultati

Come risultato dell'applicazione della metodologia di posizionamento proposta, è stato possibile dimostrare, sperimentalmente, che è valida in ogni caso di applicazione (prevedibile casi reali inclusi) e che genera un errore di posizionamento che può essere limitato con la variazione di un singolo parametro operativo. È stato inoltre possibile convalidare il metodo di applicazione della metodologia, che rende il suo utilizzo praticabile. Con tempi di applicazione dell'ordine di minuti di calcolo in un computer standard, è possibile ottenere la posizione del fuoco emettitore di raggi X con minori errori teorici di un decimo di millimetro.

Il software implementato ha permesso, inoltre, di studiare l'influenza degli oggetti localizzatori. È stato possibile determinare il numero minimo di marcatori richiesti e che esiste una sola restrizione geometrica che deve essere rispettata. È stato inoltre possibile stabilire l'influenza, nella precisione della posizione del fuoco ottenuto, del numero di marcatori degli oggetti di localizzazione utilizzati.

Conclusione

La ricerca descritta in questa relazione ha dimostrato, sperimentalmente, la possibilità di determinare accuratamente la posizione spaziale del fuoco di emissione di raggi X, di qualsiasi sistema utilizzato nella pratica clinica, senza restrizioni cliniche operative. La precisione della posizione del fuoco ottenuto è uguale o superiore a quella di tutti i sistemi commerciali, di cui sono disponibili informazioni, che eseguono indirettamente questa funzione.

La metodologia proposta può essere facilmente implementata in un computer commerciale e permetterà, a qualsiasi gruppo di ricerca o sviluppo tecnologico che ne abbia bisogno, di determinare la posizione del fuoco di emissione di raggi X in modo economico, senza dover utilizzare sistemi il cui scopo ultimo non è quello di determinare tale posizione.

E' stato dimostrato che l'applicazione diretta della metodologia per la localizzazione della posizione del fuoco di raggi X non è realizzabile nelle applicazioni pratiche prevedibili. Per superare questo problema, è stato sviluppato un metodo di applicazione, di cui è stata dimostrata la sua validità, che permette di applicare la metodologia senza appena restrizioni temporali.

La metodologia proposta non impone requisiti a l'oggetto localizzatore da utilizzare, oltre ad avere più di tre marcatori e non avereli in un unico piano geometrico. I locatori necessari saranno versatili ed economici, sia per fabbricare che per operare, il che li rende disponibili a gruppi di lavoro con risorse limitate.

Contents

1. Introduction

1.1. Scope

Prior to the beginning of the research and due to the necessity to validate the proposed methodology within the stablished time frame, it has been required to determine, not only the objectives, but the scope and the problems to be addressed. Hence, to determine what are the expected outcomes of the project. This has not only helped to conduct this work, but it will also help the future readers to understand and clarify what can be found in it.

In this thesis, an algorithmic methodology for the precise localization of the focus of emission of a standard X-ray system is developed. The first point that must be detailed is that this methodology does not apply to real but ideal radiographies, as it is a theoretical algorithmic model. Therefore, elements such as the focus of emission of X-ray, the markers of the localizer object or their projections on the radiography, are considered punctual. In addition, the developed software is intended to serve as a tool for the research on how different localizers, parameters and other variables influence the performance of the proposed methodology. This implies that it is an experimental software without commercial application.

The thesis studies the referred methodology and achieves its validation by proving the convergence of two variables: *markers error* and the *focus error*, which correspond to the differences between the theoretical and the virtual/simulated spatial position of both, the projected markers and the focus. This convergence is an unequivocal proof that, as a theoretical model, if an infinitesimal discretization of the space was achieved, the methodology would precisely find the position of the emitting X-ray focus. However, this infinitesimal discretization, unachievable in the reality, would imply an infinite calculation time as it is showed in the section Temporal study, where it is evidenced that the computation time increases exponentially as the discretization turns finer. Furthermore, values of discretization smaller than 0.1 mm make the methodology already excessively computationally expensive to be applied in a real scenario. To overcome this pitfall, an application method is developed and validated, allowing the practical application of the methodology.

The performance assessment of the methodology is contrasted against a theoretical perfect model. Functional existing methods are based in an analytical approach which theoretically reaches a precision of the 100%. Algorithms as Helbille's and Tsai's allow to deal with the errors that appear in real applications, such as non-punctual markers, distortion effects and other artifacts. Given the different nature of these algorithms, the theoretical comparison of the models shows that theoretical exact model must be set as a reference considering, in addition, that the suggested algorithmic methodology would be affected, in real scenarios, by the same kind of errors that any other currently available method.

1.2. Problem statement

The determination of the position of the focus of emission of X-ray is necessary for any application that requires the compensation of the central projection. Actual techniques have a greater or lesser dependency on the geometry of a perfectly known localizer object, placed in the radiographic scene. Predominantly, these localizer objects consist in a known spatial disposition of quasi-punctual markers. Most of these techniques determine the focus position as a necessary step for further procedures but not as its last purpose. These techniques are designed for specific systems such as RSA (consistent in two radiographic machines) or C-arms and, consequently, the mentioned localizer objects and devices are usually complex and expensive; impractical for standard X-ray systems. If the position of the focus of a standard X-ray machine wants to be precisely known for its application in research, there are no available technologies in the market that do not require from the use of specific equipment and software as the systems mentioned before, which are expensive and not present in most hospitals.

1.3. Objectives

This thesis is conducted through a main objective that consists in the development of a methodology that allows, based on the information provided by a single radiography, to spatially localize the focus of emission of a standard X-ray system without the dependence, as current methods have, of a specific geometry for the localizer object placed in the radiographic scene. Additionally, several objectives can be stated.

Development of an algorithmic methodology for the localization of the focus of X-ray. Through the implementation of an algorithmic methodology, the aim is to achieve greater flexibility than with existing methodologies, **(García Ruesgas, 2014)**, **(Kärrholm, Roentgen Stereophotogrammetry. Review of Orthopaedic Applications, 1989)**. Its application in a wide variety of cases involving diverse localizer's geometries and positions allow a dynamic redefinition of the system, serving as a powerful tool for research.

Achieve the methodology's independence from the localizer. Previously introduced analytical methods for the calculus as the one cited in **(García Ruesgas, 2014)** require the definition of equations for each marker present in the known object (named *oLRef* in the referred work). Consequently, the algorithm has a high dependency on this object allowing reduced flexibility to work with different configurations. In addition, current commercial methods require from the use of so-called *calibration cages* (as an example the ones commercialized by the company UmRSA®). Developing a methodology that works independently of the known object (named *localizer* in current project) would increase its flexibility, allowing the exploration of different designs and avoiding the necessity to appeal to of expensive commercial devices.

Implementation of a software for the testing and validation of results. The purpose of an algorithmic methodology is to be implemented in a software. In addition, as mentioned before, this methodology is oriented to be contrasted against a theoretical model. For this reason, the development of a software that incorporates the methodology, the application method and a "testing" system for their evaluation and validation is a crucial element of this project.

1.4. Structure of the thesis

This thesis is structured in 8 chapters including the present one. Additionally, an appendix with the pseudocode extends the content. The present section serves as a brief introduction of each of the subsequent chapters.

State of the art. The second chapter of this thesis brings insight into the technology relative to the field of medical images. An overview about radiology and the existent radiological systems is initially presented. Later, more specific technologies and their mathematical and geometrical principles are introduced. Finally, "state of the art" techniques that incorporate the localization of the focus of emission of radiological systems, as well as applications for which this task is highly relevant such as RSA and C-Arm based fluoroscopy are introduced.

Methodology. In the third chapter, the methodology followed for the localization of the focus as well as the difficulties that had to be faced during the resolution of the problem are presented. Initially, an introduction to the principles behind the methodology is shown. The basic geometrical formulation that serves as a support and the step-by-step procedure that defines its performance are later extended.

Application method. The forth chapter introduces a temporal study of the performance of the methodology, motivating the necessity of developing an application method that reduces the computation time and allows its execution in realistic scenarios. A temporal study, in which the improvement of the performance is assessed, is followed by a detailed description of the 4 stages in which the application method is divided.

Validation and analysis. In chapter 5, the simulation methodology employed for the performance of the tests as well as a detailed description of the results and criteria considered to validate the methodology are presented. The decrease and convergence of the errors for a finer discretization of the space prove the reliability and serves as a validation of the methodology. In addition, the results for diverse tests are collected.

Localizer. Chapter 6 studies in detail influence of the localizer in the performance of the methodology. Geometrical constraints that must be applied to their design, and a deep study of the different parameters and their effect on the methodology are presented through experimental results. In addition, a special design with potential applications is suggested.

Implementation. Chapter 7 gives an insight into the technology and the structure used for the implementation of the methodology. In addition, the Graphical User Interface of software developed is presented in detail, incorporating a user guide and a description of the different functionalities and their correspondences in the methodology.

Conclusions and future lines of research. The 8th and last chapter provides an overview of the results presented in the previous chapters of the thesis and analyses the consecution objectives. In addition, further research and developments are suggested.

2. State of the art

This chapter brings insight into the technology relative to the field of medical images. A general vision about radiology and the existent radiological systems is initially presented. Later, the mathematical and geometrical principles are introduced. Finally, state of the art technologies that allow the localization of the emitter focus of X-ray as well as applications for which this task is highly relevant such as RSA and C-arm based fluoroscopy are introduced.

2.1. Radiology

This section serves as an introduction to the field of medical images. From the general ideas about radiation and its nature, to the more specific devices used in X-ray imaging. Most of the content referenced has been extracted from (G. Webb, 2003) and (Dougherty, 2009) which serve as good reference books.

Radiology is defined as the branch of medicine that uses radiation, either ionizing and non-ionizing, for the diagnosis and treatment of diseases. Between the different kinds of radiation, several can be mentioned: X-ray and γ-rays as ionizing and ultrasounds and magnetic resonance as non-ionizing. Specifically, diagnostic radiology consists in the acquisition of biomedical images from the inner body through the conversion of invisible radiation into visible images. This thesis is allocated in this area.

2.1.1. Ultrasound Imaging

Ultrasound imaging, also known as sonography, is based on the reflection of high frequency sound waves (ultrasounds) inside the body due to the change of acoustic impedance of the mean through which the waves are propagating. A probe, which consists in a piezo-electrical transducer, acts as emitter and receiver of these waves. When transmitting, electrical impulses are converted into mechanical waves, which propagate as sound. Alternatively, during the receiving phase, in which the images are generated, the reflected waves vibrate the transducer, converting the movement into electrical impulses. The amplitude of the signal as well as the time that it takes to receive the sound are processed to generate an image, as seen in Figure 1.

Figure 1. *Fetal Ultrasound Image*

2.1.2.Medical X-ray Imaging

Medical X-ray Imaging uses X-ray, which is a kind of ionizing radiation, to generate images of the body. Ionizing radiation has, potentially, enough energy to cause damage to DNA with the consequent risk for the health of the subject. X-ray consist in a beam of high energy photons projected from a source (focus of emission) through the body and received in a detector, generating this way an image. The different body tissues present diverse absorptivity, producing changes, according to D'Alembert's law, in the intensity of the radiation reaching the sensor and allowing the visualization of the body structures. Several imaging techniques are based on X-ray: Computed tomography (CT), fluoroscopy, and radiography. The last one is developed in more detail in later sections.

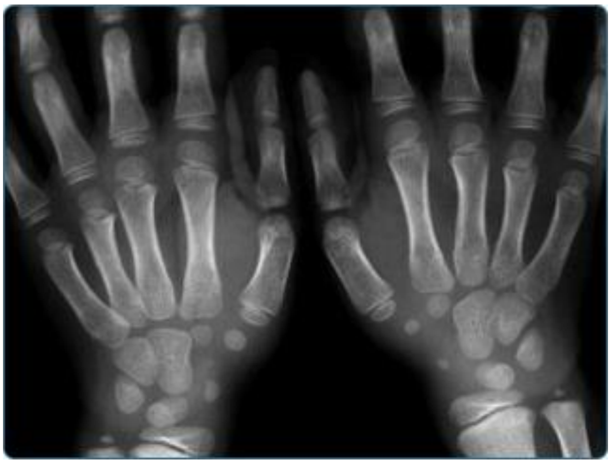

Figure 2. *Radiography of the hands.*

2.1.3.Magnetic Resonance Imaging

Magnetic Resonance Imaging (MRI), as ultrasound imaging, uses non-ionizing radiation for the generation of images. It is based on the application of strong magnetic fields and radio waves to produce the images. An electromagnet generates a strong magnetic field of around 1T inside the body altering the spins of the atoms. Complementary coils are used for the generation of radio waves that temporarily affect these spins and for the reception of the consequent signals produced by them. MRI is one the newest medical imaging methods and a promising technique thanks to its adaptability to the different characteristics of the tissues of the human body and its safety.

Figure 3. *Magnetic Resonance Image of the head.*

2.2. X-ray

Discovered in 1895 by the engineer and physicist Wilhelm Conrad Röntgen, X-rays are the oldest and most extended technique of medical imaging. Their characteristics are well described in (G. Webb, 2003) and (Dougherty, 2009).

2.2.1. Device

The generation of X-rays occurs in an X-ray tube: an evacuated tube where a high voltage (around 50 and 150 kV) is applied between a cathode and an anode. A tungsten filament within the cathode is heated, releasing a beam of electrons by thermal excitation. These electrons are accelerated due to the high voltage, towards the tungsten target where they collide, generating the X-ray. The region of collision from where the X-rays are emitted is called *focal spot* and its size and geometric properties (normally between 0.3 mm and 1.2 mm) have a crucial importance in the resolution of the X-ray images. Due to this fact, the cathode is designed to produce a tight and uniform beam of electrons, achieved thanks to the presence of a so-called *focusing cup*, negatively charged, that repels the electrons and reduces the divergence of the beam. The more negative the charge, the narrower it will become.

The anode is made of metal with a high melting point, good thermal conductivity and low vapour pressure. In addition, it is made rotate in order to avoid the incidence of the electron beam always over the same spot, what would increase considerably the temperature and lead to the damage of the element. The atomic number of the metal is selected carefully to meet with the specifications required, noticing that the higher it is, the higher the efficiency of X-ray production. In addition, it also determines the characteristic radiation, which is introduced later. For this reason, and considering its applications, the most commonly used anode metal is tungsten, having an atomic number of 74, melting point of 3370 ºC and the lowest vapour pressure, 10^7 bar at 2250 ºC, of all metals. However, for special purposes such as mammography, in which less energetic radiation is required, molybdenum, with atomic number 42, is used.

2.2.2. Generation

Because of the strong electric field applied between the cathode and the anode, the electrons are accelerated transforming the initial potential energy into kinetic energy. For example, if a potential of 100 kV is applied, the electrons released will acquire a kinetic energy of 100 keV. When these electrons strike the target, they are decelerated and most of this energy (around 99 %) is lost and transformed into heat; only the 1% is converted into X-rays, meaning a 1 % of efficiency in the conversion. These X-rays are emitted covering a wide range of energies and are generated through two mechanisms:

Bremstrahlung X-ray. Also called *general radiation*. It is the result of the reflection of an electron when it passes close to a positively charged nucleus. The energy lost by the electron is emitted as an X-ray. As the electron may not lose all its kinetic energy, further encounters occur, producing partial loss of its total energy. These interactions are the reason for the wide range of energies emitted from the anode. The maximum corresponds to the situation in which the electron is completely stopped, transferring all its kinetic energy (equivalent to the value of the external voltage) to a single X-ray.

Characteristic radiation. Observing the X-rays energy spectrum, sharp peaks can be appreciated. They arise from the second mechanism, known as characteristic radiation.

When an accelerated electron from the cathode strikes one of the electrons of the innermost shell (K shell) in a target atom, the last is ejected, leaving a hole that is occupied by an electron coming from more outer shells (L shell or M shell), with less binding energy. The loss in potential energy due to the difference between binding energies in the inner and outer shells is radiated as a single X-ray. This X-ray corresponds to a characteristic line and depends on the nature (atomic number) of the element composing the anode.

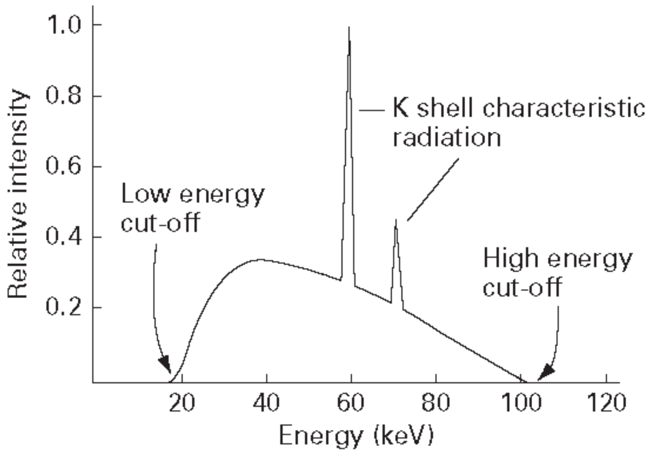

Figure 4. *X_Ray_Spectrum.*

Due to these phenomena, the energy range of the photons released covers a continuous spectrum with maximum energy equal to the one of the accelerated electrons, result of a complete loss of kinetic energy. Lower energy photons appear in cases where the electron is not completely stopped; and discrete energy levels appear related to the characteristic radiation.

2.2.3. Interaction of radiation with matter

Once the X-rays are generated, they are projected through the body towards the film or detector where the image is generated. A fraction of X-rays pass through without interacting with the matter. These conform the primary radiation. Alternatively, the photons whose trajectory is influenced by the tissue produce the so-called *secondary radiation*, which can be classified according to the way in which the trajectories are affected:

Coherent Scattering. Also known as Rayleigh scattering. In this case, the photon energy is transmitted to the electrons in the atoms of the tissue which, afterwards, reradiate the energy in a random direction as a secondary X-ray, keeping the same properties than the original photon but with different direction. This is a non-ionizing interaction that causes a reduction of the number of X-rays targeting the receptor and a variation of their angle.

Compton Scattering. Part of the energy of the photon is used to eject a loosely bound electron from an outer shell of an atom in the tissue. Consequently, the original trajectory of the X-ray is deflected, affecting to the image's quality.

Photoelectric Effect. In this case, energy from the photon is required for the ejection of a tightly bound electron of the atom from shells K or L. After that, an electron from a higher energy level occupies the vacancy. This displacement of the electron generates a characteristic X-ray with low energy that is absorbed by the surrounding tissue. The photoelectric effect implies the absorption of the X-ray, reducing the number of incident photons that reach the film and collaborating to the so-called *radiation dose*. Therefore, it is a form of ionizing radiation.

2.2.4.X-ray Detectors

To achieve a better understanding of radiological images, it is relevant to study different kind of sensors produce them. Due to the long history of X-rays and their different applications, several methods have been developed in order to extract from the attenuation of the radiation, visible and comprehensive information. Attending to the nature of these detectors, they can be classified as:

Analogical Sensors

Analogical Radiography is one of the oldest methods of X-ray imaging acquisition. A radiographic film acts as a detector for the X-rays, modifying its optical properties. Normally, the films are made of gelatine and silver halide crystals with "electron traps" called *sensitivity specks*, mainly formed by sulphur impurities and silver iodide. After the exposition of the film to the X-rays, a further processing of the film is necessary in order to obtain a radiographic image. This consists in several steps:

At first, the film is exposed to the X-ray beam, creating a latent image. Compton and photoelectric interactions of the photons with the crystals eject electrons lately absorbed by the sensitivity specks, leading to areas with negative charge and positive ions of silver (latent image). Afterwards, the latent image is immersed in a developer solution that reduces the ionized silver, precipitating it into black metallic atoms. Further labours clean and adequate the film for a long-term storage.

The film has a limited sensitivity to X-rays. In order to obtain an adequate image, a high number of photons would be needed and, therefore, an excessive dose of radiation delivered to the patient. This is a consequence of the low quantum efficiency (QE) characteristic of the films; defined as the percentage of incident photons that they can detect, usually around 2%. Aiming to increase the QE and reduce the dose, two fluorescent intensifying films are placed in both sides of the radiographic film, converting X-ray to visible light photons, to which the film is more sensitive. Through this method, a QE of around 25% is achieved and the dose to which the patient is exposed can be reduced. In addition, the time of exposition can be lowered and sharper images can be obtained.

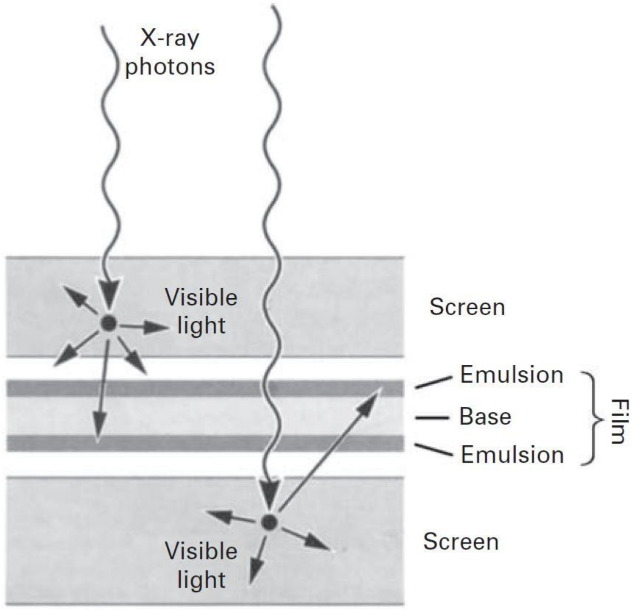

***Figure 5**. Intensifier and Film extracted from (Dougherty, 2009).*

Hybrid Sensors

Computed radiography (CR) is the main hybrid system for radiographies acquisition and an example of indirect digital radiography. It replaces the analogical system formed by the intensifying screen and the X-ray film by a photostimulable phosphor plate (PSP) or imaging plate (IP). As in the analogical sensors, the exposition of the plate to the X-ray produces a latent image thanks to the absorption of excited electrons by the phosphor. However, in this case, the latent film is not lately converted into a visible image in the film itself, but is later scanned with a laser beam. This laser releases the trapped electrons, emitting a blue light which is converted into a voltage signal by a photomultiplier. The array of voltage signals over the plate is stored as a digitalized image and the "erased plate" can be reused.

With respect to the analogical method, the use of computed radiographies implies some advantages as the linear response of the imaging plate, contrary to the sigmoidal response of the film; the reusability of the plate; the theoretical reduction of dose to the patient and, on top of all, the availability of a digital image and the consequent potential applications that this presents. The spatial resolution of the CR depends on the sampling rate when reading with the laser. Typical sampling rates in the order of 5-10 mm^{-1} bring about a spatial resolution of 2.5-5.0 lp mm^{-1}.

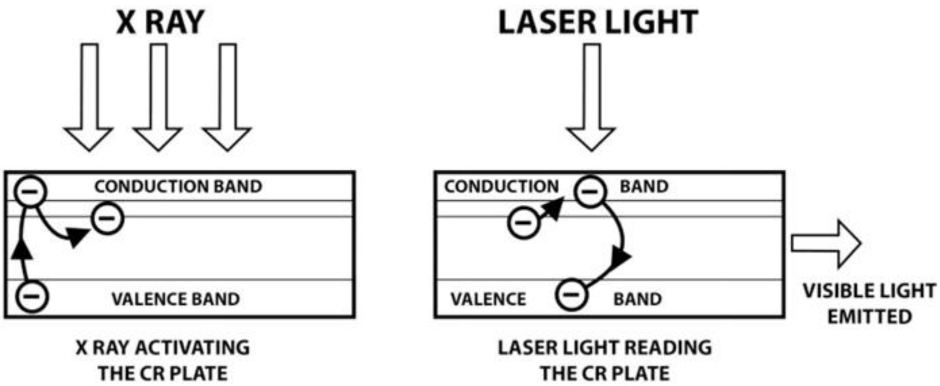

***Figure 6.** Computed Radiography extracted from (Dougherty, 2009).*

Digital Sensors

As the most modern technology, they allow to obtain a digital image without the processing of an intermediate film or panel. The device involving these sensors is called *Flat Panel Detector* and can be of two types:

Indirect Detector. The incident X-ray photon produces visible light within a scintillator material (usually Cesium Iodide) acting as an intensifying film. The visible light activates an array of silicon photodiodes, placed in the more external layer of the so-called *Active Matrix Array* (AMA), generating the digital image.

Direct Detector. Without the need for a scintillator material, the X-ray generate an electrical signal by striking an Amorphus Selenium layer.

Digital sensors, are the gold standard in X-ray imaging. In addition to the requirement from current methods of image processing of computerized images, which can be obtained through hybrid detectors as well, additional features allowing real-time applications such as fluoroscopy or X-ray in-room registration systems need an instant image not achieved with other available technology.

2.2.5.Geometry of X-ray imaging

This section introduces the geometrical principles that define the X-ray images, which are subject to the well-known central projection. Additionally, the effects of the distortion caused by the perspective are presented.

Central projection

X-ray images are one of the most widespread medical imaging techniques due to their great potential in medical applications. However, unlike ultrasound, CT or MR images, they do not directly provide depth information. If this information wants to be extracted, it is necessary to perform a further processing of the image in order to compensate the distortion generated by the central projection. Central projection can be defined as the projection of a point located in a plane into another point with the peculiarity that the projection lines are not parallel (as in orthographic projection) but concurrent in a point called *focus*

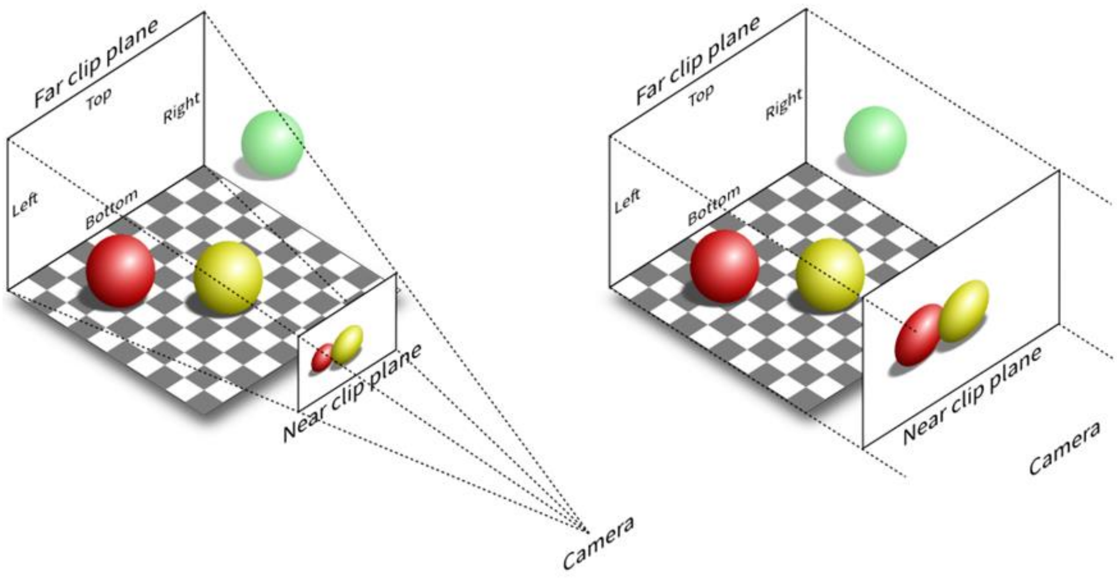

Figure 7. *Perspective projection vs orthographic projection..*

X-ray Cone Beam

In in X-ray imaging, X-rays are emitted from the focus, travel through the object and strike the projection plane, located after the object. In this area, two terms are defined in the DICOM standard to refer to the distance between focus and projection plane and the distance between focus and object respectively: *Source to Image Distance* (SID) and *Source to Object* Distance (SOD). In addition, a third variable can be defined as Object to Image Distance (OID). The configuration of these variables adopted for the X-ray image influences the obtained image in several ways:

Recorded Detail. Large SID and SOD increase the *Recorded Detail*, which corresponds to the sharpness of the image**.**

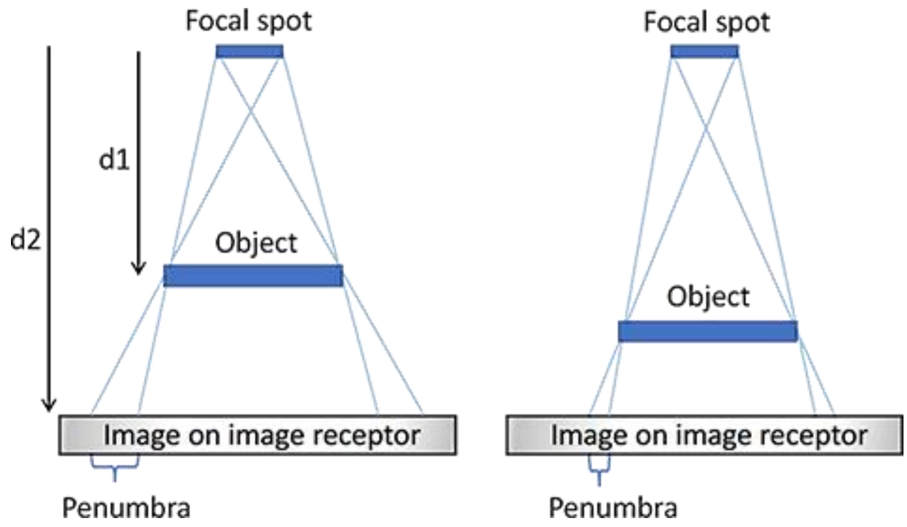

Figure 8. *Blur effect due to the change of SOD and OID.*

Size Distortion. Large SID and SOD decrease magnification or *Size Distortion*. It can be seen how increasing SID the system approximates to a cylindrical projection, which does not present the magnification effect (in X-ray imaging, this case would correspond to a pencil beam).

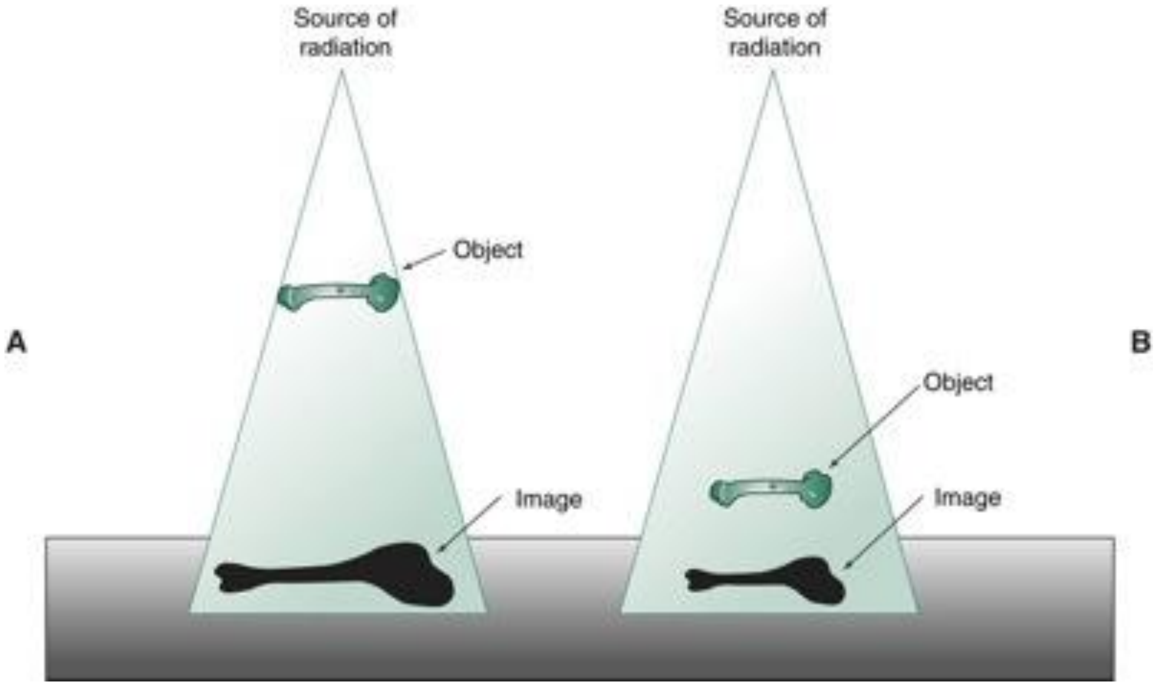

Figure 9. *Magnification effect as a consequence of the change of SOD and OID.*

Density. Large SID contributes to lower intensity of the beam as Lambert's law states. As it has been previously stated, real distances cannot be directly measured from the 2D image, requiring from the use of alternative techniques to achieve this task. Binocular vision helps to improve metrical assessment in human vision, method which is imitated in the Roentgen Stereophotogrammetric Analysis (RSA) **(de Bruin, et al., 2008)**.

2.3. State of the Art technologies

In this section, the RSA and the C-arm technologies are introduced. These systems determine the localization of the emitter focus of X-ray as a necessary information for their performance although this localization is not their last purpose.

2.3.1.Roentgen Stereophotogrammetric Analysis (RSA)

To find the origin of RSA it is necessary to go back to 1974. In that year, Göran Selvik introduced a technique for the accurate assessment of spatial displacement of prostheses (Selvik, 1989).This technique, which is based in the use of two roentgen machines (X-ray sources), a known object (calibration box) and a variable number of markers placed in both the human body and the prosthesis, consists in several steps (Valstar, Digital Roentgen Stereophotogrammetry: Development, Validation, and Clinical Application, 2001) presented next.

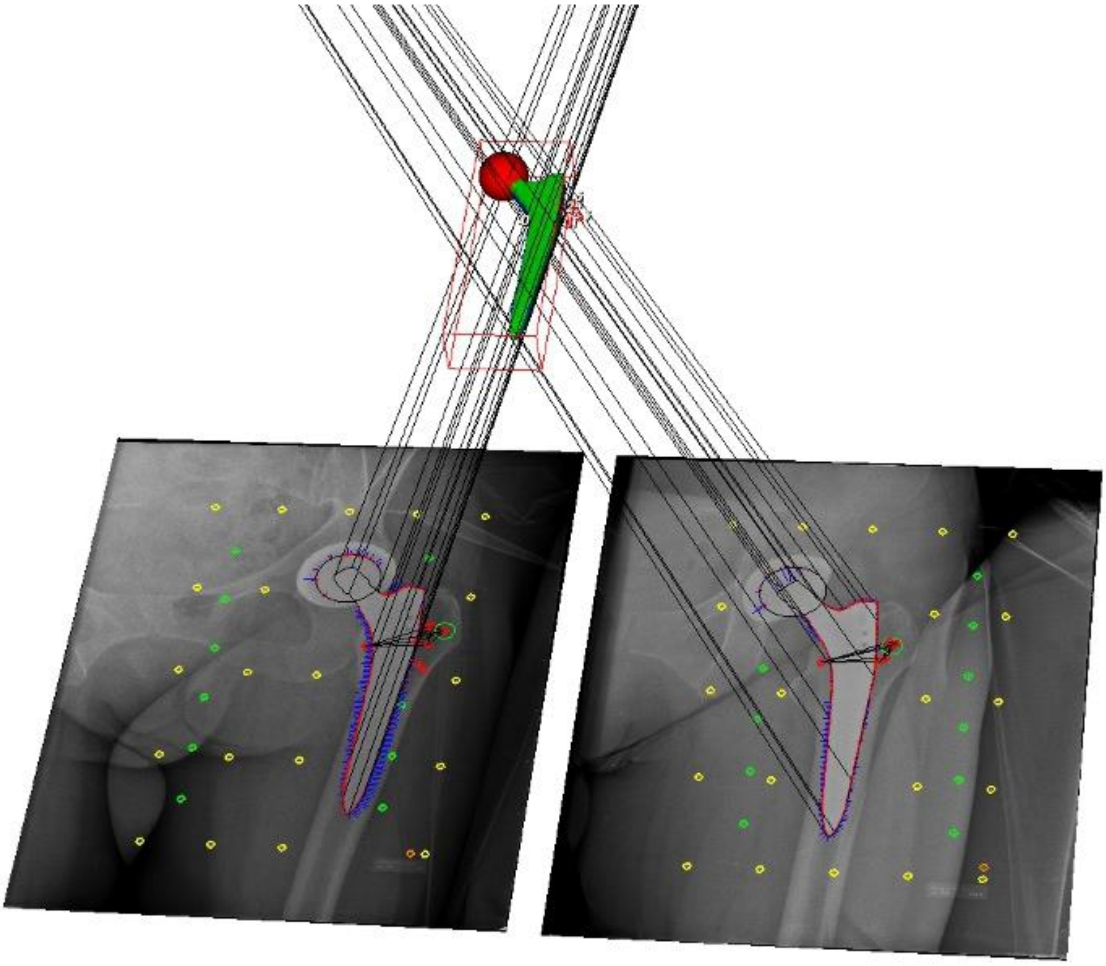

Figure 10. *RSA simulation applied in a hip prosthesis.*

Marking of the bone and prosthesis with tantalum beads. The insertion of markers in the bone allow to obtain well-defined measurement points whose position can be determined accurately. These marks act as a reference coordinate system for the evaluation of the prosthesis position. Due to basic geometrical principles, a minimum of three non-linear points is required. The marking of the prosthesis follows the same principle. Although some implants may present landmarks that allow its spatial definition, the use of appropriately located markers is recommended. Again, a minimum of three non-linear marks is required in order to define its spatial arrangement.

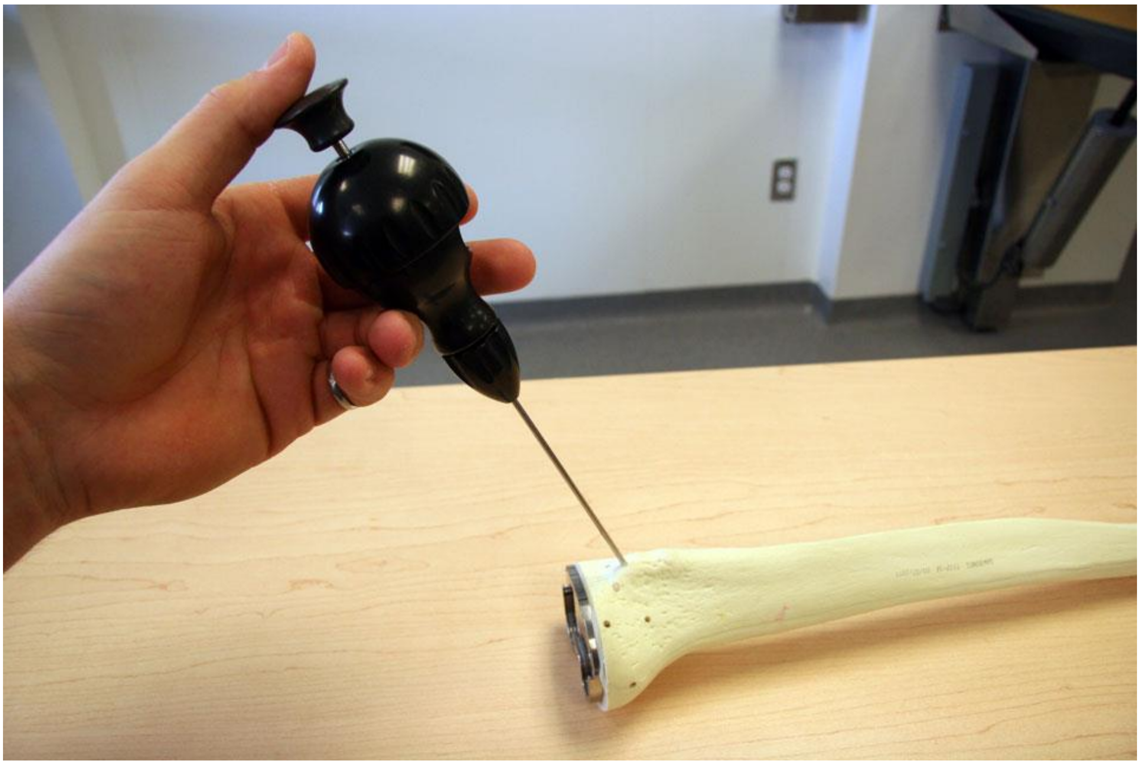

Figure 11. *Simulation of a bone marking procedure.*

Roentgen setup. The setup of the system has to comply with the requirements of the method. The geometry and position of the calibration box and the location of its markers must be perfectly defined. In addition, the orientation of the roentgen machines (X-ray machines) as well as their operationg parameters (intensity, voltage, etc) must be adjusted**.**

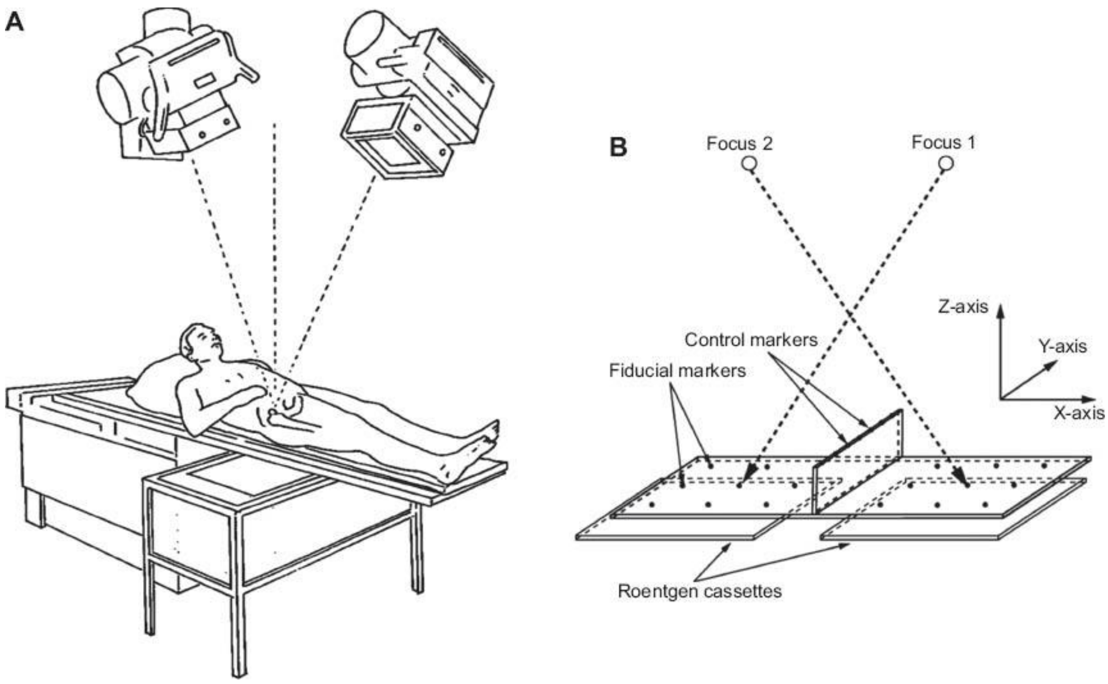

Figure 12. *RSA setup. A) shows the in-room setup, B) shows the geometrical configuration.*

Calibration of the roentgen set-up. As an initial step, the projection of the markers of the calibration box on the radiography must be defined. Years ago, this was made with the help of a measuring table. However, in recent times, the widespread use of digital and digitized systems has allowed the automatization of this procedure. With the information about the calibration box, its markers and the corresponding projections, the position of the foci is determined as the intersection of the projection lines corresponding to each of the markers. Due to the errors that may appear, these lines do not intersect at the same point and, therefore, a least squares problem needs to be solved in order to localize the foci.

Determination of the spatial coordinates of the markers. In a similar way to the calibration of the foci, the 3D coordinates of the bone and prosthesis markers is determined. Particularly, the intersection of the markers' projection lines (connecting foci spatial coordinates with those of the radiography) and the geometrical plane to which they belong, defines their 3D coordinates. This step depends on the accurate determination of the foci so the accuracy in the previous calibration is crucial.

Calculation of micromotion. Once the bone and prosthesis markers' positions have been determined, the micromotion can be calculated as a variation of the distance of the seconds with respect to the firsts. According to bibliography **(Kärrholm, Gill, & Valstar, The history and future of radiostereometric analysis., 2006)**, this method has reported an accuracy that ranges between 0.05 and 0.5 mm for translations and between 0.15º and 1.15º for rotations (with a 95% confidence interval) in determining prosthesis micromotion. However, this precision is strongly related to accuracy of the calibration of the foci. For different calibration methods (manual processing of radiographies and scanned ones), this last accuracy has given errors ranged from 0.70 mm to 6.66 mm **(Valstar, Digital Roentgen Stereophotogrammetry: Development, Validation, and Clinical Application, 2001)**.

2.3.2. C-Arm registration

C-arm X-ray systems are used as typical imaging methods during interventions thanks to its ability to perform 2D/3D overlays (Thürauf, et al., 2018); however, in order to execute this task, the C-arm must be accurately calibrated. Current techniques for the calibration are based on the projection images of a known geometry, calibration phantom, which is at a constant position and allows to estimate the so-called *projection matrix*, P, for each pose of the C-arm during the calibration procedure. This matrix consists in a set of equations that define the necessary transformations in order to spatially map 3D coordinates of the space into 2D coordinates of the detector. Calling P to the projection matrix that allows to map a point X from the 3D world coordinate system to a point Y in the 2D image coordinate system, the transformation is applied following the equation shown next:

$$Y = P(X)$$

The matrix P can be decomposed in three transformations: Euclidian transformation, central projection and affine transformation (transformation of the point to image coordinates) (Hoppe, Noo, Dennerlein, & Lauritsch, 2007). Its parameters depend on the geometry of the system and the projective scene. Conversely, using algorithms such as Helbille's and Tsai's it is possible to use it in the determination of the geometry characteristics of the scene, as it could be the distance SID, which allows to obtain the position of the focus of emission.

For the calibration of the C-Arms, typically, a cylindrical phantom with a helical distribution of markers is used. As an example, the PDS-2 manufactured by Siemens AG, Medical Solutions, consisting of a cylindrical wall made of a low-attenuation material with a total of 108 markers arranged in a spiral path, showed in Figure 14.

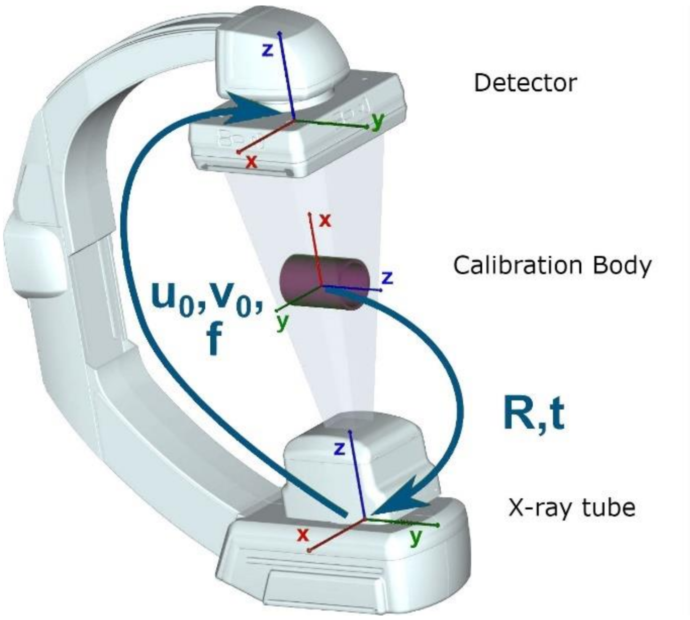

Figure 13. *C-arm pose relative to calibration body. Extracted from (Thürauf, et al., 2018).*

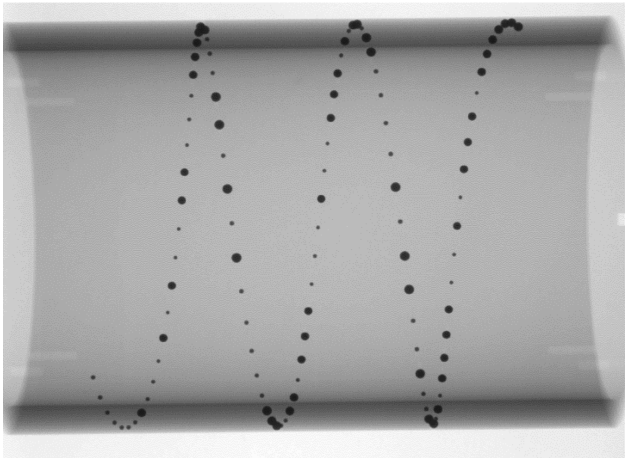

Figure 14. *X-ray image of a helical calibration phantom PDS-2 from Siemens ®.*

2.3.3.Calibration object

The determination of the precise coordinates of the focus in a roentgen/X-ray machine is of crucial importance for diverse diagnostic and interventional applications. In addition, the need of a known object of perfectly defined geometry is needed for this calibration procedure. Different authors design this object with particular names: *oLRef* (García Ruesgas, 2014), *calibration phantom* (Thürauf, et al., 2018), *calibration box* (Valstar, Digital Roentgen Stereophotogrammetry: Development, Validation, and Clinical Application, 2001). In this research, the equivalent element, is denoted as *localizer*. The calibration object locates in the space a series of points (markers) with respect to a defined coordinates system, facilitating its projection towards the radiographic film and the localization of the focus of emission of X-ray. It consists in two functional elements:

Markers. The markers serve as reference points perfectly positioned in the space with a precision of a few micrometres. Normally consist in small spheres of between 0.8 and 1.5 mm **(Valstar, Digital Roentgen Stereophotogrammetry: Development, Validation, and Clinical Application, 2001)** made of a radio-opaque material, mainly tantalum, due to its radiologic properties. This material is also used in markers placed inside the human body thanks to its biocompatibility. For these purposes, a special device, denoted as *injector*, serves physicians for their insertion.

Figure 15. *UmRSA® tantalum markers injector.*

Calibration box. It serves as a support for the markers, performing a purely structural task. The materials must be radio-transparent and meet with other characteristics as non-deformability. Several research groups use Plexiglas, however, due to the effects of temperature changes, glass is also utilized, although its heavy weight and its characteristic roentgen opacity. Some authors suggest the use of carbon fibre sandwich plates to overcome these limitations **(Valstar, Digital Roentgen Stereophotogrammetry: Development, Validation, and Clinical Application, 2001)**.

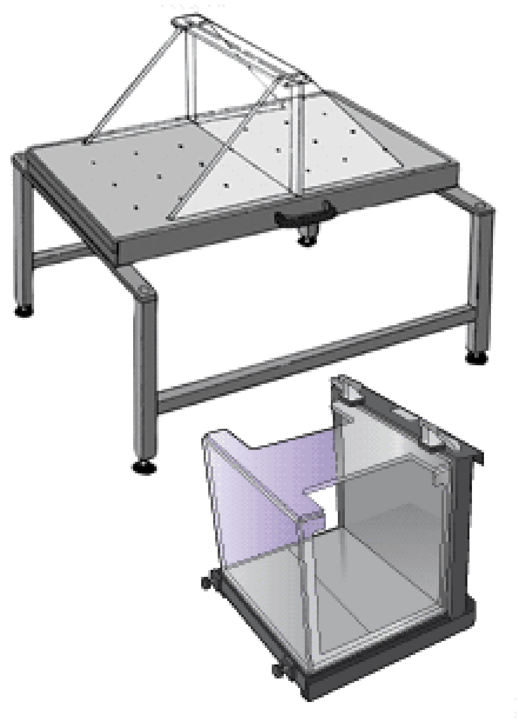

Figure 16. *UmRSA® Calibration Cages.*

Commercial elements

Although several companies manufacture X-ray equipment worldwide: General Electrics, Philips, Siemens... The market of calibration boxes and tantalum markers is reduced and coped by a few companies, mainly in the area of Scandinavia, where most of the research about RSA and X-ray calibration has been performed. Note UmRSA® and X-Medics®. Consequently, the availability of suppliers and alternatives is reduced.

Calibration studies

Due to the strong necessity for calibration methods in current applications and the low availability of software destined for this purpose, different researches have been conducted in order to develop a standardized method. In this direction, Dra. L. García Ruesgas (García Ruesgas, 2014) stablishes a geometrical model (mgpro) for the accurate localization of the X-ray emission focus from a standard radiographic system. To complete the functionalities of the software developed, a calibration object (oLRef) is designed. In contrast to the present thesis, her work uses an analytical method for the determination of the focus spatial coordinates, achieving remarkable results, nonetheless, the validity of this method, due to its analytical nature, is dependent on the designed oLRef, needing to adapt the methodology if a different object were employed. In addition, the oLRef that suggests is subject to various geometrical restrictions as: size, number of markers and parallelism between faces and the projection plane.

Figure 17. *oLRef comercialized by MBA Incorporado 2014. Extracted from (García Ruesgas, 2014).*

3. Methodology

In this chapter, the algorithmic methodology for the focus spatial localization is presented. Initially, an introduction to the principle under the methodology is stated. The basic geometrical formulation that supports it and the step-by-step procedure that defines its performance are later developed. The previously introduced Doctoral Thesis (García Ruesgas, 2014) suggests an analytical approach for the localization of the focus of an X-ray machine using a calibration object particularly named *oLRef*. Other techniques such as RSA and C-arm calibration introduce, in addition, techniques for the localization of the emitter focus in other complex and expensive systems. The difficulty to impose some restrictions to the oLRef stated as needed in her project and the possibility to develop simpler and more economic localizers, make it interesting to study the feasibility and performance of an approach sustained by an algorithmic methodology, based in a "brute force" method.

3.1. Fundament

The X-ray imaging geometry basics do not present a high complexity and can be perfectly understood with the comprehension of the central projection. Considering the source of X-ray (focus) as punctual, the image projected on the projecting film is the result of applying D'Alembert's law to the rays directed from the focus and through the volume in between the source and the plate (radiographed scene). Current methods place a calibration object, which consist of a perfectly known arrangements of spatially distributed markers, in this volume and its projection serves to analytically determine the coordinates of the emitting focus with the help of algorithms such as Helbille's or Tsai's.

If the global coordinates of the calibration object are known, a digital simulation of the projection can be generated for a given focus position using a DRR (Digital Reconstructed Radiography) software. However, for the case that concerns this thesis, neither the object nor the source location are known and, therefore, they must be determined. For simplicity, the calibration object used in this thesis is referred as "localizer". This localizer consists in a set of markers with a perfectly defined disposition. This means: the coordinates of all the markers with respect to the object's coordinates system is known.

As a brute force method, the algorithm suggested, denoted by *LoFX*, iteratively relocates the localizer varying its x, y, z coordinates, as well as the X-ray emission source, within all the possible combinations inside a range of exploration, simply named as *range* in this project, finding, with minimum error, the configuration that projects the same information than the radiographic scene given by the radiography.

Based on the previous studies, by choosing an appropriate geometry for the localizer, a single solution should exist, and this should correspond to the configuration (absolute position of the localizer and the focus) of the real system. Moreover, in later sections this statement is proved, and the methodology is validated, based on the convergence of the errors in the projected markers (*markers error*), which is defined as the sum of linear distances between the real projections given in the radiography and the projections of the virtual/simulated configuration; with the errors in the determination of the focus (*focus error*), defined as the linear distance between the exact focus and the virtual one. A more detailed explanation is performed in (chapter 4).

It is important to remark that this project studies the feasibility and implementation of an algorithmic methodology for the calibration of a standard X-ray system. By stating this, must be clarified that the processing of radiographies and images interpretation lies outside of the scope of the project. Hence, the "real world" can be simplified and focus, markers and projected markers can be considered as points. In addition, X-ray artifacts are not contemplated, leaving their study apart.

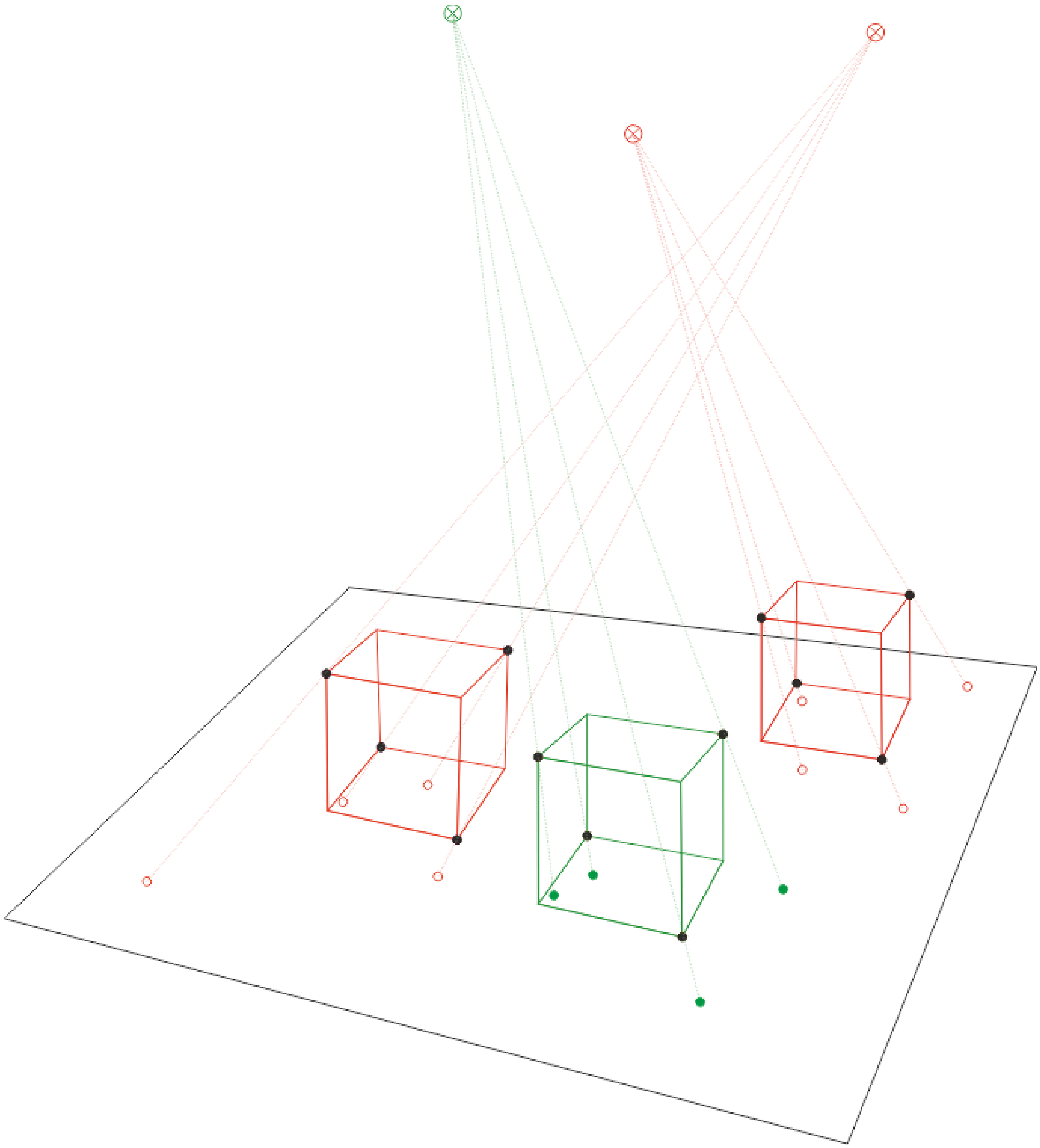

Figure 18. *Introductive geometry.*

Figure 18 illustrates the principle in which the methodology is based. The crossed circles in the top of the figure represent localizations in which the focus is explored. The cubic shapes represent different positions that the localizer adopts during the iterations. Black circles illustrate the markers, considered as punctual (with no volume) by the methodology. The respective markers projections are presented as circles in the projective plane; also considered punctual by the methodology. In red, configurations of focus-localizer that do not produce the same projective data than the radiographic scene. In green, the correct layout.

3.2. Projective space

Although the apparent simplicity of the method, such an algorithm requires of several considerations that allow an almost unbearable number of iterations and computational time to become reasonable for a feasible solution. As mentioned before, the geometry and, consequently, the mathematical formulation of the system is simple. The coordinates of the projection of a marker on a reference plane can be determined defining the equation of a line through two points: focus and marker; and setting its intersection with the given plane. For this explanation an orthonormal coordinates system is used. As well, the nomenclature assigned to the relevant elements is introduced as: F for the emitter focus, with coordinates Fx, Fy, Fz; M_i for any marker in the space with M_ix, M_iy and M_iz coordinates respectively. The plane Ω corresponds to the projection plane and l_i is the projective line that passes through F and M_i. The vector equation of l_i can be expressed as:

$$l_i = F + \lambda(M_i + F) \qquad (1)$$

If the X-ray are supposed to project vertically on a horizontal plane, the equation of the plane becomes as simple as $\Omega = z$, making it easy to find the projections.

$$l_i = F + \lambda(M_i - F) \qquad (2)$$

$$l_ix = Fx + \lambda(M_ix - Fx) \qquad (3)$$

$$l_iy = Fy + \lambda(M_iy + Fy) \qquad (4)$$

$$l_iz = Fz + \lambda(M_iz - Fz) \qquad (5)$$

For a given system in which the coordinates of the focus, the localizer and the plane $\Omega = z$ are known, the coordinates of the projections P_i can be easily determined by intersecting the projective ray with the plane:

$$P_i = \begin{cases} l_i = F + \lambda(M_i - F) \\ \Omega = z \end{cases} \qquad (6)$$

Solving in (5), λ can be determined and substituted in (3) and (4), to find P_ix and P_iy respectively.

$$\lambda = \frac{l_i\mathrm{z} - Fz}{M_i\mathrm{z} + Fz} \qquad (7)$$

3.2.1.Geometrical Optimization

When considering a real application for the methodology, some practical considerations must be taken into account. Although from a theoretical point of view, the previous equations are perfectly defined, the selection of an appropriate coordinates system and, specially, an adequate origin may imply a significant improvement in the performance of the algorithm. Although computers have more computational power each day, an optimized method, able to save even 1ms per iteration could make a difference when solving a problem with billions of iterations. At first sight, the most intuitive location for the origin would be placed in the radiographic plane. This idea was initially considered for the implementation of the algorithm.

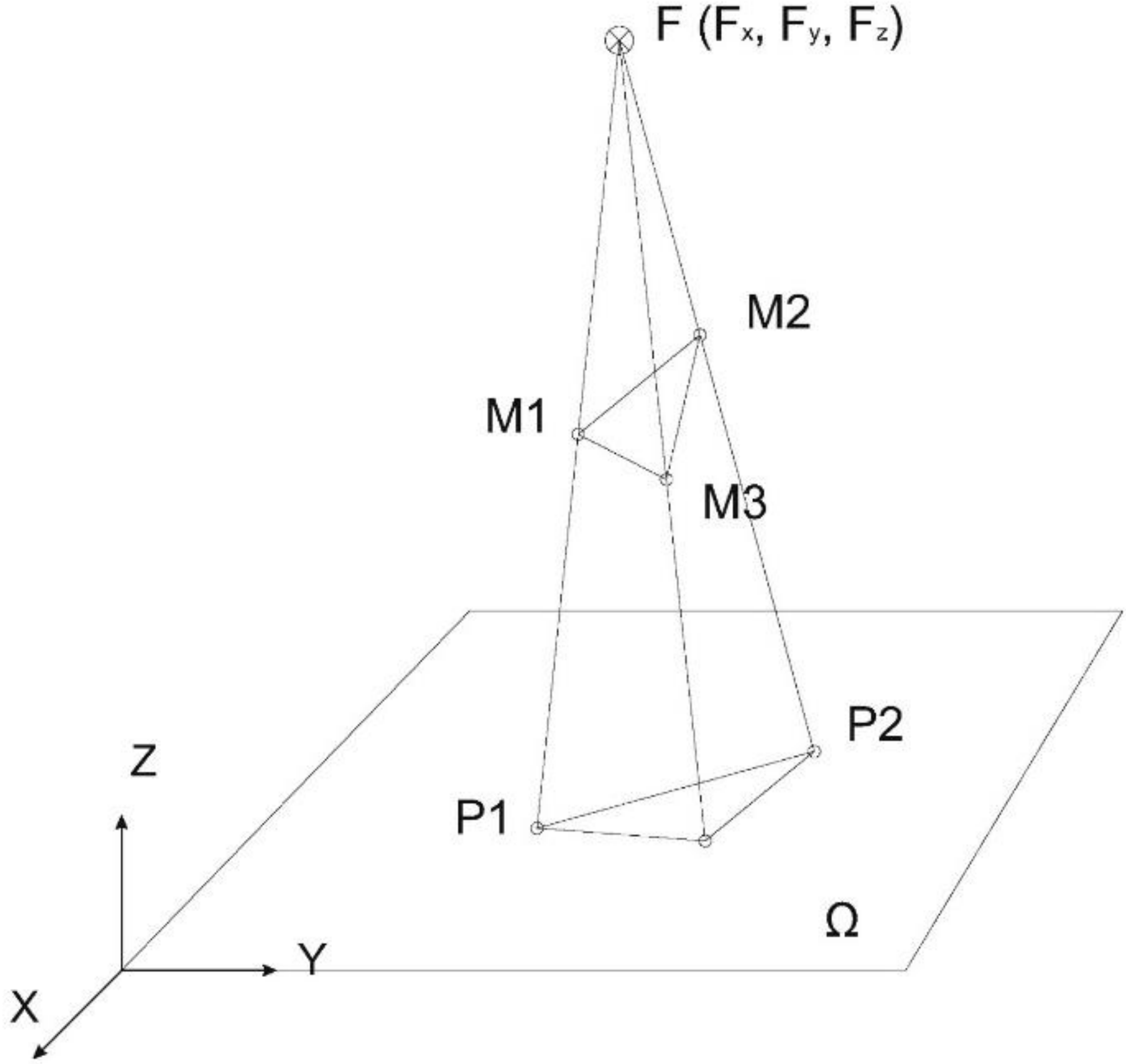

Figure 19. *Initial configuration.*

However, for each iterative location of the focus, the equations should be redefined, taking into account the three spatial coordinates of the focus. This was noted in the first phases of implementation of the methodology, where the main objective was to design and test a valid and refined algorithm. In order to improve this performance, the origin of coordinates is located in the focus as it is considered in (García Ruesgas, 2014).The same reference is used in the formulation of the equations of the homology, in which analytical methods are based. If the focus coordinates become $Fx = Fy = Fz = 0$, then, the equations of the projective beam can be simplified as in (8).

$$l_i = \lambda P_i \quad (8)$$

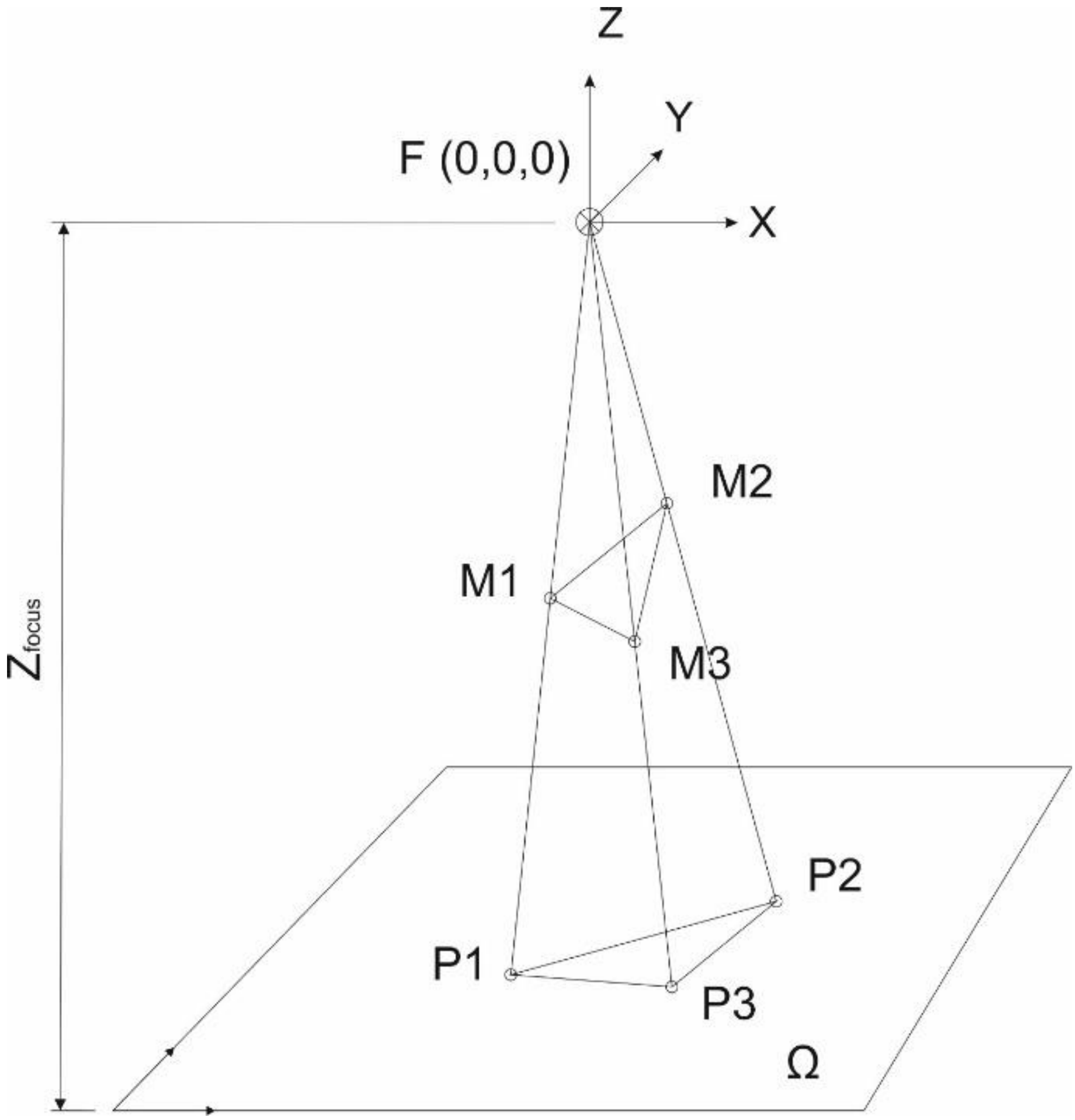

Figure 20. *Origin of coordinates set in the focus.*

The simplification achieved justifies the selection of the source of emission of X-ray as the origin of coordinates. However, this implies an additional study in the definition of the problem. It must not be forgotten that the only real data manipulated by the software concerns the geometry of the localizer (number of markers and relative position between them) and the radiographic image and, hence, it may not be intuitive to locate the origin of coordinates in the point whose position wants to be determined, here it lies the complication that requires from a rigorous study and improvement of the method.

The position of the localizer can be easily managed with respect to the focus: Selecting a point as origin of the object's coordinate system (can be a marker or a significant point of the geometry such as the barycentre), the coordinates of each marker in a global reference system can be obtained as the addition of the marker's coordinates with respect to the object's coordinate system with those defined as coordinates of the object. Nonetheless, the radiographic image characteristics need from some considerations stated below.

The data available when handling a digitalized radiograph refers to an array of pixels with a specific brightness assigned to each of them. The location of features/pixels in the image is indicated by two pixel indices: i, referred to the x spatial direction and j, for the y direction. Traditionally, for image processing, the index $(0{,}0)$ corresponds to the top-left corner of the image; however, this can be easily manipulated with the aid of any modern software, reason why, initially, the bottom-left corner was used in this project. Later, this reference was displaced to the centre of the radiograph because of reasons presented next in the text. As mentioned in previous sections, the image processing is outside the scope of this project and, therefore, the spatial coordinates of the projected markers (treated as punctual) in the radiography are considered as known.

3.3. Procedure

In this section, the methodology implemented is explained in detail looking into the reasons that motivate each of the steps of the algorithm. The first and one of most important elements of the method is the positioning of the focus at the origin of coordinates. As mentioned in 3.2.1, this simplifies the calculus and saves time during the operation. Consequently, all the model must be built on this basis.

As introduced before, a brute-force method explores a huge number of different spatial configurations for the localizer and the focus, determining this way, the configuration that generates the virtual projections that match with those present in the radiograph. This means that the radiographic scene has been identified. Note that the computational cost and precision are intrinsically related to the size of discretization of the space, denoted as *increment*. If the focus lies on the origin of coordinates, it implies that it is intrinsically static, and its position does not vary. In order to be able to implement the suggested methodology, it is necessary to compensate this restriction of movement and allow the system to explore the spatial variations that would correspond to the displacement of the focus. The solution explored consists in the application of the displacements to the projection plane. This criterion implies a change of mind with respect to the variable Z_{focus}. This variable indicates the distance between the focus and the projective plane, necessary in order to achieve a perfect definition of the projections. Therefore, the iterations related to the Z coordinate of the focus are applied to the distance between focus and projective plane. An important consequence of this fact is that, for each Z_{focus} explored, the distance between the localizer and the projective plane varies; whereas the distance between localizer and focus remains constant. An illustrative schema of the variations on Z_{focus} is shown in Figure 21.

It is important to note that the consideration of the coordinates Fx , Fy and $Fz = 0$, serves as a tool for the generation of the different projections in order to optimize the algorithm. However, the focus coordinates when an eventual localization has been achieved are given with respect to the X-ray film, with different x, y, z coordinates and, at least z different from 0.

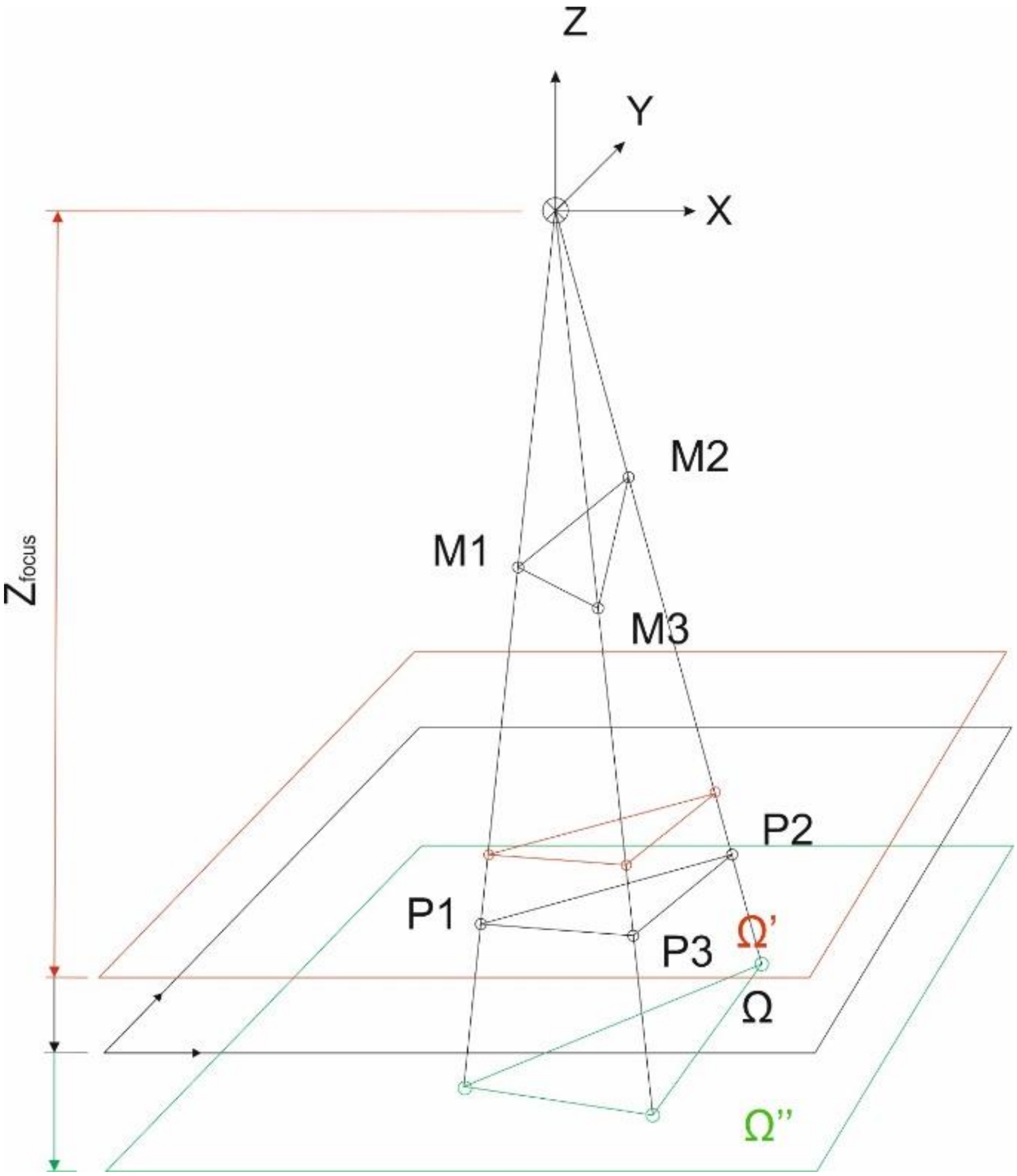

Figure 21. *Variations on the distance between X-ray focus and X-ray film (Z_{focus}).*

This statement is crucial in order to understand and proceed with the next steps of the methodology. According to this criterion, the methodology considers 6 degrees of freedom in the system: x, y, z variations of the localizer and plane positions respectively. Initially in this project, a 6 concatenated *for* loops were implemented exploring all the possible combinations for the localizer and the projection plane in each software execution. This algorithm was tested in a close surrounding of the "true/exact positions" using a small range for the variation of the coordinates and a considerably large increment value. Although the results were positive, meaning that the methodology was valid, the computational cost exceeded the expectations, showing the necessity to improve the performance. The clue to this improvement came from the implemented transformation within "plane displacements" and "focus coordinates". This permitted to refine the methodology and increase its speed as it is explained in the next section 3.3.1.

3.3.1.X-Y translations of the projection plane

The following text explains an optimization that permits to speed up the methodology and, therefore, to target more precise localizations of the focus. As an example, consider the centre of the radiography as a reference point (with i, j axes referring to indexes instead of cartesian coordinates). Notice that the centre is geometrically constrained and does not require from a dimensional definition. In the radiographic plane, place the "data points" given by the radiography (real projections) as D_1, D_2, D_3, D_4 as it can be seen in the Figure 22.

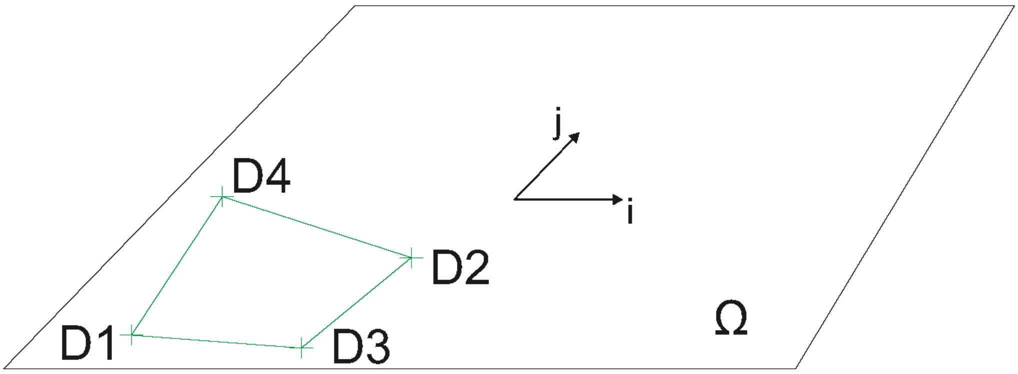

Figure 22. *Radiography data.*

After iterating through the 4 degrees of freedom that refer to the localizer spatial position and the z coordinate of the plane, next, prior to the implementation of this improvement, it would be necessary to repeat those iterations for different values of x and y of the projective plane. As mentioned before, this algorithm was proved to be slow and computationally expensive. However, the transformation between the projective plane displacements to the focus coordinates gave an idea on how to optimize the methodology modifying part of the algorithm. This improvement stands on the existing reciprocity between focus and plane displacements; meaning that a displacement of the plane, given by a vector [x, y, z] with respect to the focus, causes that the focus is seen with respect to the plane as displaced according to a vector of same module but opposite direction, analogously [-x, -y, -z].

Additionally, it can be observed that, in order to generate a unique projection, four parameters play a role in the system: x, y, z position of the localizer with respect to the focus and the distance to the projective plane. The latter affects through the magnification effect. The x and y coordinates of the plane have a secondary role here. Their variation implies the creation of "displaced" versions of the same projection without varying its shape. Therefore, it can be stated that from the variation of x, y and z coordinates of the localizer and the z coordinate of the plane, the algorithm has explored all the combinations of parameters that generate a unique projection. Considering that further variations in x and y of the plane would only move the same projection on the radiography.

Then, instead of repeating iterations and with knowledge of the geometrical characteristics of the system, the x and y coordinates of the focus can be obtained through the decomposition of the displacement d required to superimpose the virtual projection on the data present in the radiography, as seen in Figure 23. The perfect matching is very unlikely and, as a consequence, the displacement needed for each of the markers is different. In order to unequivocally define this displacement, d is determined as the displacement required to superpose the virtual projection of the first marker on the data corresponding to the first marker on the radiograph. This method makes the algorithmic independent on the position of the radiographic data and on the size of the radiography.

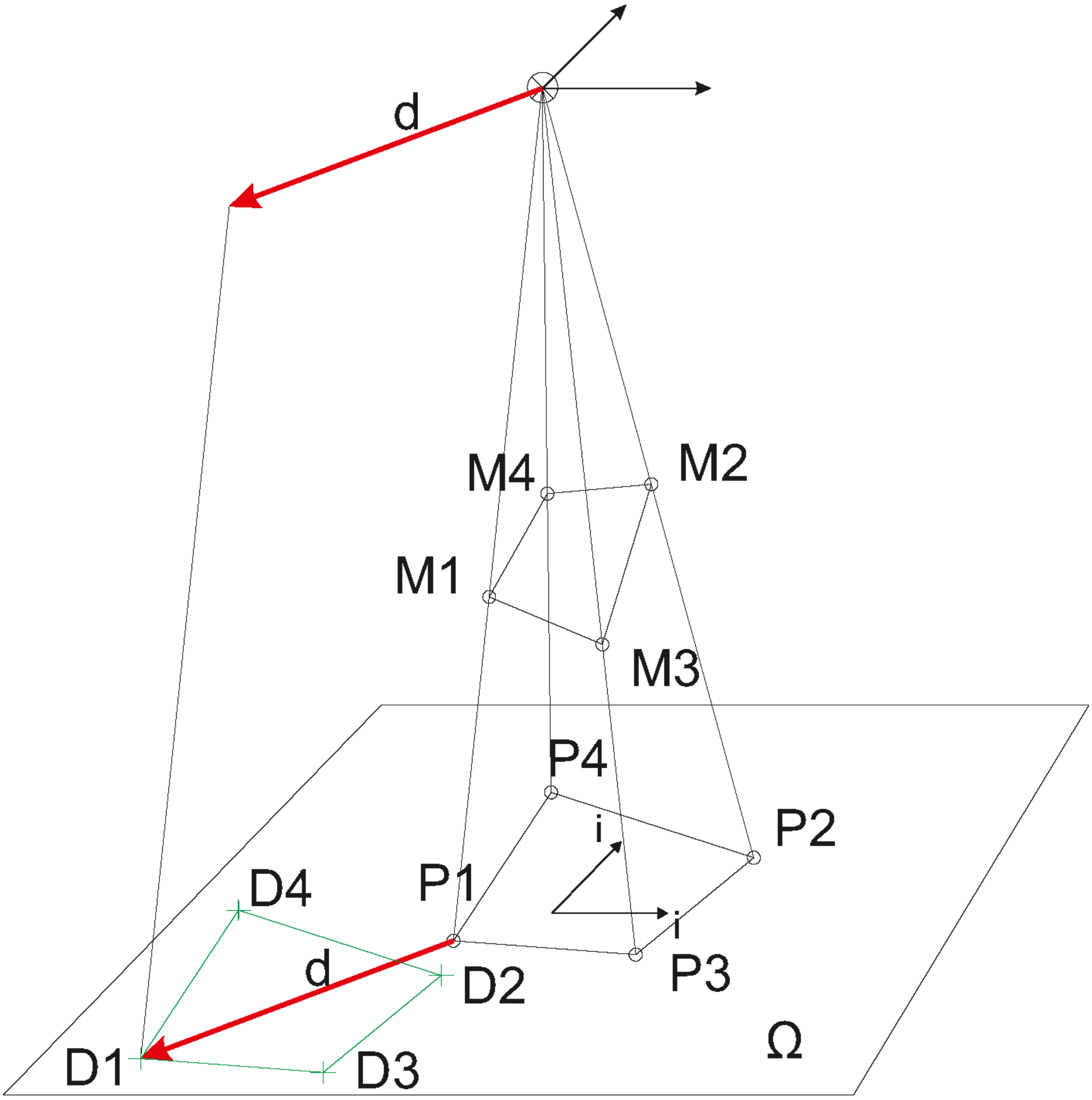

Figure 23. *x, y position of the focus derived from the decomposition of the displacement of the projections.*

This approach is present in the pseudocode under the procedure **CalculateFocus**, and can be seen in the next lines:

```
Xfocus=RadiographMarker(0).X-ProjectedMarker(0).X
Yfocus=RadiographMarker(0).Y-ProjectedMarker(0).Y
```

Here, **RadiographMarker(0**) corresponds to the radiographic data (D1). The x and y coordinates of the focus, **Xfocus** and **Yfocus** respectively, are obtained subtracting its coordinates to those of the projected marker 1 (P1), named **ProjectedMarker(0).**

3.3.2.Iterative exploration

As an initial idea, spatial location of the focus and the localizer were explored iteratively within the algorithm. However, it has been shown how maintaining the focus stationary during the whole process optimizes the method. In order to compensate this "restricted movement", two successive displacements are implemented:

On one hand, the variation that would be applied to Fz is replaced as a variation in the distance between the focus and the projection plane. This variable is introduced as Z_{focus}, referencing the relative Z of the focus with respect to the projection plane. Considering an initial value or "seed", the algorithm expands a window that covers a set of values delimited by $\pm range$ (remember that range was introduced as a variable that defined the exploration range) and initiates the process. This is considered as the first and most external iteration of the algorithm. Notice how considering the projection plane as a moving element, the distance between it and the localizer is changed twice per loop. The first one corresponds to the iteration in Z_{focus} and the second to that of the localizer Z_{loc}.

On the other hand, the iterations applied to the localizer in its x, y and z coordinates are executed. As in the case of the application of the displacement introduced in 3.3.1, these translations are defined for a reference point (either a marker or a significant point) and applied to each of the markers composing the localizer; the corresponding components are named X_{loc}, Y_{loc} and Z_{loc} respectively. As in the case of Z_{focus} the area of exploration is centred in an initial seed and covers $\pm range$. The number of iterations is directly dependent on the size of the range of exploration and the increment value. In this way, as the same range and increment are applied to both Z_{focus} and the localizer in its three coordinates (an additional feature of the software implemented incorporates the possibility to individually define the ranges for each spatial variable), after a whole process has been completed, the number of iterations performed by the algorithm correspond to:

$$variables^{\frac{2*range+1}{increment}}$$

With 4 variables: $Z_{focus}, X_{loc}, Y_{loc}$ and Z_{loc}. As an example, if the range of exploration were 10 mm and the increment 0.1 mm, the total number of iterations would be:

$$4^{201} = 1.03\,exp\,121$$

For the assessment of this algorithm, variations in the sequence of iteration of the variables have been explorer with no significant effect. On the contrary than rotations, the translations are commutative, which introduces independence in the selection of the order. The iteration loops are registered in the pseudocode under the procedure **CalculateFocus** and shown next.

```
Zfocus=ZfocusREF+Zfocus_INI
DO
    Xlocalizer=Xlocalizer_INI
    DO
        Ylocalizer=Ylocalizer_INI
        DO
            Zlocalizer=Zlocalizer_INI
            DO

                [Inner code]

            Zlocalizer=Zlocalizer+Zlocalizer_INC
            LOOP UNTIL Zlocalizer>Zlocalizer_FIN
        Ylocalizer=Ylocalizer+Ylocalizer_INC
        LOOP UNTIL Ylocalizer>Ylocalizer_FIN
    Xlocalizer=Xlocalizer+Xlocalizer_INC
    LOOP UNTIL Xlocalizer>Xlocalizer_FIN
Zfocus=Zfocus+Zfocus_INC
LOOP UNTIL Zfocus>(ZfocusREF+Zfocus_FIN)
```

The following graphs show the iterative nature of the methodology. In the x-axis, the iteration number is indicated, while in the y-axis, the *focus error* associated with it. Three successive augments are shown to bring insight into the inner loops of the procedure. It is possible to observe the oscillating behaviour of the methodology based on the different variables: Trying to draw attention to the existing envelope in each image, it is possible to window a range of values of each variable for which the error is minimum. For the case of the first figure, the outer envelope relates to Z_{focus} although not easily observed, it can be intuited a minimum error in the region around the iteration number $2.7 * 10^5$, associated to a certain value of Z_{focus}.that can be identified knowing the increment, range and initial value. The second figure corresponds to a higher level of magnification, between iterations 0 and 18000. Here, the external envelope is associated to the behaviour of the X_{loc}. Lastly, the third figure, gathering the errors associated to the iterations 16800 to 17700 brings insight into the influence of the Y_{loc} showing, as well, the oscillations related to Z_{loc}. It is important to remark that these variables are interrelated and, consequently, it is not possible to determine a value of minimum error for each of them, since it depends on the values that the others are adopting. However, it can be delimited a region for this minimum, as it is introduced 4.

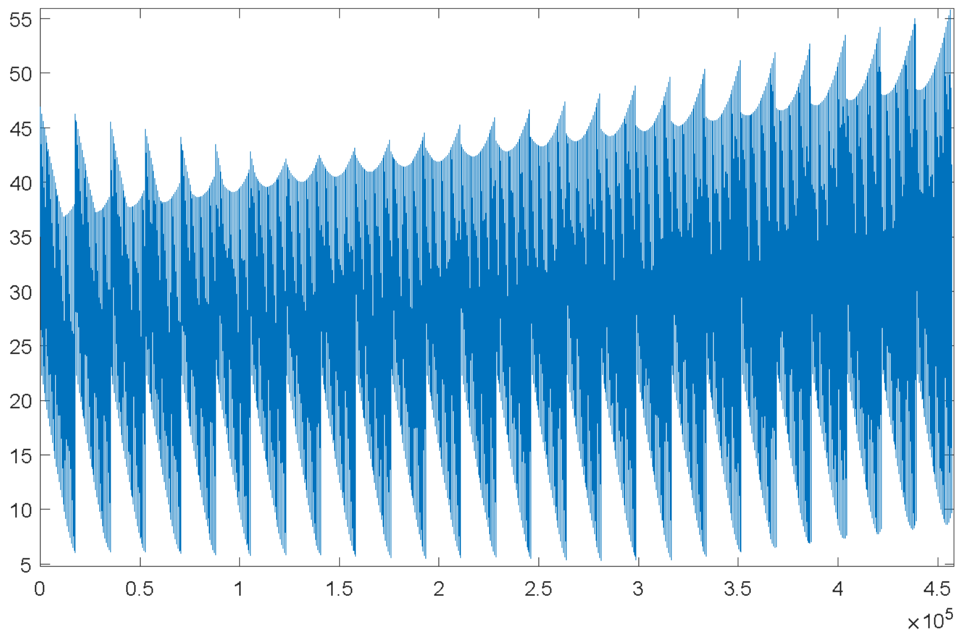

Figure 24. *Iterations Zfocus.*

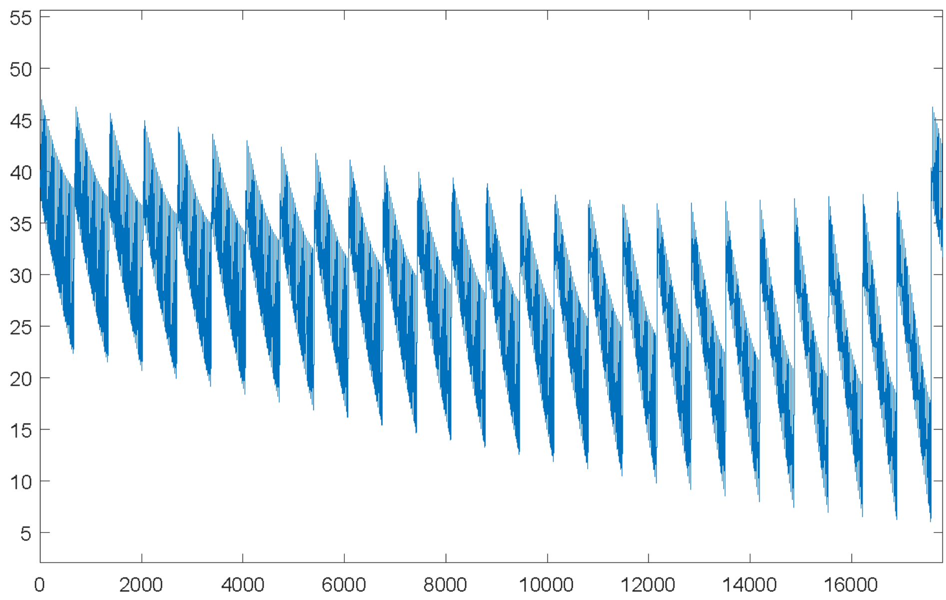

Figure 25. *Iterations Xloc.*

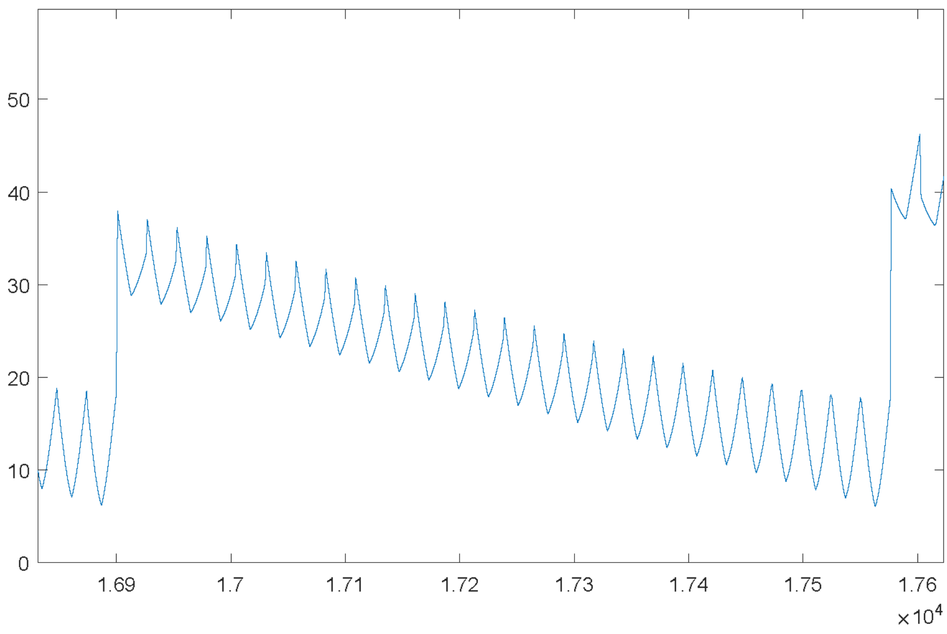

Figure 26 *Iterations Yloc.*

3.3.3.Position verification

As for any iterative algorithm, a stopping criterion is crucial when determining a "solution". Intrinsically to this case, a necessary parameter from which the computational time depends directly, is the order of discretization of the space or, in a more intuitive way, the spatial separation between one position of the focus/localizer and the corresponding to the next iteration, introduced under the name of increment. In addition, other parameters can be considered in order to try to implement a stopping criterion. The first and more important is the error in the hypothesized projection, *markers error*, explained below:

When studying the conditions that apply to his research, it is important to bear in mind what is the data available and how is it possible to manage it. Up to now, the only known data are the spatial location of the previously introduced radiographic data (projection of the markers in the radiography). Analogous to this information, virtual/hypothesized projections are generated as the projections of the localizer's markers for each combination of focus/localizer position in the space during the iterations. An interesting variable to examine is the difference between the radiographic data and the virtual projections; this is named *markers error*, already introduced in previous sections. This error is defined as the sum of linear distances between each of the markers of the radiographic data and those of the virtual projections. Experimental results show that the error in the determined position of the focus, *focus error*, is reduced in concordance with *markers error* and *increment* value. This correlation between the both errors can be seen in Figure 27. Correlation between Markers error and Focus error, in mm, for values of discretization ranging from *2 mm* to 0.15 mm

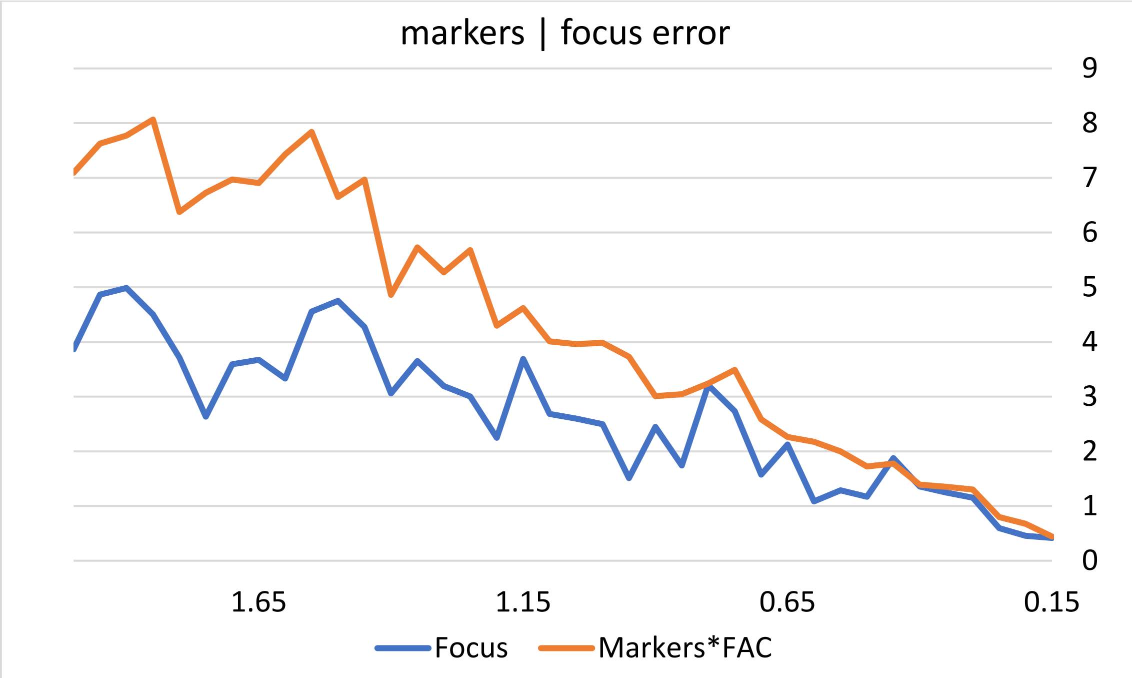

Figure 27. *Correlation between Markers error and Focus error, in mm, for values of discretization ranging from* 2 mm *to 0.15 mm.*

Once the aforementioned correlation has been proved, the position of the focus must be determined according to the principle that minimal *markers error* leads to a minimal *focus error*. This *markers error* is checked for each iteration of the program and compared with the previous instance of minimum *markers error*, in case it is smaller than the previous one it is stored and compared with the value of the following iterations. Through this method, it is possible to reach a solution after all the iterations that explore the *range* have been completed. The following lines contain the pseudocode relative to this test. There, **MarkersError** corresponds to the *markers error* and **MinimumMarkersError** with the minimum *markers error*. Additionally, **Solution-Number** registers the number of occurrences of minimum error, which is explained later in the text.

```
If MarkersError<=MinimumMarkersError Then
    If MinimumMarkersError=MarkersError Then
    SolutionNumber = SolutionNumber+1
END IF
```

From the iteration with minimal *markers error*, the coordinates of the focus with respect to the centre of the radiography are determined as: Z_{focus}, distance between focus and projection plane; X_{focus} and Y_{focus}, decomposition of the coordinates of the displacement d applied to the first projected marker to match the corresponding projection in the radiographic data.

$$X_{focus}, Y_{focus} = (D_1x, D_1y) - (P_ix, P_1y)$$

4. Application Method

In the previous chapter 3, the LoFX methodology was explained. This is the core algorithm for the entire software and the ultimate responsible of the calculus of the position of the focus. However, the performance of the methodology in an acceptable time is restricted to a small area around the actual position of both the focus and the localizer. The reason is that, as a brute force method the number of iterations rises exponentially with increasing range of exploration and decreasing value of increment, which is, in fact, determinant for the accuracy. Consequently, if the methodology is applied directly for example, in a range of exploration of $\pm$ 200 mm with an increment value of 0.5 mm (in order to warranty a reasonable accuracy), the number of iterations rises to:

$$4^{\frac{2*200+1}{0.05}} = 3.32\, exp\, 4828$$

Considering the number of intermediate steps that the processor has to perform, the calculus time would exceed any reasonable limit.

4.1. Temporal study

As suggested before, the nature of the methodology implies an exponential increase of the iterations as the range of exploration increases or the discretization of the space is smaller. In order to transform this idea into a quantitative amount of time, several tests have been carried out, with a consequent study of the results, showing a potential function associated with the time, directly related to the increase in precision. This study is presented in the next pages.

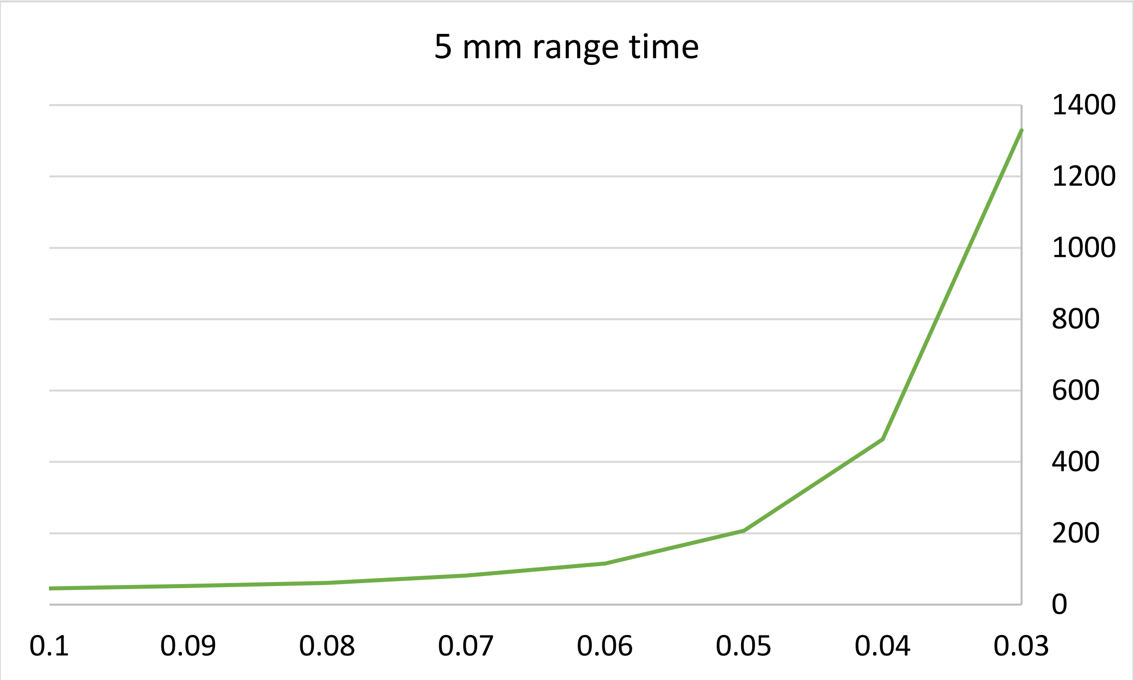

Figure 28. *Calculus time, in seconds, of the LoFX methodology for a range of 5 mm and increment values from 0.1 mm to 0.03 mm.*

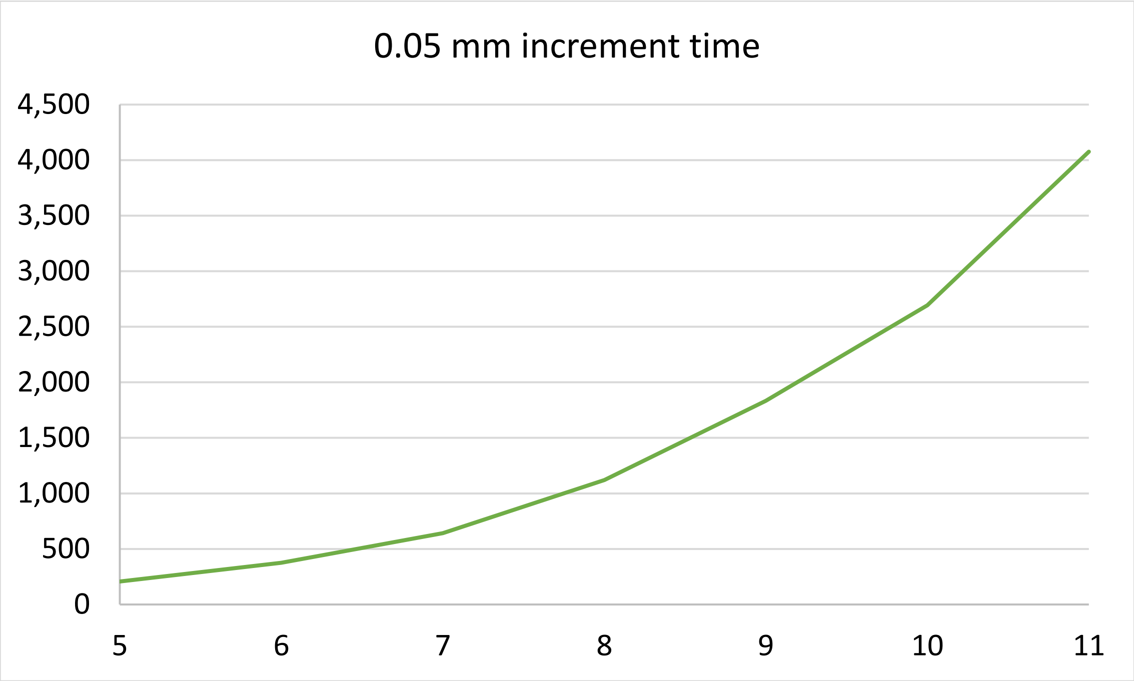

Figure 29. *Calculus time, in seconds of the LoFX methodology for an increment of 0.05 mm and range values from 5 mm to 11 mm.*

In Figure 29, the relation between the increment (x-axis) and the calculus time (y-axis) is shown. Evaluating this data with the software MATLAB® and the *Curve Fitting Tool*, some considerations can be extracted from its behaviour.

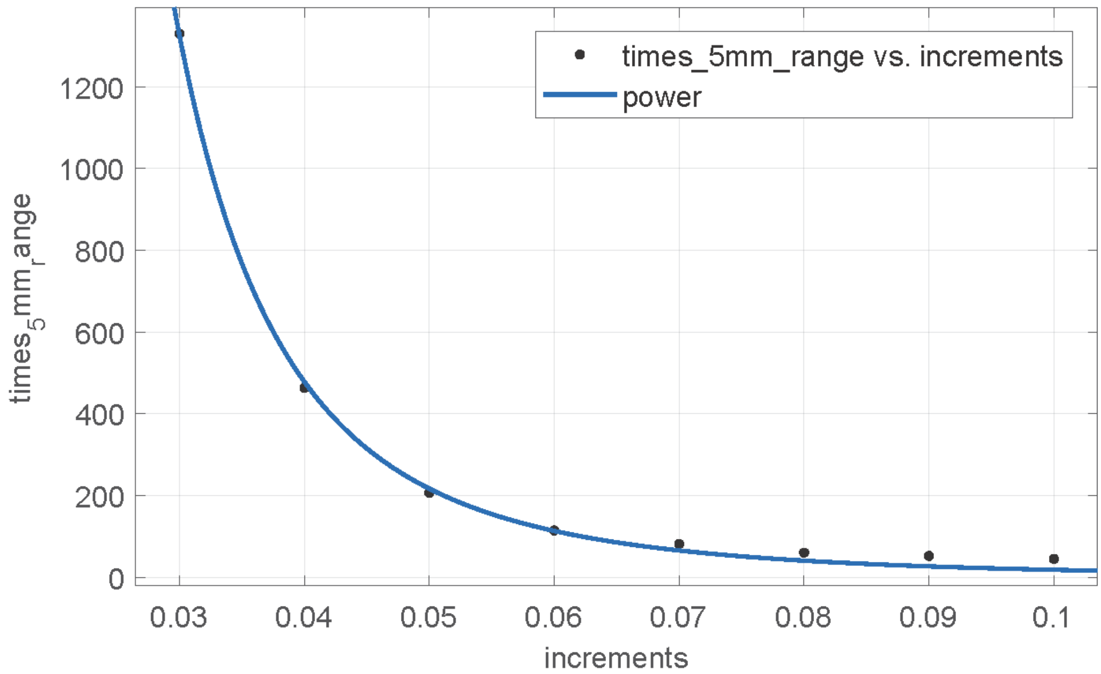

Figure 30. *Power function curve fitting for the calculus time, in seconds of the LoFX methodology for an increment of 0.05 mm and range values from 5 mm to 11 mm.*

Notice that, due to the increasing values presented in the x-axis, the curve is shown inverted with respect to the previously presented graphs. The obtained results for this fitting with a power function curve are showed in Figure 30, allowing the extrapolation of calculus times for decreasing increment values.

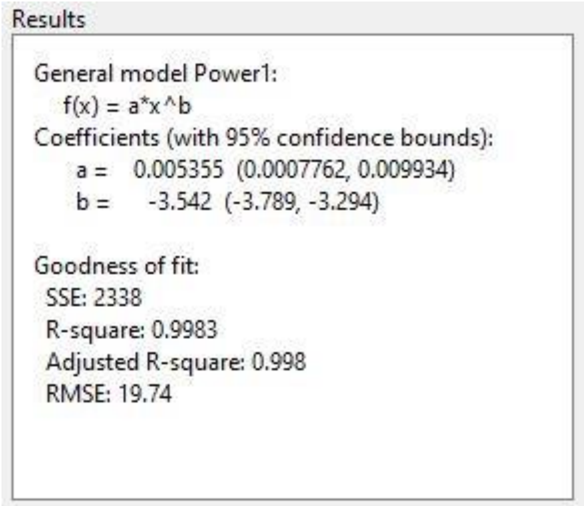
Results

General model Power1:
f(x) = a*x^b
Coefficients (with 95% confidence bounds):
a = 0.005355 (0.0007762, 0.009934)
b = -3.542 (-3.789, -3.294)

Goodness of fit:
SSE: 2338
R-square: 0.9983
Adjusted R-square: 0.998
RMSE: 19.74

Figure 31. *Numerical results for the power function curve fitting for the calculus time, in seconds of the LoFX methodology for a range of 5 mm and increment values from 0.1 mm to 0.03 mm.*

More relevant in order to justify the need of an application method are the results related to the increase of the range, showed in Figure 32 for an increment of 0.05 mm and a range up to 11 mm. To advance information, the application method explained in this chapter allows the application of the methodology in ranges up to 200 mm in a reasonable time. As for the previous calculus, the software MATLAB® and, specifically, the Curve Fitting Tool is used. Obtaining the numerical results presented in the Figure 33.

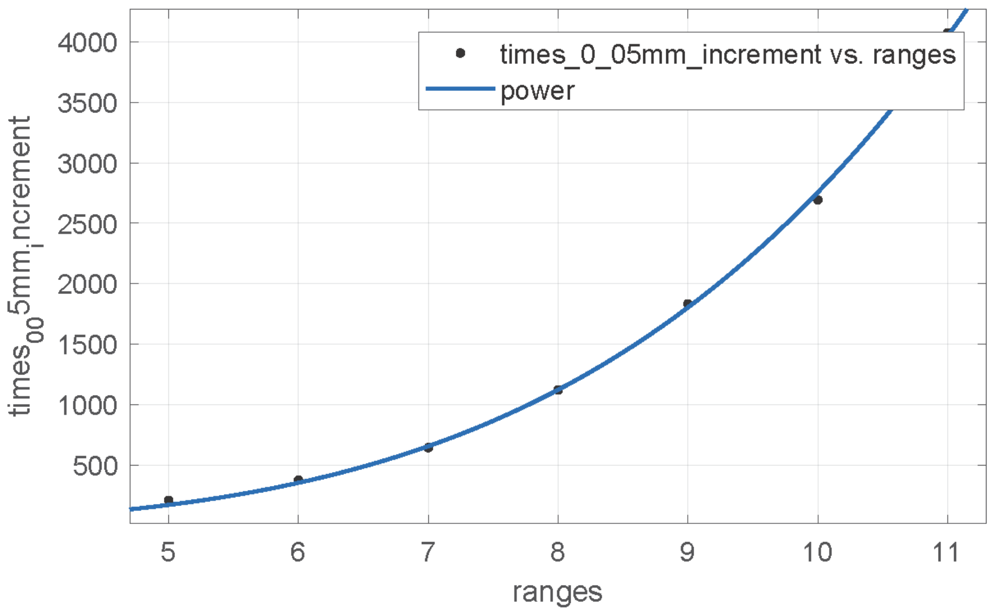

Figure 32. *Numerical results for the exponential curve fitting for the calculus time, in seconds, of the LoFX methodology for an increment of 0.05 mm and range values from 5 mm to 11 mm.*

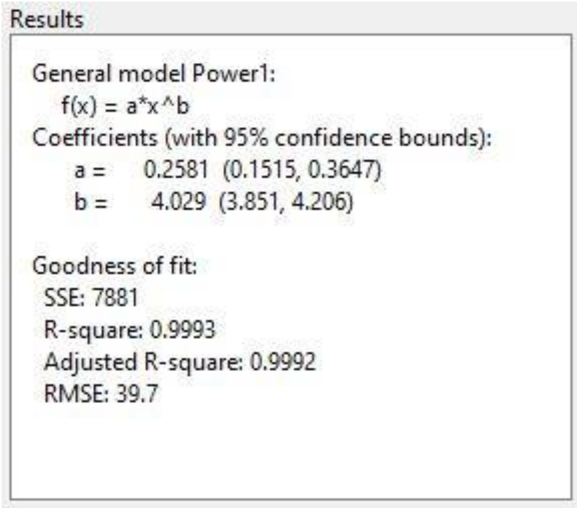

Figure 33 *Numerical results for the exponential curve fitting for the calculus time, in seconds, of the LoFX methodology for an increment of 0.05 mm and range values from 5 mm to 11 mm.*

With these data, if a range of 200 mm wants to be explored using an increment of 0.05 mm, the expected time is more than 48,000,000 seconds (a total of 557 days). In contrast with the achieved results showed in section 4.1, in which this time is reduced to just 14 min thanks to the implementation of the *Application Method*. In addition, for the determination of the calculus times, a DELL 7720 workstation with 64GB of RAM and a processor of 2400MHz was used. The comparison with a standard PC ASUS F556U gives an idea of the magnitude of this time for a standard equipment as it can be seen in the Figure 34. Calculus time (in seconds) for a Workstation vs a user PC for a range of 5 mm and increment values ranging from 0.1 mm to 0.03 mm, evidencing the importance of a reduction in the calculus time.

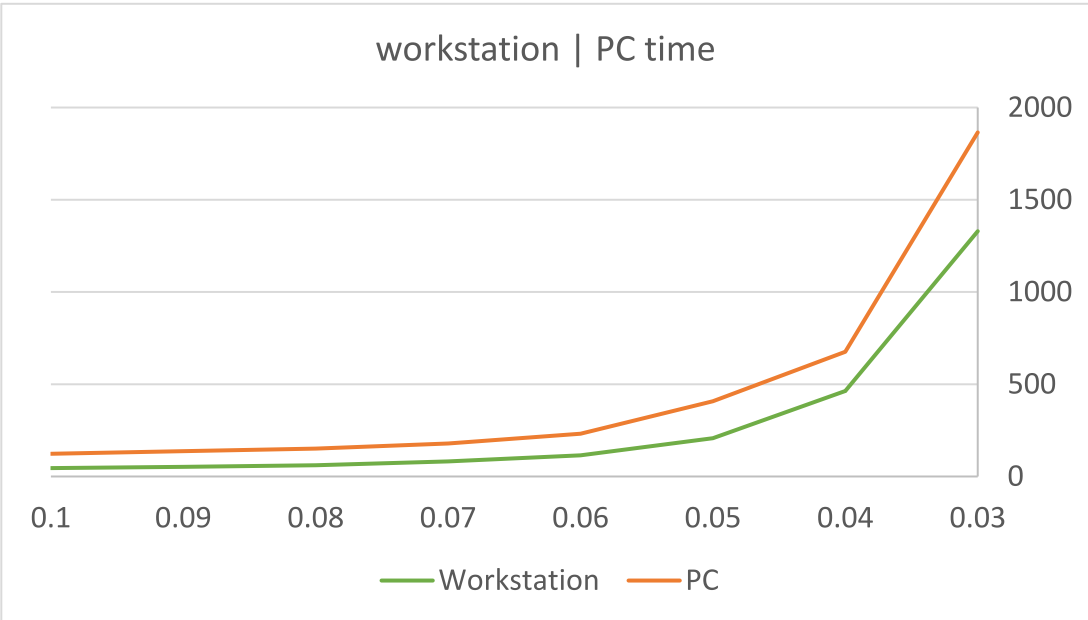

Figure 34. *Calculus time (in seconds) for a Workstation vs a user PC for a range of 5 mm and increment values ranging from 0.1 mm to 0.03 mm.*

The excessive computational cost introduces the need to implement a method to initially narrow the space before performing a precise calculus with the smaller increment value The method developed in this thesis consists in 4 steps that are introduced in the next pages.

4.2. Prepositioning

As indicated in the previous chapter, initial positions (seeds) for the focus and the localizer are required to initialize the exploration. These values must be provided by the physician or researcher attending to the specific positioning of the X-ray machine. Under standard operating conditions, the focus is placed at an approximate distance from the radiograph of 1.5 m, in an almost centred position; and the localizer is expected to be centred and close to the radiography. Although standardized procedures exist, these values can be reintroduced depending on the characteristics of each study case. These initial values can help to have an approximate idea of the position of the focus, however, the range of uncertainty exceeds the possibilities of the LoFX if a high level of precision wants to be achieved. For this reason, an initial stage that can handle a large area of exploration is introduced under the name of *prepositioning*.

Thanks to the prepositioning, the precision of this initial seed loses importance, since a range of $\pm$200 mm is explored. The main reason for this choice relies on the typical size of an X-ray film, which rarely exceeds 40 cm. With the aid of the light beam collimation available in most of the conventional X-ray machines as well as the available information about the position of the X-ray machine, it is reasonable to expect an accuracy higher than $\pm$200 mm in these initial data.

One of the problems associated to the LoFX methodology is the concatenation of loops, which exponentially increases the computational cost if a wider range of the space or a finer value of increment wants to be used. This fact motivated the procedure described as prepositioning. Starting at an initial value or seed, the algorithm operates based in an "isolation" of iterative variables. First, Z_{focus} is isolated. A whole exploration of its range is performed without any intermediate change of the other variables ($X_{loc}, Y_{loc}, Z_{loc}$, which remain locked at their initial position). Thus, values of Z_{focus} between $\pm$200 mm with an increment of 1 mm are explored around this seed. The x and y translations in the projective plane are performed according to the procedure introduced in the previous chapter and the *markers error* is assessed for each of the different values of Z_{focus}. The reduction achieved in the variability of the system leads to a global minimum close to the real and exact value. As it is done in the main algorithm, the Z_{focus} associated with the minimum *markers error* is kept as a "temporal solution". Next, the same procedure is repeated with X_{loc} It is important to remark that for this and future exploration of variables, Z_{focus}, instead of returning to the initial value, is updated with the value obtained in the previous step. Again, the X_{loc} associated with the minimum *markers error* is saved. The procedure is repeated for Y_{loc} and Z_{loc} ensuring that all the variables are redefined based on their respective global minima, serving as a new seed to introduce to the next stage.

Although in the main algorithm, the *increment* value had a crucial relevance in the precision, consequence of the multiple local minima that appeared due to the 4 degrees of freedom (one per each variable), this stage (prepositioning) shows a small dependence on the value thanks to the existence of a single and global minimum for each variable. In Figure 35, the evolution of the *Focus error* for different cases after the prepositioning phase, using the same initial conditions is shown. Increment values of 1 mm and 0.1 mm are used for these tests. However, due to the similarity between both errors, the corresponding lines appear superposed making it difficult to appreciate the difference between them.

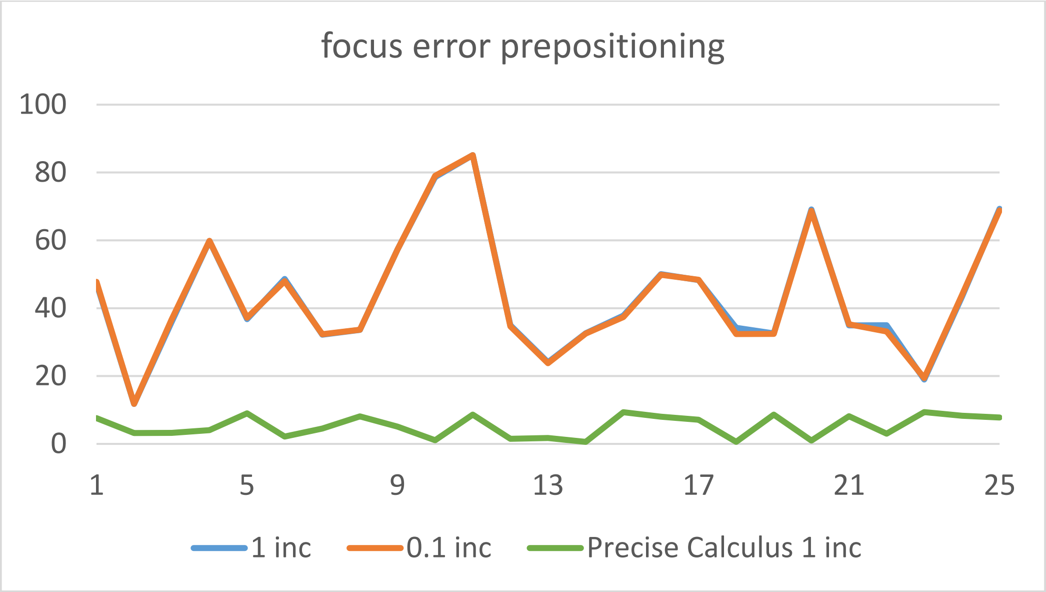

Figure 35. *Focus error in mm after prepositioning for 25 random cases. In blue increment of 1 mm. In orange, increment of 0.1 mm. Error after the Proximate Positioning in green.*

The evolution of both *markers error* and *focus error* for the independent variation of the different variables is shown in the following figures: Figure 36, Figure 37, Figure 38 and Figure 39.

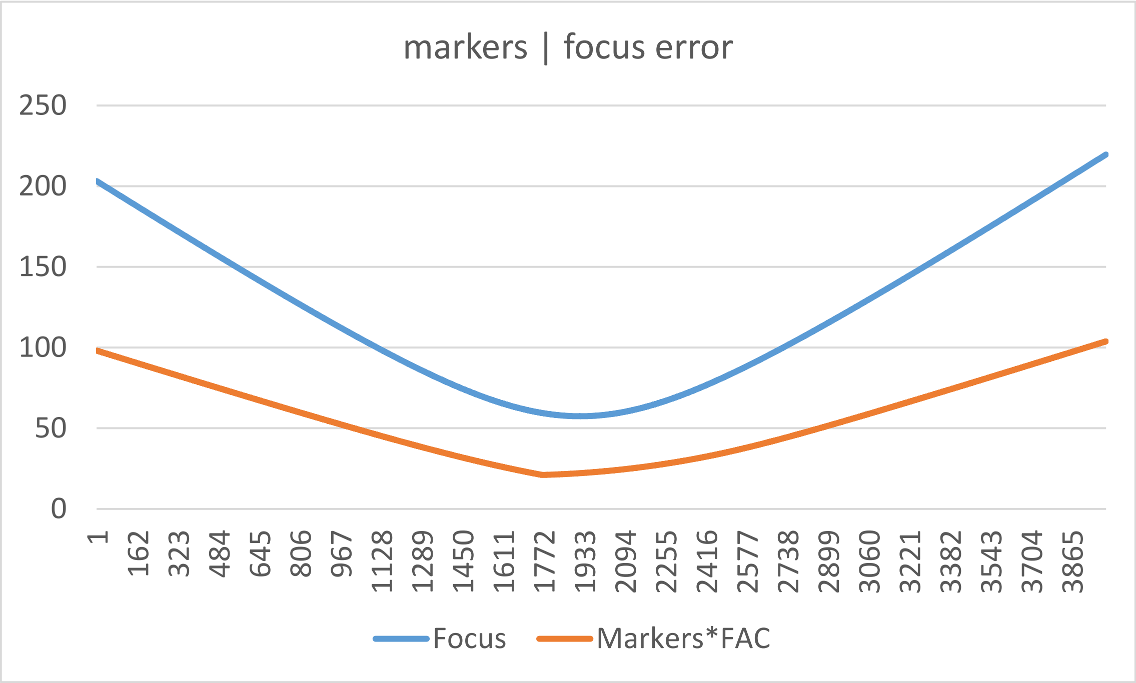

Figure 36. *Zfocus variations.*

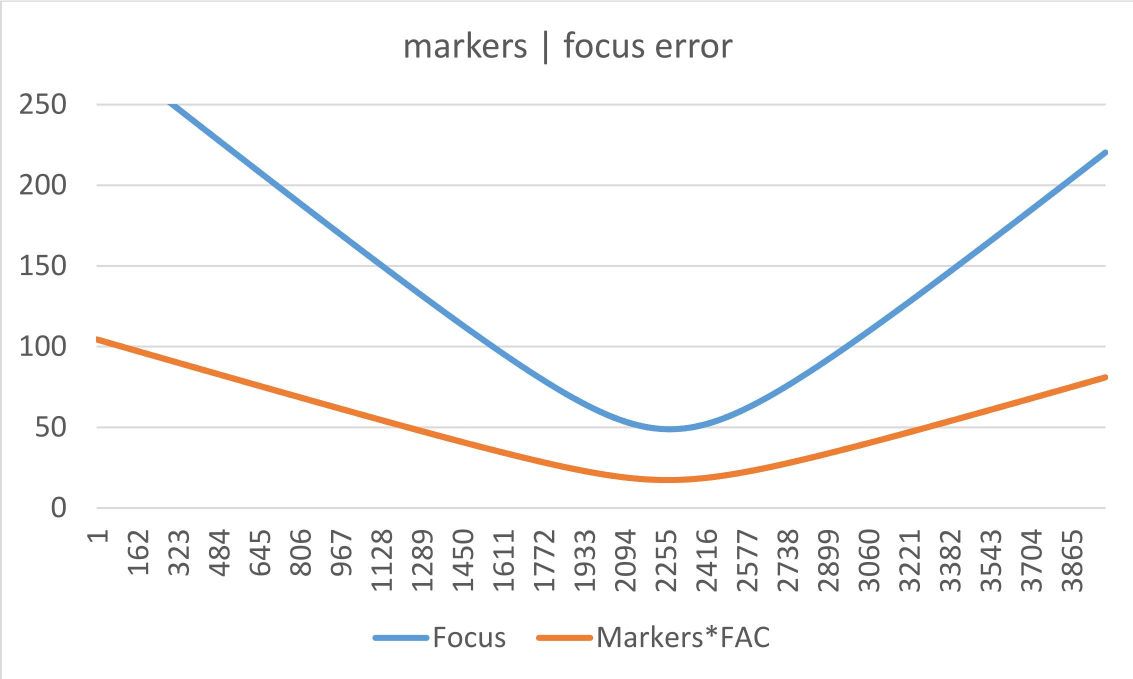

Figure 37. *Xloc variations.*

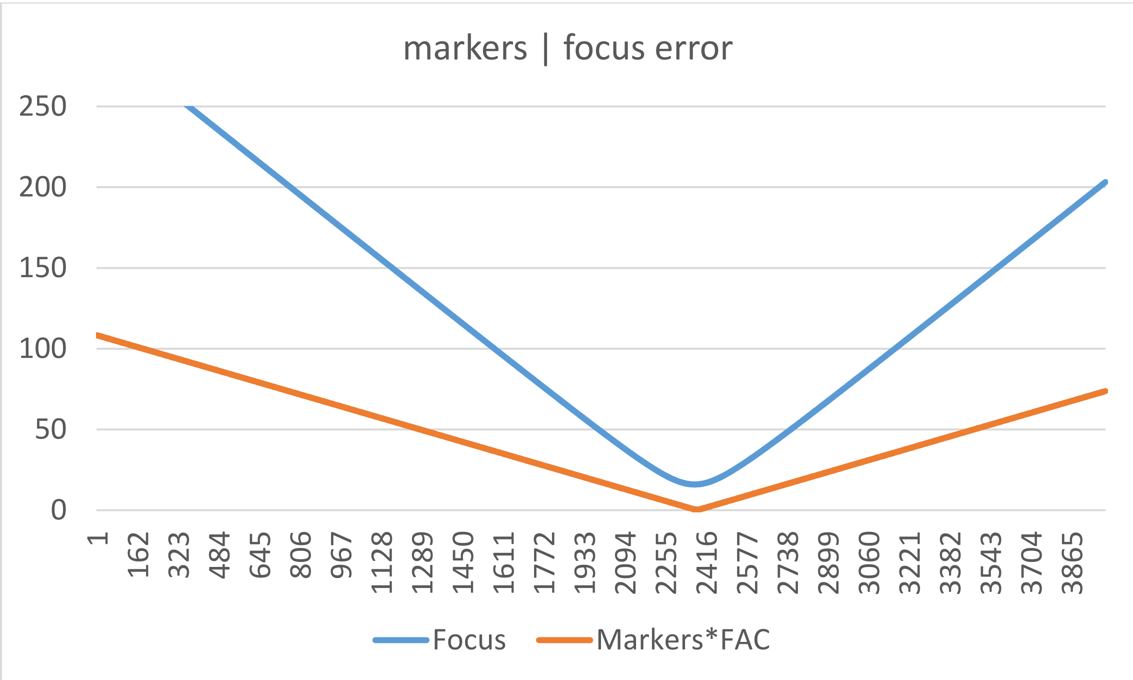

Figure 38. *Yloc variations.*

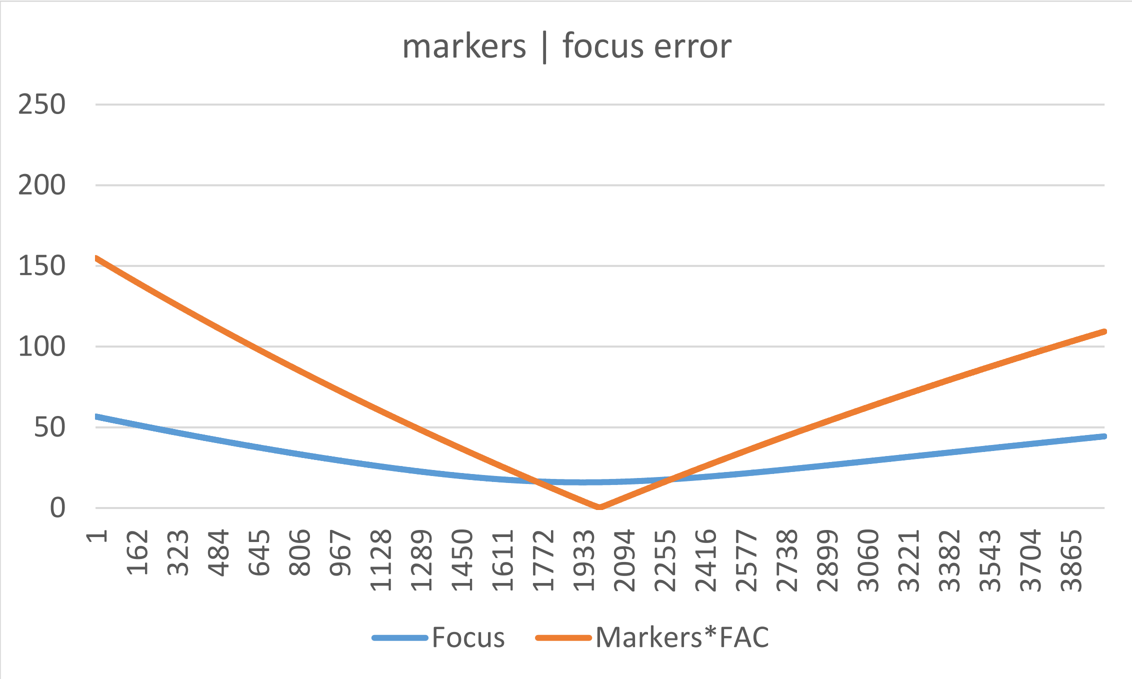

Figure 39. *Zloc variations.*

It can be observed the existence of a single minimum for each variable, that serves as an approximate seed for the next stage of the algorithm.

4.3. Proximate Positioning

The previous stage, prepositioning, introduced in the section Prepositioning established a new seed for a more precise calculus of the methodology (remember that the seed is composed by a Z_{focus}, X_{loc}, Y_{loc} and Z_{loc}). However, this seed is still subject to a big error as seen in Figure 35. Again, if the precise calculus wants to be applied around it in a region where it is sure that the focus will be found it is necessary to determine the size of this area. After numerous tests, experimental results have shown that a range of $\pm$100 mm is necessary. A significant improvement from the 200 mm used for the prepositioning but still an excessively large area to be examined with a small increment value. In order to narrow this area, a new method is used: proximate positioning.

This method takes the same steps and procedures than the main methodology, LoFX, but uses different parameters. Both range and increment are significantly larger than those applied in the precise calculus: 100 mm and 1 mm respectively. After numerous tests the accuracy of the prepositioning has been proven to be greater than $\pm$100 mm, ensuring the existence of a solution in this range. In addition, an increment of 0.1 mm has proven to find a new seed in a reasonable time. Furthermore, it can be observed how the errors of the green line in Figure 35, which corresponds to the errors after the proximate positioning, are bounded below 10 mm, suggesting that the window for the new search can be considerably reduced.

4.4. Minimal Opening

The previous sections showed methods for locating a new seed closer to the true solution. In addition, the results of the proximate positioning suggest that a small range around the provided seed could be enough to window the exact position of both localizer and focus. This new stage, minimal opening, has the aim of determining a minimum range in which applying the precise calculus. As the proximate positioning, this stage is based on the use of the main methodology, LoFX, to wisely determine which is the minimum range around the seed provided by the previous stage, that ensures that the real position is contained within.

Starting centred at the seed provided by the proximate positioning, the method executes the LoFX with a small *range* and *increment*. 5 mm and 0.5 mm respectively have proved to perform perfectly in all the trials. Although some cases were satisfactorily solved with a smaller increment, a dominant proportion of cases found the solution in a range of 5 mm. In addition, the time spent in the exploration of smaller areas could be neglected against the iterative procedure that is required for the increase of the range.

Given the small relative size of the range with respect to that of the increment, a whole cycle of iterations consumes few resources. Through this cycle, a minimum value for the *markers error* is found and stored, together with the value of the *range* associated to it. It is relevant to point out that, in this case, the values of the variables Z_{focus}, X_{loc}, Y_{loc}, and Z_{loc}. are not relevant, as the purpose of this stage is to determine a minimum value for the range. Afterwards, the range value is increased and, again, another full cycle is run to find the minimum *markers error*. If the value matches with the previous one, it implicates that the minimum was found within the first range explored, as the larger range includes the first; if not, the minimum was found in the increased range.

This procedure of increasing the range and exploring it is repeated until the minimum *markers error* reappears for certain number of times. After numerous trials, 5 repetitions have shown to be sufficient to ensure that the minimum found is close to the global minimum. The first range associated to the mentioned minimum (proven to be the smaller range containing the real position) is recovered and provided for the next and last stage. This algorithm is presented in the following lines of pseudocode:

```
IF PreviousMarkersError=PreviousMarkersError THEN
    CoincidenceCounter=CoincidenceCounter+1
    IF CoincidenceCounter=5 THEN Condition=TRUE
    ELSE
        MinimalOpening= Range
    CoincidenceCounter=0
END IF
```

Here, **PreviousMarkersError** corresponds to the minimum *markers error* obtained when exploring in the previous range. **ExternalMarkersError**, meanwhile, represents the minimum *markers error* found after the exploration in the extended range.

4.5. Precise Calculus

As the last and definitive stage, the precise calculus runs the main methodology, LoFX, based on the information generated in the previous stages. On one hand, the proximate positioning stage determined a seed to serve as initial values for the variables; on the other, the minimal opening determined the minimum range to explore. These parameters are used in the main algorithm to obtain an accurate position of the focus. Thanks to the reduced size of the range, it is possible to use increment values smaller than 0.1 mm with still reduced calculus times.

5. Validation and analysis

In this chapter, the validation and analysis of the main methodology and the application method are presented. The different utilities developed for testing the performance and accuracy of the algorithm are explained and justified.

5.1. Simulation Methodology

As mentioned in previous chapters, in a real application, the only data available for the calculus of the focus is contained in the radiography. Due to the theoretical nature of this thesis, the tools and features necessary to process radiographic data and, hence, to test the methodology in real scenarios are not implemented. This highlights the need to develop a testing system to virtually simulate and validate the methodology.

The methodology suggested is based in the iterative combination of focus and localizer position together with the corresponding projections generated (from now-on, this combination of focus/localizer position is denoted *projective case)*, in order to match them with the projective data (information contained in the radiograph). The best way to compare a virtual projection with a real case is to simulate the second one. Based on the same geometrical principles that serve the main algorithm for the creation of virtual/hypothesized cases, the testing method creates "real cases" to serve as a reference of the exact position of both focus and localizer. In order to achieve a reasonable but "controlled" simulation, capable of providing experimental data, some requirements are considered. As in a real case, both localizer and focus position must be unknown (randomized in a certain area). However, a known approximate location is strongly recommended so that a possible influence of this positions in the capability of the main algorithm to find a solution can be tested. Additionally, different cases of localizers must be tested; facilitating the variation of the number of markers, dimension, and geometry in order to explore their effects on the methodology. Eventually, a flexible and intuitive method has been implemented meeting these characteristics.

Initially, a localizer can be designed. The number of markers and their relative coordinates are defined with respect to a local reference frame in the localizer. As the next step, both the approximate distance between the focus and the X-ray film (Z_{focus}) and the position of the localizer are set. The last one is defined in global coordinates, using the X-ray focus as origin of the system. In this project, this definition of parameters is denoted as *positioning*. After this, the localizer is randomly displaced in an aleatory range (Range of Aleatory Displacement or RAD) around the initial position. The projection of the displaced markers is simulated, keeping the focus at the origin of coordinates and positioning the projective film a randomized distance around its initial location.

For a completely flexible "case generation", the x-y position of the focus must be defined. According to the procedure introduced in the main methodology, a displacement on the focus can be simulated applying the same displacement to the markers and their projections, considering that all the system composed by focus, markers and projected markers moves as a block. These procedures bring about the following data, which can be hold under the name of *projective case*.

Positioned localizer. Initial position and coordinates of the markers of the localizer in the global reference system.

Positioned and randomized markers. Coordinates of the markers after their "initial" positioning and the corresponding random displacement in the surroundings. These coordinates are not affected by the x-y displacement applied to the focus.

Approximate distance of the focus. Approximate distance between focus and radiographic film, ideally given by the physician (value introduced in the variable $\boldsymbol{Z_{focus}}$).

Simulated focus. x and y coordinates of the source of emission to be found and distance from the X-ray film. These are generated by the simulation algorithm.

Dimensions of the X-ray film. Size of the sides of the radiographic film in mm.

Range of displacement. Displacement around the seed data (focus and localizer) to be explored during the methodology.

Projected markers. Coordinates x and y of the projected markers in the X-ray film.

It is worth remembering that the only information available for the main methodology are the defined localizer and the projected markers (corresponding to the radiographic data). Once a *projective case* is generated, both the defined localizer and the projected markers are transferred to the localization methodology for its operation, and the simulated focus is used for the assessment of the performance and accuracy. After the main routine, corresponding to the localization methodology, has been proven to work correctly and the testing method ensures a valid system to track the behaviour of the software, it is necessary to assess the reliability, accuracy and performance of the methodology.

5.2. Validation of the methodology

The localization methodology relies on the fact that studying the *markers error* (sum of linear distances between the hypothesized projected markers to those conforming the *projective data*) it is possible to determine, with high accuracy, the position of the X-ray focus. Hence, with a sufficiently small *markers error*, a small *focus error* must be achieved. In chapter 3, the correlation between *markers error* and *focus error* was shown for a single localizer; presenting the results for increment values ranging from 20 mm to 0.15 mm, and achieving a *focus error* smaller than 0.5 mm. This result was enough in the initial phases of the project to motivate a further study in the feasibility of the methodology. In the current section, a more thorough evaluation is performed.

The methodology is based in the statement that for an infinitesimal value of the increment, the error in the determination of the focus disappears. Due to the impossibility of reaching such small increment values, the validation must be achieved with the smaller values achievable. The test presented next serves as a confirmation of the mentioned tendency of the *focus error* for decreasing values of increment. For a rigorous validation, it is necessary to define the parameters and conditions for the evaluation. The localizer used corresponds to the named *reference localizer*, explained in detail in the section 6.1, which consists in a spatial disposition of 5 markers, homogeneously distributed in a cubic form with dimensions 200x200x200 mm as it can be seen in the Figure 40. Reference localizer of 5 markers.

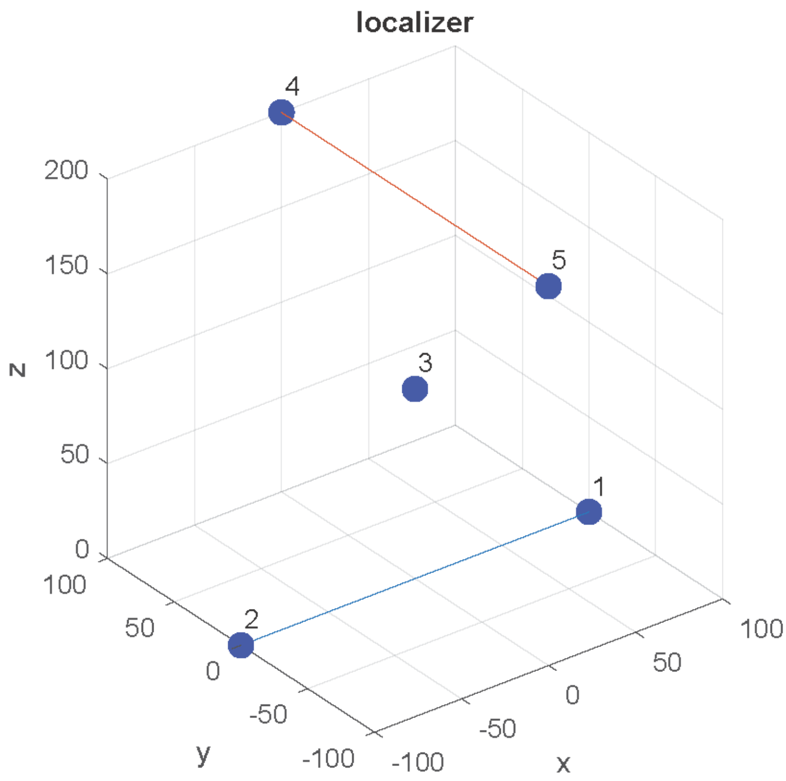

Figure 40. *Reference localizer of 5 markers.*

In addition, the positioning is defined according to the standardized conditions, applied in all the tests conducted in this research and given by the values present in the Table 1. Positioning for the tests. Coordinates of the localizer are applied to the reference or 0 marker.

Positioning

	X	Y	Z
Localizer	100	- 100	1200
Focus	0	0	1500

Table 1. *Positioning for the tests. Coordinates of the localizer are applied to the reference or 0 marker.*

For a better visualization of the positioning, the corresponding spatial configuration is represented with the help of MATLAB® and can be seen in Figure 41. Positioning representation for the focus (red), the markers (blue) and the respective projections (green). Additionally, the numeric values of the case 1, presented in the image, is expressed in the Table 1.

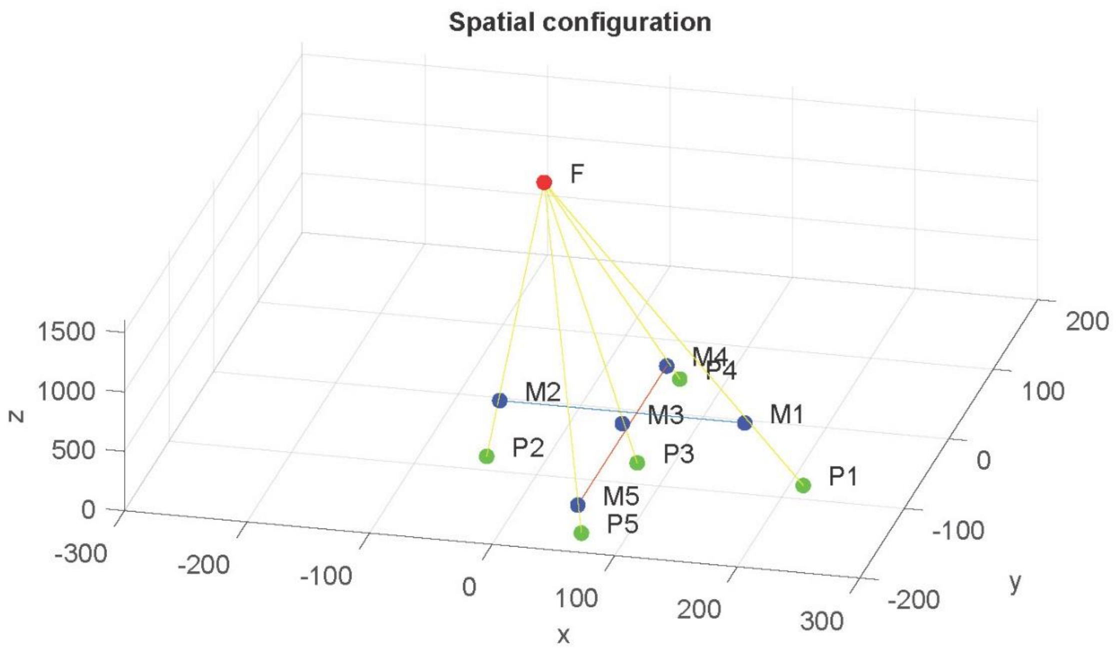

__Figure 41.__ Positioning representation for the focus (red), the markers (blue) and the respective projections (green).

Case 1

Marker	X	Y	Z
M1	196.80	-85.88	1163.20
M2	-3.18	-85.88	1163.20
M3	96.82	-85.88	1263.20
M4	96.82	14.12	1363.20
M5	96.82	-185.88	1363.20
Focus	-47.45	47.83	1549.99

***Table 2.** Projective case for the standard positioning of the reference localizer and a RAD of 50 mm.*

The testing method consist in an initial application of the methodology in a range of exploration of 25 mm, in correspondence with the RAD defined in the generation of the cases. In this range, increment values varying from 5 mm to 0.25 mm are used for the resolution of the same *projective case* (same positioning and same aleatory displacement). The time required for the methodology to find a solution with the smaller increments showed the necessity to narrow the range of exploration; as it can be seen, for a range of 25 mm, the computation time expands from 387 s with an increment of 0.20 mm to 1232 s with an increment of 0.15 mm. Consequently, for the next tests, both the range of exploration and the RAD are reduced to 15 mm. This implies that the *projective cases* are different (same positioning but different aleatory displacement). The importance of the variation between *projective cases* with the same positioning is studied later. Eventually, a total of 24 evaluations corresponding to increment values ranging from 5 mm to 0.05 mm are executed with the results shown in Table 3 and Figure 42.

Range (mm)	Increment (mm)	eM (mm)	eF (mm)	Time (s)
25	5.00	0.35980	15.59450	0.094
25	4.75	0.94920	17.00910	0.097
25	4.50	0.51770	9.28140	0.093
25	4.25	0.41620	15.10900	0.091
25	4.00	0.60110	7.81300	0.094
25	3.75	0.65870	4.94470	0.095
25	3.50	0.50890	16.12820	0.097
25	3.25	0.63330	2.47270	0.100
25	3.00	0.23810	4.58630	0.118
25	2.75	0.41070	15.85560	0.113
25	2.50	0.35980	15.59450	0.125
25	2.25	0.36390	6.98050	0.125
25	2.00	0.21540	2.51430	0.145
25	1.75	0.17010	3.77100	0.173
25	1.50	0.21890	3.13860	0.227
25	1.25	0.17960	4.53760	0.384
25	1.00	0.12550	0.60210	0.825
25	0.75	0.05570	1.51990	2.262
25	0.50	0.05930	2.03830	11.054
25	0.25	0.04690	0.29650	175.311
25	0.20	0.03210	0.50360	387.947
25	0.15	0.01990	0.58880	1232.084
15	0.10	0.01210	0.21990	2511.098
15	0.05	0.00520	0.06470	41823.261

Table 3. *Test results for the reference localizer of 5 markers and increment values ranging from 2 mmm to 0.05 mm.*

These results show the correlation and convergence between *markers error* and *focus error* stated in previous chapters, reaching a *focus error* of 0.0647 mm. The tendency in the data suggest that if an infinitesimal increment value was used, the error in the determination of the focus would be negligible, serving as a confirmation of the validity of the methodology. Additionally, thanks to the occurrence counter incorporated in the simulation software, which registers in every execution the number of solutions found, it has been possible to prove the existence of a single solution for each *case*. However, the computation time required for these values, 41823 s (11.6 h) exposes the necessity of an application method that delivers accurate results in a more reduced and acceptable time.

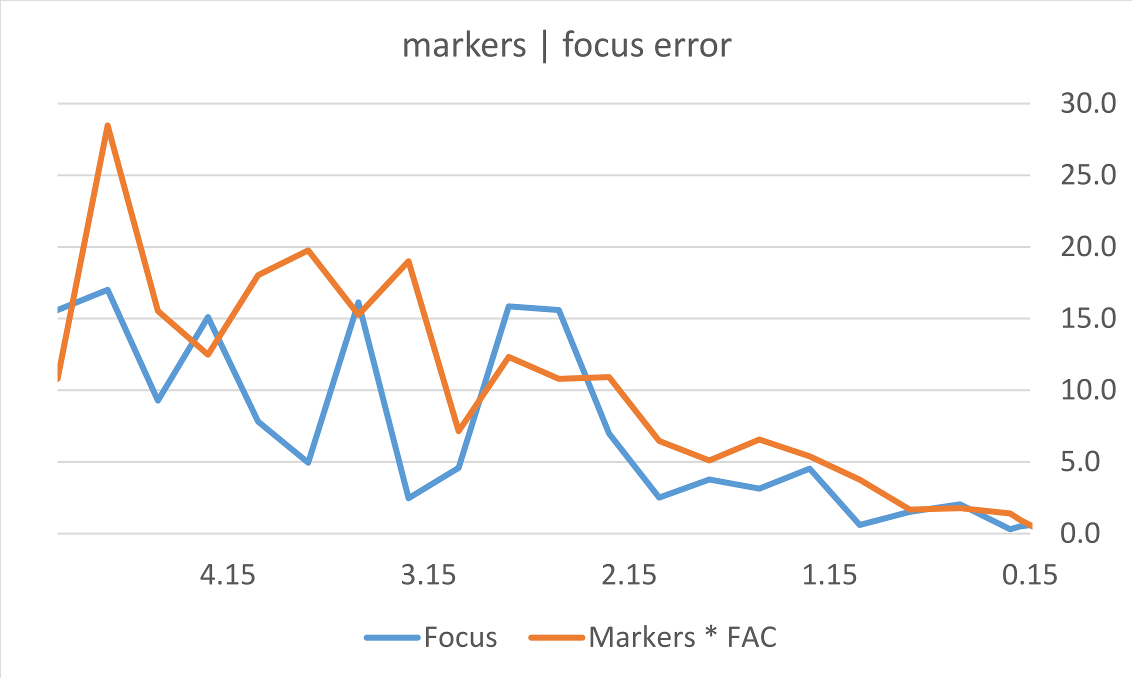

Figure 42. *Focus error (blue) and markers error (orange), in mm, for increment values ranging from 5 mm to 0.05 mm.*

Variability between projective cases

Previously in this section, the existence of different *projective cases* with the same positioning parameters was mentioned. To achieve a better understanding about this circumstance, it is interesting to reintroduce the "simulation methodology”. The simulation is performed using the so-called *projective cases*, each of which contains manually introduced information about the geometry of the localizer, its positioning (review 5.1). and 4 additional variables which are automatically randomized by the software, around the positioning: x, y, z coordinates of the localizer and distance between focus and projective plane Z_{focus}. Due to the variation between the initializing seed (start position for the iterations) of the cases as, together with the effect of the size of discretization of the space (referred as increment), variability in the behaviour of solutions is obtained for different cases, even with the same positioning.

The *Random Displacement Range*, applied around the positioning, is studied in order to explore its influence when determining the focus position. For this test, 25 different cases with the same positioning, localizer (reference localizer) and increment are studied. Figure 43 shows the effect of the random displacement of the markers, the focus and, consequently, the projected markers for 25 different cases generated with random displacement of 50 mm (the seed of the localizer and focus for the localization algorithm is placed randomly in a cube of side 50 mm and centre located in the real solution) and both the *focus error* (blue) and the *markers error* (orange) are represented in a graph in which the y-axis represents the error (*markers error* is multiplied by a factor of 30 in order to facilitate its comprehension) and the x-axis makes allusion to each of the 25 cases. This result shows the necessity of evaluating a significative number of cases (25 have proven to be sufficient for a high confidence) in order to extract reliable information.

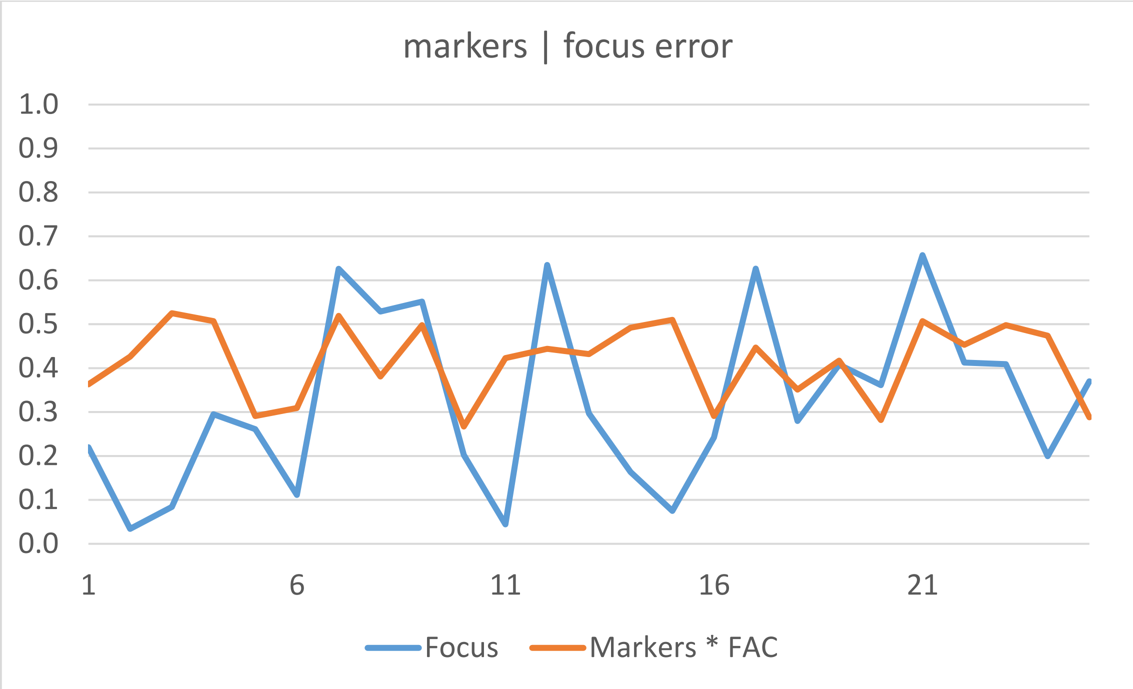

Figure 43. *In blue Focus error, orange Markers error*30 and in light orange with no multiplication, in mm, for 25 cases, represented in the x-axis. An increment of 0.1 mm is used*

As it can be observed in Figure 43, both *focus error* and *markers error* obtained when applying the localization methodology show a high variability. This precise data is characterized by a mean value of the *focus error* of 0.3180 mm and a standard deviation of 0.1900 mm.

5.3. Validation of the application method

The methodology was validated in the previous section, where the results showed an increase of the precision achieved by the reduction of the increment value. Moreover, the necessity of an application method to avoid the excessive computational time and permit the practical execution of the methodology was presented. The application method developed, named *ApLoFX*, is thoroughly explained in chapter 4. In this section, its validation is achieved showing the correspondence between the errors obtained with the use of the standard methodology, LoFX, and those of the application method. Additionally, in the section 5.4. the trials carried out (all of them using the application method), show the same convergence previously presented in the validation of the methodology. These results serve as an additional proof of the validity of the ApLoFX.

The test performed utilizes the previously defined standard positioning (see Table 1), a RAD of 10 mm, an increment value of 0.05 mm for both the LoFX and the precise calculus stage of the ApLoFX, and a localizer of 5 markers and dimensions 200x200x30 mm, which is later introduced in section 6.4. The results obtained are shown in Table 4.

Case	eM (mm)	eF (mm)	Time ApLoFX (s)	Time LoFX (s)
1	0.0015	0.2882	229	4436
2	0.0024	0.0531	389	5379
3	0.0012	0.1217	205	5345
4	0.0022	0.1296	203	5355
5	0.0021	0.0851	198	5449
6	0.0014	0.2450	197	3291
7	0.0012	0.1444	199	5887
8	0.0022	0.0926	217	6152
9	0.0018	0.3030	1130	6017
10	0.0011	0.1982	3867	5873
11	0.0019	0.1273	7401	6181
12	0.0013	0.0223	199	6019
13	0.0018	0.4081	199	6172
14	0.0018	0.2739	204	6226
15	0.0012	0.0962	226	6056
16	0.0008	0.0759	1625	6079
17	0.0019	0.2020	6102	5732
18	0.0022	0.3448	572	6151
19	0.0016	0.3217	1811	6061
20	0.0020	0.1812	5350	5708
21	0.0022	0.3086	245	5450
22	0.0017	0.0294	1902	6106
23	0.0012	0.1435	813	6048
24	0.0016	0.2040	571	5729
25	0.0017	0.0833	1402	5391
Average	0.0017	0.1793	1418	5692

Table 4. *Test results for 25 cases, a localizer of 5 markers and an increment value of 0.05 mm. Calculus time for the methodology and the application method are presented.*

Both *markers error* and *focus error* are equal for the methodology and the application method. The difference lies on the computation time, with a remarkable reduction in the case of the ApLoFX, showing an average time of 1418 s, in contrast to LoFX, with 5692 s, meaning a reduction of 4 orders of magnitude. Additionally, ApLoFX shows a higher variability, characterized by a standard deviation of 2000 s against 634 s. The reason can be found in the stages that define the application method, concretely in the 3rd one: minimal opening, which determines the range of exploration in which the precise calculus is applied, adding, hence, variability in the time of calculus.

5.4. Test results

In the previous sections, the proposed methodology and the application method that allows its application in practice were validated. The principle that associates a minimum *focus error* and, hence, an accurate localization of the focus, with a minimum *markers error* was shown in section 5.2.

During this section, the results obtained from the execution of the application method are presented and analysed. In earlier stages of the project, multiple localizers were used during the development of the LoFX with no significant differences between them. However, given the relevance that the localizer occupies, its consideration as a variable to be studied shows to be determinant. Consequently, in order to initially isolate its influence from the other variables under study, a *reference localizer*, standard for all the tests, is used. The reference localizer has been designed according to neutral characteristics (see Figure 40) and is denoted as *5M-200 mm* regarding to the 5 markers and dimensions of 200x200x200 mm. Additionally, the following tests are conducted overcoming the variability existent between cases which was mentioned in section 5.2. For this reason, 25 *projective cases* with the same positioning introduced in Table 18 Positioning for the tests. Coordinates of the localizer are applied to the reference or 0 marker. are evaluated. The *Range of Aleatory Displacement* (RAD) for the definition of the cases and the range of exploration evaluated during the prepositioning stage are both set to 200 mm. With these parameters, decreasing values of increment, ranging from 0.1 mm to 0.03 mm are tested and the corresponding results recorded in the next pages.

Test results for an increment value in the precise calculus of 0.1 mm

Case	Range (mm)	eM (mm)	eF (mm)	Time (s)
1	9	0.0142	0.0340	154
2	5	0.0175	0.0839	47
3	5	0.0169	0.2951	47
4	5	0.0097	0.2611	47
5	8	0.0103	0.1113	109
6	5	0.0173	0.6262	47
7	6	0.0127	0.5287	59
8	10	0.0166	0.5513	217
9	5	0.0089	0.2024	50
10	5	0.0141	0.0443	48
11	8	0.0148	0.6349	101
12	5	0.0144	0.2966	45
13	5	0.0164	0.1633	43
14	5	0.0170	0.0750	43

15	11	0.0097	0.2422	272
16	9	0.0149	0.6266	140
17	9	0.0117	0.2798	142
18	5	0.0139	0.4077	43
19	9	0.0094	0.3612	143
20	5	0.0169	0.6572	43
21	5	0.0151	0.4126	43
22	5	0.0166	0.4090	43
23	6	0.0158	0.1994	54
24	7	0.0096	0.3699	83
25	8	0.0102	0.1749	100
Average		0.0138	0.3219	86

Table 5. *Range, Markers error (eM), Focus error (eF) and calculus time for 25 cases evaluated with an increment of 0.1 mm.*

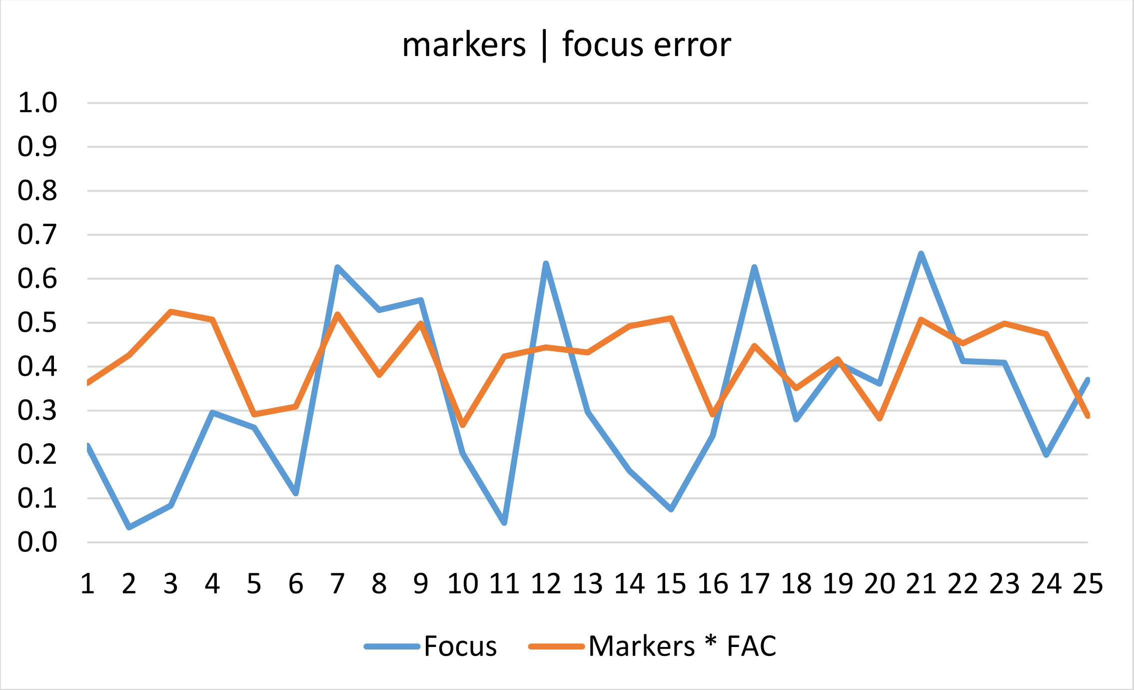

Figure 44 *Focus error (blue) and Markers error*30 (orange), in mm, for 25 cases evaluated with an increment of 0.1 mm.*

Test results for an increment value in the precise calculus of 0.09 mm

Case	Range (mm)	eM (mm)	eF (mm)	Time (s)
1	9	0.0121	0.0588	211
2	5	0.0148	0.5060	52
3	5	0.0086	0.2192	52
4	5	0.0073	0.2142	51
5	8	0.0118	0.1446	140
6	5	0.0122	0.3026	50
7	6	0.0084	0.1436	90
8	10	0.0117	0.3093	309
9	5	0.0079	0.0274	53
10	5	0.0097	0.2395	55
11	8	0.0103	0.4521	153
12	5	0.0160	0.0597	52
13	5	0.0108	0.3576	53
14	5	0.0131	0.2914	54
15	11	0.0146	0.0924	433
16	9	0.0137	0.5050	214
17	9	0.0098	0.4000	208
18	5	0.0090	0.1912	52
19	9	0.0113	0.3730	213
20	5	0.0144	0.0492	53
21	5	0.0050	0.1872	53
22	5	0.0168	0.4570	68
23	6	0.0103	0.3455	71
24	7	0.0160	0.4667	110
25	8	0.0053	0.1755	148
Average		0.0112	0.2627	120

Table 6. *Range, Markers error (eM), Focus error (eF) and calculus time for 25 cases evaluated with an increment of 0.09 mm*

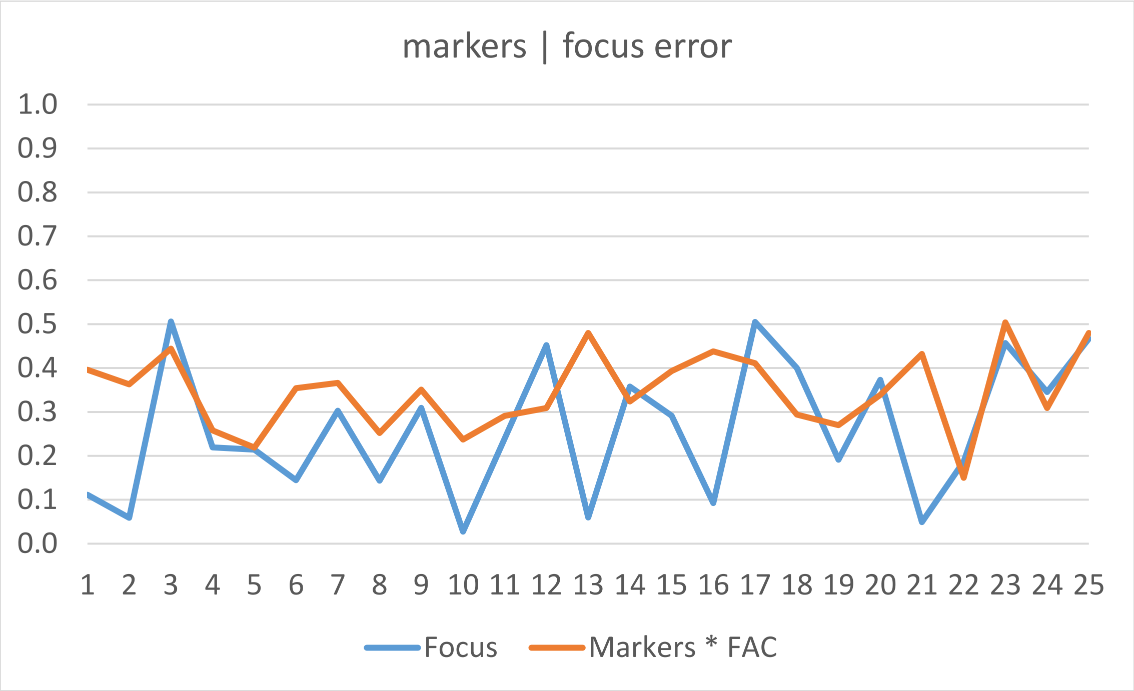

Figure 45 *Focus error (blue) and Markers error*30 (orange), in mm, for 25 cases evaluated with an increment of 0.09 mm.*

Test results for an increment value in the precise calculus of 0.08 mm

Case	Range (mm)	eM (mm)	eF (mm)	Time (s)
1	9	0.0062	0.2349	297
2	5	0.0149	0.3585	58
3	5	0.0047	0.1150	59
4	5	0.0049	0.0269	59
5	8	0.0073	0.2737	199
6	5	0.0107	0.3421	58
7	6	0.0131	0.0365	87
8	10	0.0093	0.2842	456
9	5	0.0098	0.4021	63
10	5	0.0097	0.4590	63
11	8	0.0105	0.2759	204
12	5	0.0139	0.3947	61
13	5	0.0075	0.2254	63
14	5	0.0122	0.2813	61
15	11	0.0093	0.2221	637

16	9	0.0120	0.3812	315
17	9	0.0068	0.0147	321
18	5	0.0099	0.4598	61
19	9	0.0087	0.2583	315
20	5	0.0141	0.2568	63
21	5	0.0126	0.3824	62
22	5	0.0142	0.4232	61
23	6	0.0139	0.3986	93
24	7	0.0147	0.0956	135
25	8	0.0077	0.1968	208
Average		0.0103	0.2720	162

Table 7. *Range, Markers error (eM), Focus error (eF) and calculus time for 25 cases evaluated with an increment of 0.08 mm.*

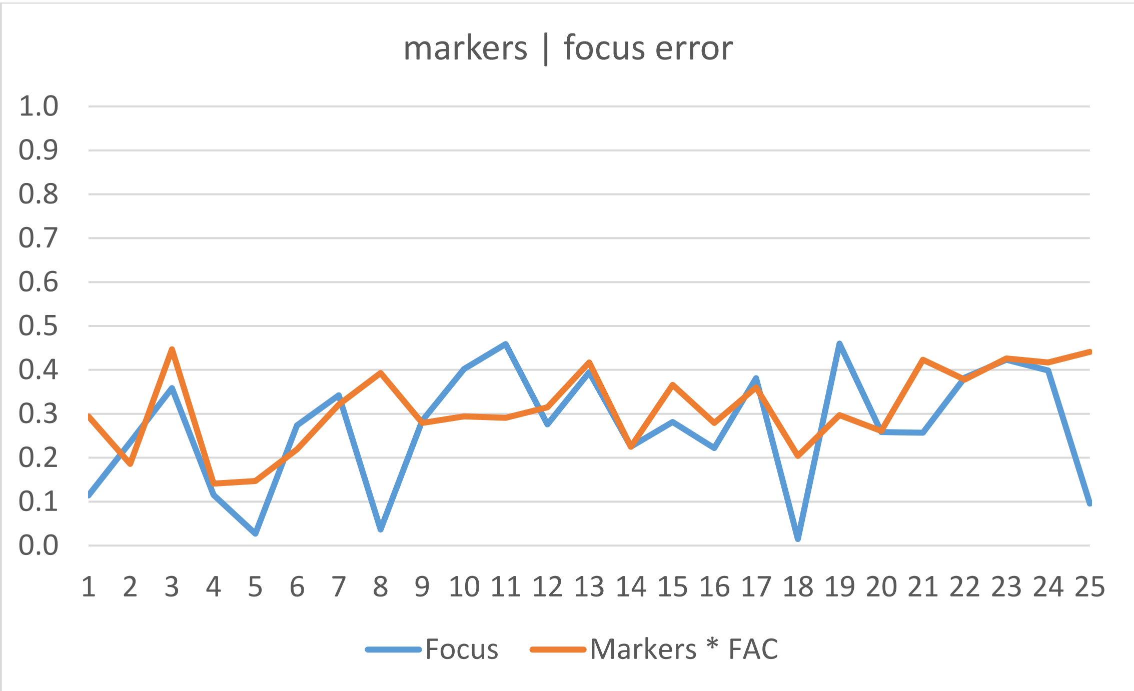

Figure 46 *Focus error (blue) and Markers error*30 (orange), in mm, for 25 cases evaluated with an increment of 0.08 mm.*

Test results for an increment value in the precise calculus of 0.07 mm

Case	Range (mm)	eM (mm)	eF (mm)	Time (s)
1	9	0.0078	0.0227	514
2	5	0.0119	0.1845	83
3	5	0.0100	0.4009	83
4	5	0.0085	0.1708	83
5	8	0.0102	0.3956	328
6	5	0.0072	0.2914	82
7	6	0.0113	0.1762	128
8	10	0.0107	0.4163	751
9	5	0.0081	0.2524	83
10	5	0.0095	0.3777	80
11	8	0.0107	0.0266	360
12	5	0.0093	0.1131	83
13	5	0.0044	0.1624	79
14	5	0.0049	0.1173	80
15	11	0.0061	0.0518	1129
16	9	0.0094	0.1987	501
17	9	0.0119	0.3945	494
18	5	0.0112	0.3721	75
19	9	0.0092	0.2042	488
20	5	0.0121	0.0704	76
21	5	0.0093	0.2680	77
22	5	0.0079	0.0285	77
23	6	0.0065	0.2622	122
24	7	0.0078	0.3111	193
25	8	0.0068	0.2669	342
Average		0.0089	0.2215	256

Table 8.. *Range, Markers error (eM), Focus error (eF) and calculus time for 25 cases evaluated with an increment of 0.07 mm.*

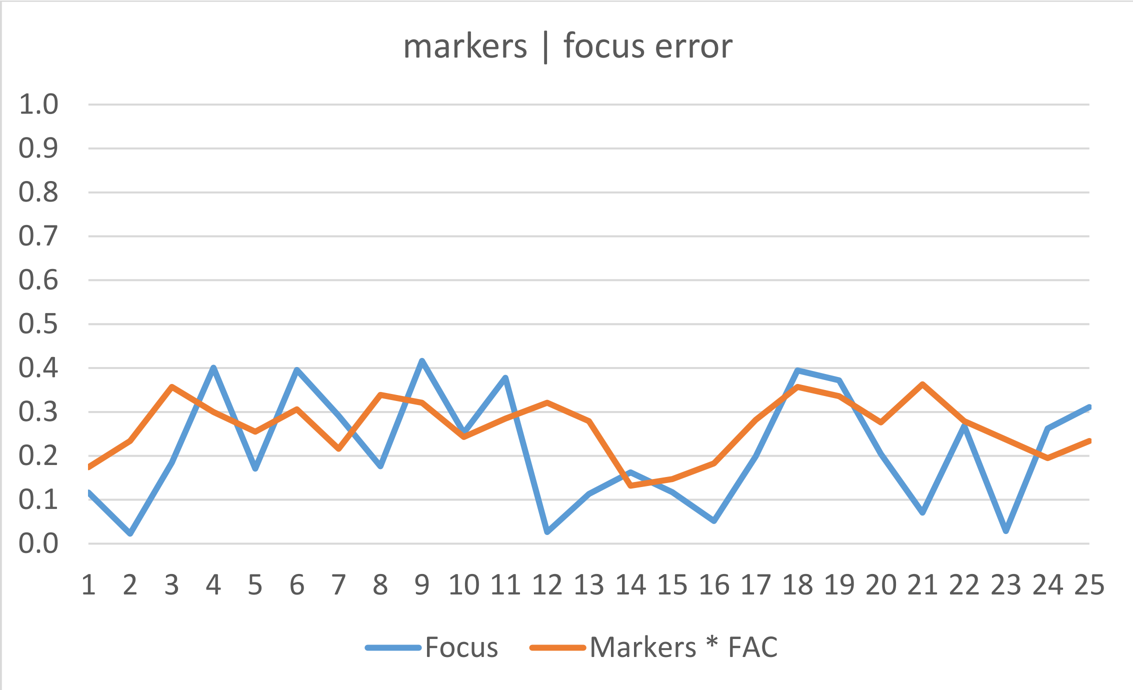

Figure 47 *Focus error (blue) and Markers error*30 (orange), in mm, for 25 cases evaluated with an increment of 0.07 mm.*

Test results for an increment value in the precise calculus of 0.06 mm

Case	Range (mm)	eM (mm)	eF (mm)	Time (s)
1	9	0.0024	0.0464	867
2	5	0.0100	0.2535	112
3	5	0.0031	0.0538	111
4	5	0.0107	0.2424	112
5	8	0.0066	0.2493	594
6	5	0.0084	0.3633	115
7	6	0.0089	0.2055	202
8	10	0.0115	0.0688	1346
9	5	0.0072	0.0829	112
10	5	0.0087	0.1799	111
11	8	0.0086	0.3353	599
12	5	0.0085	0.1151	115
13	5	0.0060	0.0256	114
14	5	0.0082	0.0511	137
15	11	0.0114	0.0505	2030
16	9	0.0042	0.1439	972
17	9	0.0074	0.1622	980

18	5	0.0083	0.1479	117
19	9	0.0062	0.2648	881
20	5	0.0063	0.2122	112
21	5	0.0071	0.2365	112
22	5	0.0046	0.0621	113
23	6	0.0078	0.2924	208
24	7	0.0068	0.2346	334
25	8	0.0093	0.1869	543
Average		0.0075	0.1707	442

Table 9. *Range, Markers error (eM), Focus error (eF) and calculus time for 25 cases evaluated with an increment of 0.06 mm.*

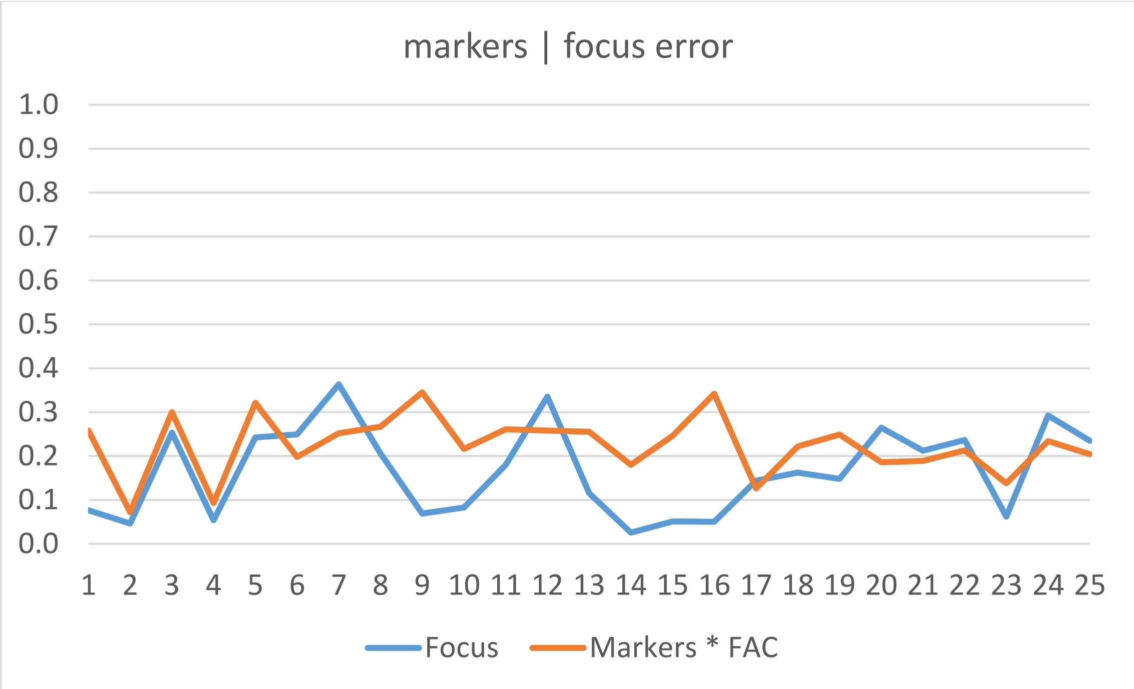

Figure 48 *Focus error (blue) and Markers error*30 (orange), in mm, for 25 cases evaluated with an increment of 0.06 mm.*

Test results for an increment value in the precise calculus of 0.05 mm

Case	Range (mm)	eM (mm)	eF (mm)	Time (s)
1	9	0.0081	0.2680	1745
2	5	0.0065	0.1842	198
3	5	0.0064	0.2878	198
4	5	0.0073	0.0951	196
5	8	0.0063	0.2594	1086
6	5	0.0072	0.2734	198
7	6	0.0031	0.0286	387
8	10	0.0079	0.1609	2694
9	5	0.0089	0.2024	207
10	5	0.0076	0.2263	201
11	8	0.0051	0.0794	1125
12	5	0.0053	0.1901	217
13	5	0.0062	0.2608	214
14	5	0.0055	0.0564	217
15	11	0.0079	0.1934	4076
16	9	0.0039	0.1288	1862
17	9	0.0084	0.0767	2012
18	5	0.0071	0.1046	208
19	9	0.0078	0.2949	1715
20	5	0.0071	0.2035	240
21	5	0.0041	0.0550	193
22	5	0.0082	0.2036	194
23	6	0.0053	0.0170	363
24	7	0.0062	0.1712	642
25	8	0.0015	0.0252	1152
Average		0.0064	0.1619	862

Table 10. *Range, Markers error (eM), Focus error (eF) and calculus time for 25 cases evaluated with an increment of 0.05 mm.*

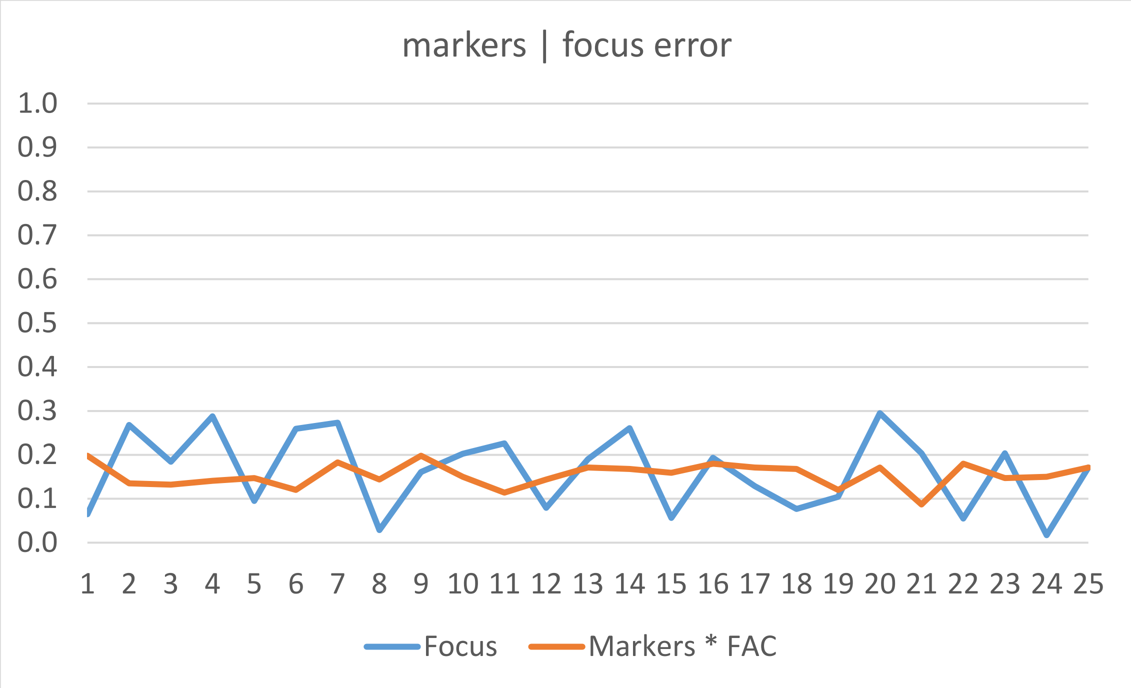

Figure 49 *Focus error (blue) and Markers error*30 (orange), in mm, for 25 cases evaluated with an increment of 0.5 mm.*

Test results for an increment value in the precise calculus of 0.04 mm

Case	Range (mm)	eM (mm)	eF (mm)	Time (s)
1	9	0.0045	0.0763	4212
2	5	0.0044	0.1708	446
3	5	0.0047	0.1150	449
4	5	0.0049	0.0269	468
5	8	0.0040	0.0750	2768
6	5	0.0061	0.0620	477
7	6	0.0048	0.1989	855
8	10	0.0066	0.1651	6133
9	5	0.0050	0.2019	414
10	5	0.0038	0.1058	474
11	8	0.0048	0.1128	2875
12	5	0.0057	0.1121	431
13	5	0.0056	0.2203	433
14	5	0.0053	0.0162	459
15	11	0.0060	0.1812	9773
16	9	0.0057	0.0606	4391
17	9	0.0056	0.1234	4844
18	5	0.0040	0.0268	506

19	9	0.0057	0.0662	4855
20	5	0.0029	0.0320	508
21	5	0.0060	0.1874	499
22	5	0.0049	0.0617	493
23	6	0.0050	0.2107	983
24	7	0.0057	0.2507	1775
25	8	0.0061	0.0873	2828
Average		0.0051	0.1179	2094

***Table 11**. Range, Markers error (eM), Focus error (eF) and calculus time for 25 cases studied with an increment of 0.04 mm.*

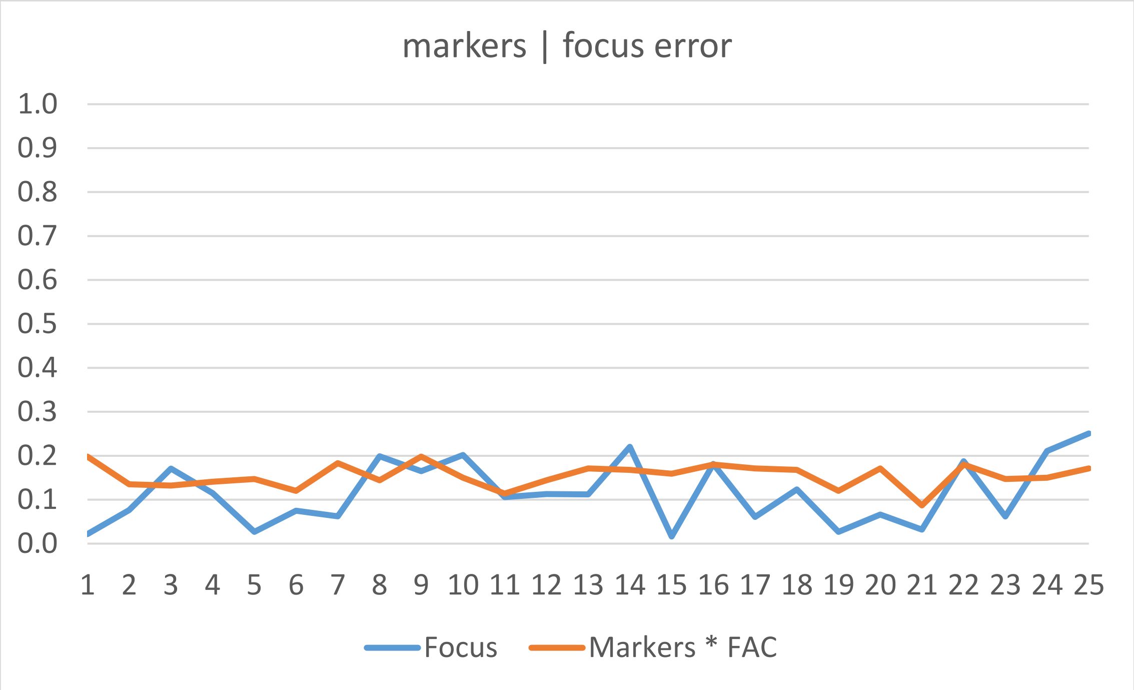

***Figure 50.** Focus error (blue) and Markers error*30 (orange), in mm, for 25 cases evaluated with an increment of 0.04 mm.*

Test results for an increment value in the precise calculus of 0.03 mm

Case	Range (mm)	eM (mm)	eF (mm)	Time (s)
1	9	0.0024	0.0464	15985
2	5	0.0021	0.0199	1371
3	5	0.0031	0.0538	1376
4	5	0.0028	0.0601	1390
5	8	0.0050	0.1442	8753
6	5	0.0007	0.0023	1317
7	6	0.0040	0.0674	2655
8	10	0.0035	0.0890	25193
9	5	0.0039	0.1013	1305
10	5	0.0035	0.0864	1344
11	8	0.0040	0.0327	8403
12	5	0.0039	0.0133	1318
13	5	0.0043	0.0993	1299
14	5	0.0029	0.1061	1320
15	11	0.0032	0.0810	30582
16	9	0.0042	0.1439	14071
17	9	0.0027	0.0831	13275
18	5	0.0029	0.0541	1279
19	9	0.0029	0.1283	13994
20	5	0.0050	0.1229	1269
21	5	0.0037	0.1468	1283
22	5	0.0035	0.0908	1369
23	6	0.0042	0.0719	2923
24	7	0.0027	0.0701	5226
25	8	0.0045	0.0571	8750
Average		0.0034	0.0789	6682

Table 12 *Range, Markers error (eM), Focus error (eF) and calculus time for 25 cases studied with an increment of 0.03 mm.*

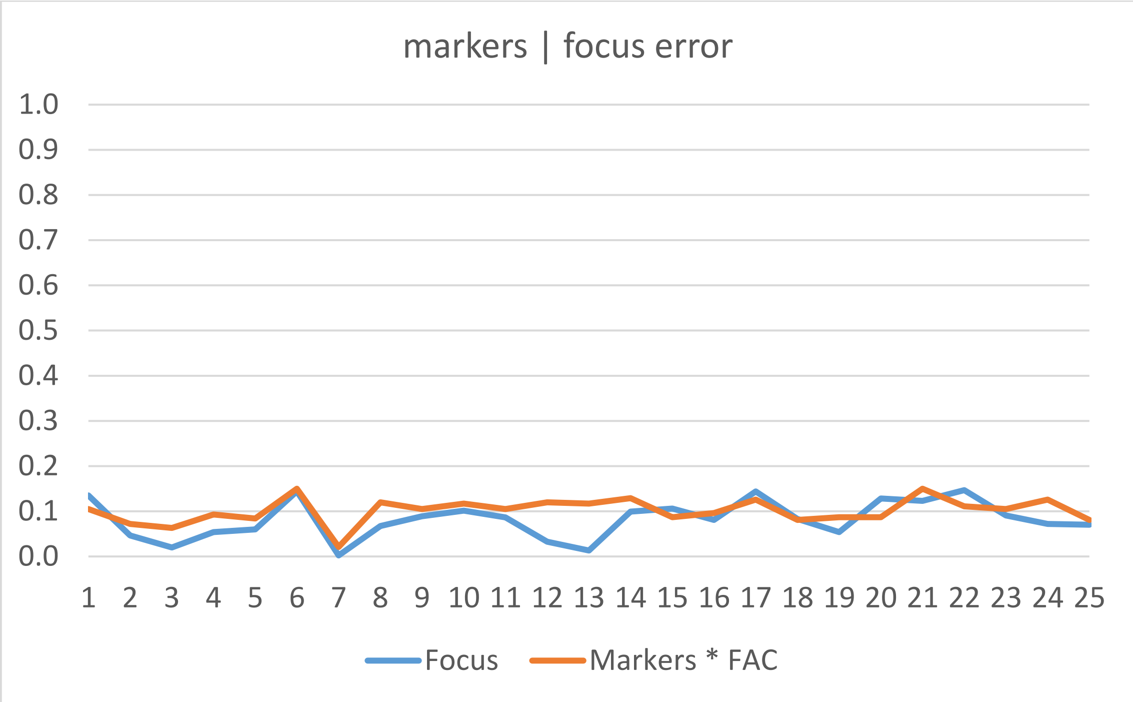

Figure 51 *Focus error (blue) and Markers error*30 (orange), in mm, for 25 cases evaluated with an increment of 0.03 mm.*

5.4.1.Summary

The averaged results from the previous tests are gathered in the following tables and in Figure 52. The exponential relation between the decreasing increment value and the calculus time can be observed. At the same time, the increase of precision achieved is also noticeable.

	0.1	0.09	0.08	0.07
Focus error (mm)	0.3180	0.2569	0.2659	0.2159
S.D (mm)	0.1938	0.1511	0.1344	0.1291
Markers error (mm)	0.0137	0.0113	0.0103	0.0088
Av. Time (s)	85	117	158	250
Av Time (min)	1.4	2.0	2.6	4.2

	0.06	0.05	0.04	0.03
Focus error (mm)	0.1671	0.1581	0.1142	0.0811
S.D (mm)	0.0979	0.0895	0.0705	0.0408
Markers error (mm)	0.0076	0.0063	0.0052	0.0034
Av. Time (s)	429	837	2030	6478
Av Time (min)	7.2	13.9	33.8	108.0

*Table 13**.** Average values of Focus error, SD of the Focus error, markers error and calculus Time for increment values from 0.1 mm to 0.03 mm.*

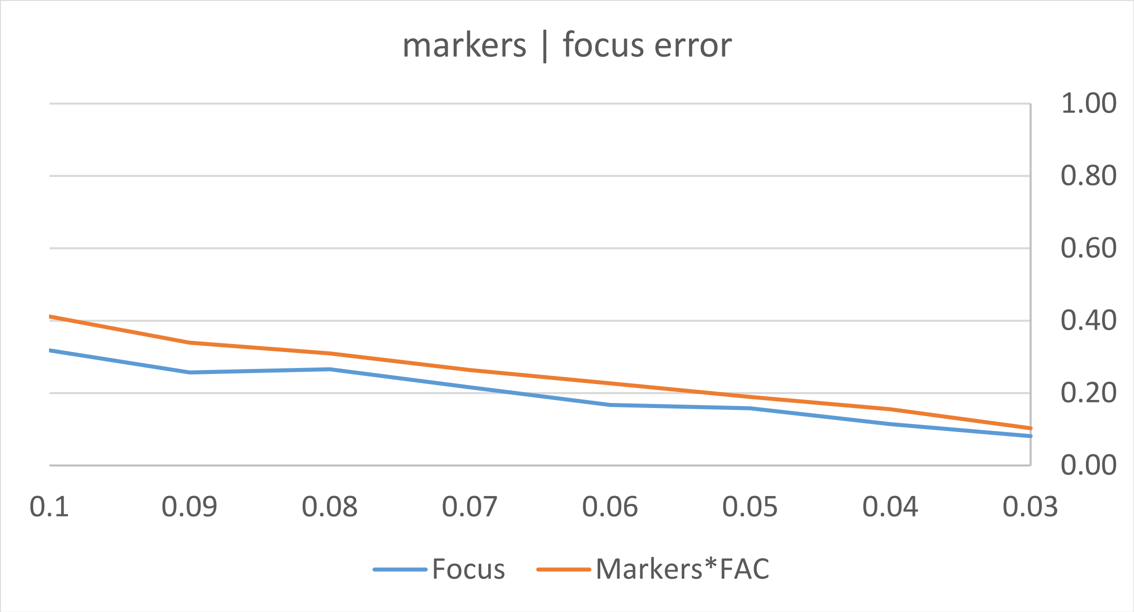

Figure 52. *Evolution of Focus error (blue) and Markers error*30 (orange), in mm, for increment values ranging from 0.1 mm to 0.03 mm.*

5.4.2.Analysis

Precision. From the previous data, it can be observed how smaller values of increment permit a higher accuracy in the determination of the position of the focus. As in previous sections of the project, the convergence between *markers error* and *focus error* continues present.

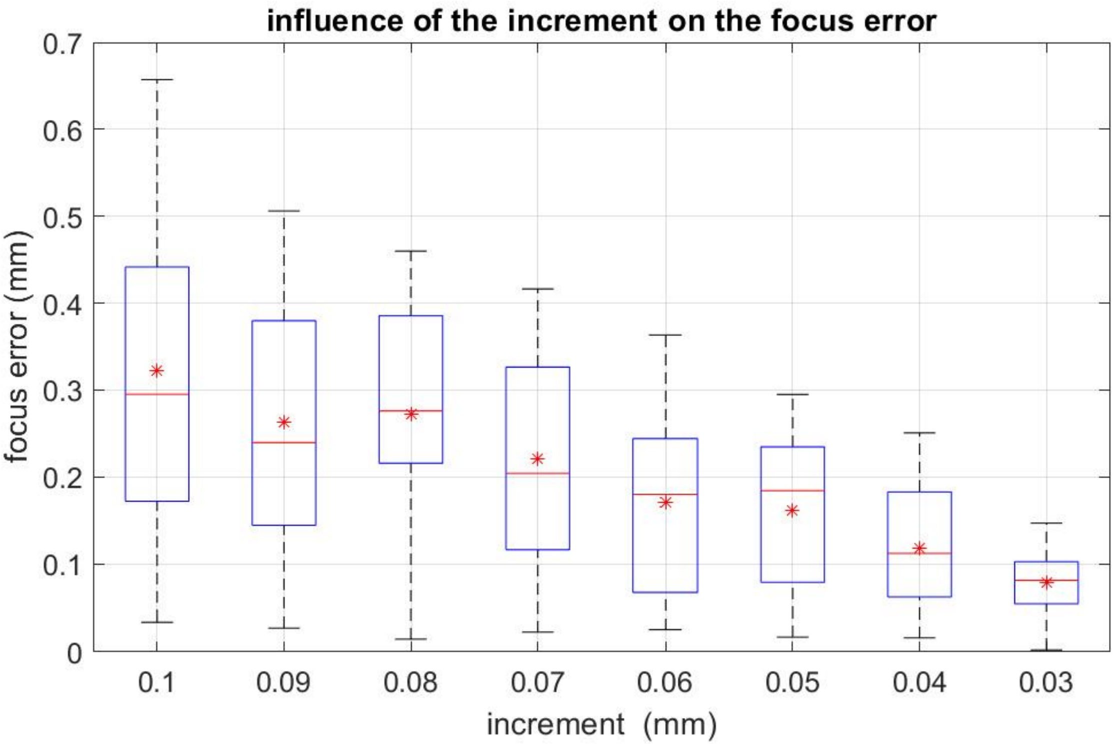

Figure 53. *Boxplot of the Focus error for increment values ranging from 0.1 mm to 0.03 mm. Red asterisks indicate the mean value for each increment.*

The presented boxplot gathers the *focus error* for the different increment values. In this graph, the 25, 50 and 75 percentiles are shown. In addition, for this special case, the mean values have been indicated with red asterisks. A decreasing tendency in the error as well as in the SD is shown accordingly with the increment value, evidencing the increase of precision. For an increment of 0.1 mm, a mean *focus error* of 0.3180 mm and a SD of 0.1938 mm are achieved. Together with an average calculus time of 85 s it is possible to state that these results are more than acceptable for most of the potential applications. If the precision wants to be maximized, an increment of 0.03 mm has shown to obtain a mean *Focus error* of 0.0811 mm and a SD of 0.0408 mm, however, rising the calculus time up to an average of 5523 s (65 times more).

Considering that the methodology has been tested in a theoretical study, greater errors should be expected if applied in real scenarios. Nevertheless, such a high precision must be remarked as an important achievement if compared with the real size of the focal spot in the X-ray machines, which ranges between 0.3 mm in mammographs up to 1.2 mm in general radiographs, making the obtained error negligible. In addition, other studied techniques, as the previously stated RSA, experience errors (in real scenarios) ranging from 0.70 to 6.66 mm (Valstar, Digital Roentgen Stereophotogrammetry: Development, Validation, and Clinical Application, 2001) significantly higher than those obtained by this methodology. Furthermore, the low standard deviation associated with the increment value of 0.03 mm, 0.04 mm support the reliability of the methodology and show that the errors are tightly bounded.

Time. When assessing the time spent for each of the cases, a high variability can be observed (see Figure 55). It is relevant to point out that the time for each case depends on the performance of the application method, more specifically on the *range* set by the phase of *minimal opening* (this explanation was previously used with reference to the validation of the application method). Large ranges are associated with long calculus times whereas small ranges can be quickly explored by the precise calculus stage.

As an interesting feature, the same cases explored with an increment of 0.04 mm and 0.03 mm show the same time profile. This is because the increment (0.04 mm and 0.03 mm) defines the operation of the precise calculus, last stage of the application method; meanwhile, the range of exploration, set by the minimal opening stage, is unaltered regardless of the increment and varies only between the different cases. However, although the shape is analogous, the order of magnitude for the time is significantly lower for the 0.04 mm.

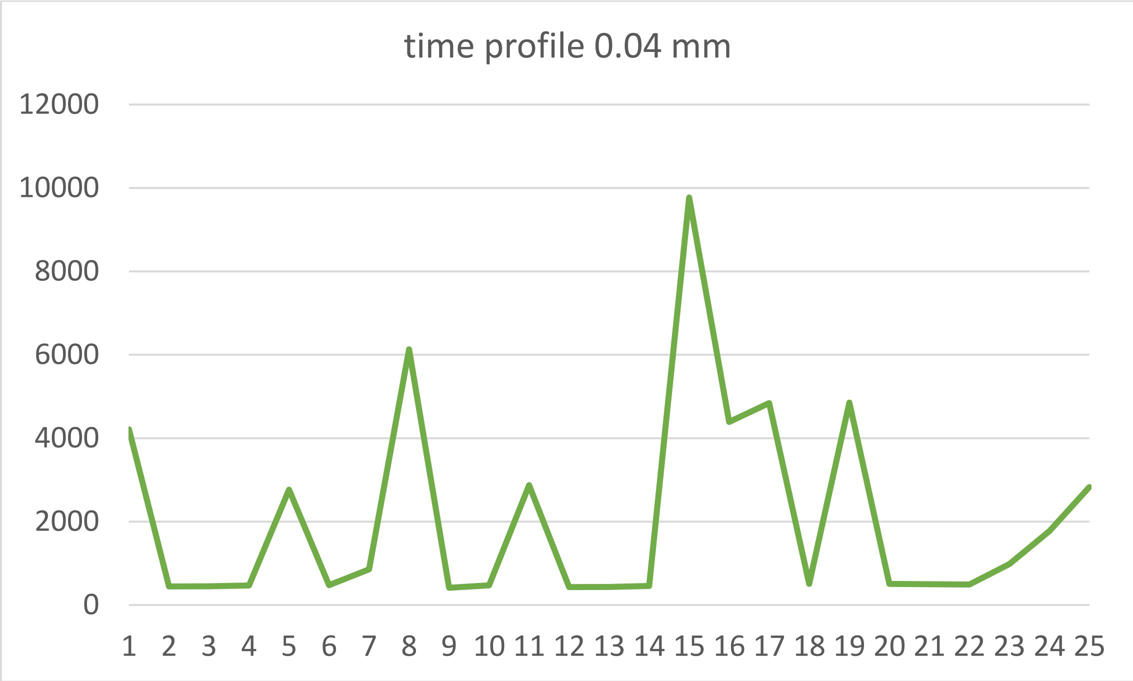

Figure 54. *Calculus time, in seconds, for 25 cases with an increment of 0.04 mm.*

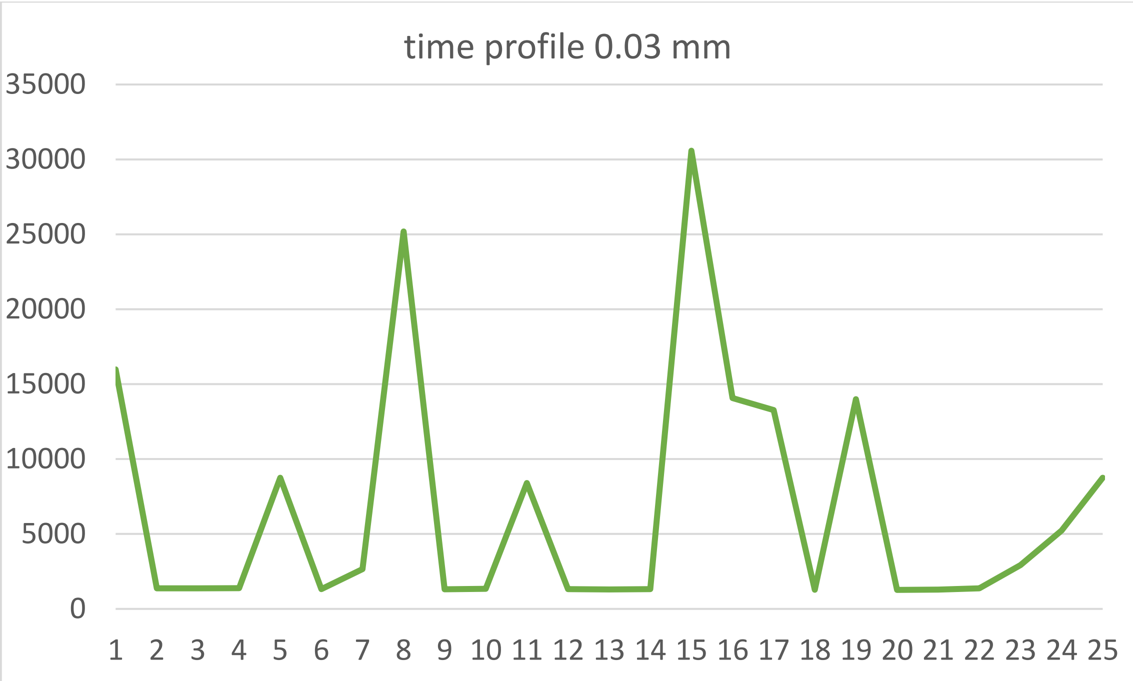

Figure 55. *Calculus time, in seconds, for 25 cases with an increment of 0.03 mm.*

6. Localizer

In previous chapters, the algorithmic methodology developed in this research project was exposed, validated and assessed. These studies where performed with a so-called *reference localizer* (Figure 40) due to its neutral properties. The influence that the design of localizer and its different characteristics have in the performance of the ApLoFX is studied in this chapter.

6.1. Reference Localizer

As it was previously mentioned. A reference localizer for the study of the several variables influencing the methodology has been used. In chapter 5, the convergence of the LoFX for different localizer configurations was mentioned. This circumstance was noticed in the earlier stages of development of the methodology, where a variety of sizes and shapes for the localizer were used, with no significant influence on the results obtained. The study of the influence that the localizer could have in the overall performance of the method creates the necessity of initially isolating its effect on the methodology, setting a "reference point" for both, the analysis of other variables and the study of the parameters that characterize the localizer itself. This motivates the definition of a *reference localizer* with "neutral" properties to serve a base for future modifications. The selection of its characteristics is based on the following criteria:

Cubic form. In the search for simplicity, the cubic form has a major advantage over other shapes since it can be defined with a single parameter: the dimension of its side. From this point, any variation on its dimensions can be applied with the modification of this parameter.

Size. 200x200x200 mm. In chapter 6, different variations are applied to the size and shape of the localizer. The 200 mm cubic form, selected with half the size of a standard radiograph, can be easily moved above the projective plane without exiting the limits of the radiograph.

Octant based. A cube can be easily divided in octants. Selecting points in the intersection between the faces of the cube and three axial planes that define the octants, it is possible to locate up to 9 markers without any overlapping in its top projection. The coordinates of the reference localizer are indicated in the Table 14.

Geometrical Design

	X	Y	Z
M1	100	0	0
M2	-100	0	0
M3	0	0	100
M4	0	100	200
M5	0	-100	200

Table 14. *Markers' coordinates for the 5 markers reference localizer.*

6.2. Geometrical Restrictions

In this chapter, the criteria that have to be considered in the design of a valid localizer are explained and proved experimentally. Eventually, only two restrictions limit the free design of the localizer.

6.2.1.Minimum Number of Markers

The first consideration that must be evaluated when exploring the influence that different parameters of the localizer have on the way in which the application method, ApLoFX behaves, is the existence of any restrictions that prevents reaching an appropriate solution for the localization of the focus. During the development of the software, different localizers, mainly with 4 and 5 markers were used without presenting any issues. According to (García Ruesgas, 2014), a minimum number of 4 markers are required for the design of a functional calibration object. This statement motivated the study of localizers with a lower number of markers. In addition, several studies mention the fact that the markers cannot be coplanar, being also 4 the minimum number of points that can meet with this constraint. The results of tests for a localizer with 3 Markers are displayed in Figure 56**,** showing that this construction cannot serve the methodology for its adequate operation. In order to better comprehend the spatial distribution of the markers, Table 15 shows their coordinates.

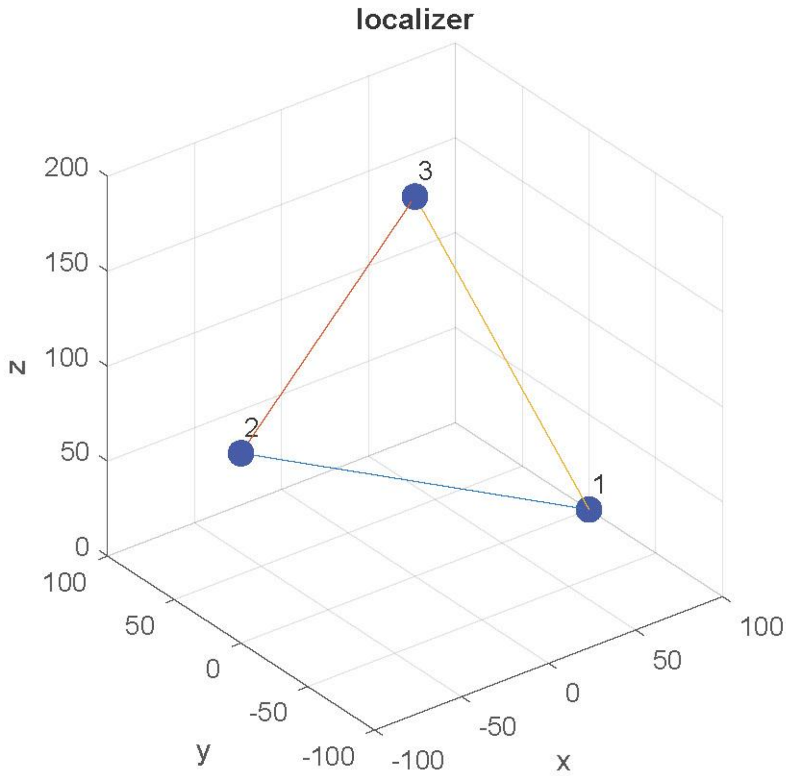

Figure 56. *3 markers localizer used to explore restrictions concerning the number of markers.*

Geometrical Design			
	X	Y	Z
M1	100	0	0
M2	-100	0	100
M3	0	0	200

Table 15 *Markers' coordinates of the 3 markers localizer*

The tests are performed following the same procedure stated in section 6.3, this means: increment value of 0.05 mm, positioning given by the values indicated in Table 1, and same variables recorded. The results are gathered in Table 16, where the mean *focus error* for this 3 markers localizer, 22.4542 mm, as well as the high Standard Deviation, 16.3533 mm, indicate that its use is not possible if a precise determination of the position of the focus wants to be obtained. In comparison with the results presented in 6.3 and in 6.5, this error considerably exceeds the values obtained for a geometry of similar characteristics. This evidences the necessity of incorporating a minimum of 4 markers in order to design a proper localizer.

Case	Range (mm)	eM (mm)	eF (mm)	Time (s)
1	5	0.0073	15.4524	128
2	6	0.0140	28.9819	247
3	8	0.0092	19.5687	772
4	9	0.0193	42.2339	1122
5	7	0.0069	15.0563	455
6	8	0.0255	58.7035	705
7	5	0.0050	10.5196	133
8	5	0.0040	8.3079	136
9	7	0.0038	7.4652	428
10	6	0.0082	17.0440	235
11	6	0.0034	4.7862	247
12	8	0.0058	10.4858	713
13	5	0.0193	42.0053	127
14	5	0.0035	6.9819	127
15	7	0.0013	0.4287	462
16	7	0.0148	31.2077	430
17	8	0.0013	0.3103	722
18	5	0.0034	6.4061	132
19	8	0.0168	36.8775	1153
20	8	0.0127	28.4746	714
21	5	0.0152	31.3303	134

22	8	0.0145	32.0650	722
23	7	0.0066	12.7203	426
24	5	0.0172	38.8986	127
25	8	0.0242	55.0438	711
Average		0.0105	22.4542	188.49

Table 16. *Range, Markers error (eM), Focus error (eF) and calculus time for 25 cases studied with a localizer of 3 markers.*

6.2.2. Planarity

Another condition imposed on the characteristics of the calibration objects is the fact that the markers have to be placed in different geometrical planes, as mentioned in (García Ruesgas, 2014) and (Yuan, Ryd, & Tanner, 2002). Previously, a localizer with 3 markers was studied, concluding that a minimum number of 4 markers is required for a localizer to allow the methodology to find an adequate solution. Although the 3 markers localizer defines a single plane, the disposition employed was such that the defined one was not parallel to the projective plane. Apart from the required specifications indicated in the mentioned bibliography, the trials carried out about the influence of the size of the localizer (see 6.3) and, specifically, the results observed in section 6.4, motivated a rigorous study on the effects that planar localizer, parallel to the projection plane, could have in the behaviour of the ApLoFX.

Continuing with the systematic approach to the study of the effect of different variables, the same parameters are used: increment value of 0.05 mm and positioning given in Table 1 as well as the same kind of data recorded, with one particularity, the addition of an extra variable: the numbers of solutions found after the application of the method. In addition, the planar localizer design is based in the reference localizer (Figure 40), modifying the z coordinate of all the markers and setting it to 0. In early stages of the project, due to a different implementation of the "error criteria" that determines the position of the focus, the application of the methodology showed the existence of several solutions. For this reason, an extra feature was implemented in the software in order to obtain information on the number of solutions found. A refinement of the methodology conducted to the fact that no more multiple solutions were found during the tests, however, this feature of the software was kept.

With the study of a planar localizer, the number of solutions found by the ApLoFX showed to be, as it is registered in the Table 17, multiple again. The explanation of this feature must be found in the nature of the central projection and the Thales Theorem, which explains how multiple combinations of localizer and focus positions may generate the same projection in the radiography.

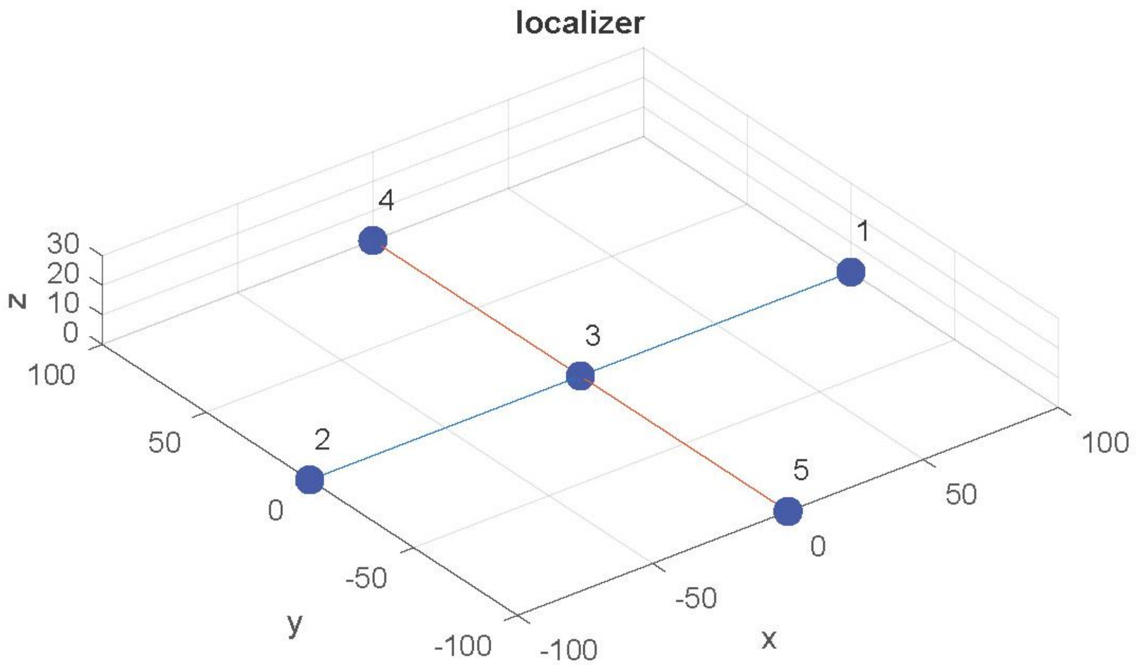

Figure 57. *5 markers planar localizer used for the study of the geometrical restrictions*

Case	Range (mm)	eM (mm)	eF (mm)	Time (s)	n. solutions
1	5	0.0001	470.8046	801.00	81
2	5	0.0001	398.6903	815	72
3	5	0.0000	294.6133	797	1,211
4	5	0.0000	405.5349	808	214
5	5	0.0000	284.2792	743	285
6	5	0.0000	408.2595	235	176
7	5	0.0001	269.8820	264	314
8	5	0.0000	465.6941	269	879
9	8	0.0000	618.3089	1528	356
10	7	0.0000	471.3267	694	488
11	5	0.0000	313.7451	204	3,013
12	5	0.0003	96.1355	319	118
13	5	0.0000	530.1485	309	652
14	5	0.0002	350.9198	307	103
15	9	0.0000	476.4117	3063	1,852
16	5	0.0001	389.7666	339	1,682
17	12	0.0000	363.7854	8536	158
18	9	0.0000	173.5345	1782	223
19	10	0.0000	344.3562	4238	650
20	5	0.0003	340.3997	366	1,495

21	5	0.0001	199.3713	389	282
22	5	0.0000	256.1683	339	609
23	5	0.0000	410.5052	474	378
24	5	0.0000	288.9393	469	455
25	5	0.0000	276.8730	329	147
Average		0.0001	355.9381	473	636

Table 17. *Range, Markers error (eM), Focus error (eF) calculus time and number of solutions for 25 cases studied with a flat localizer.*

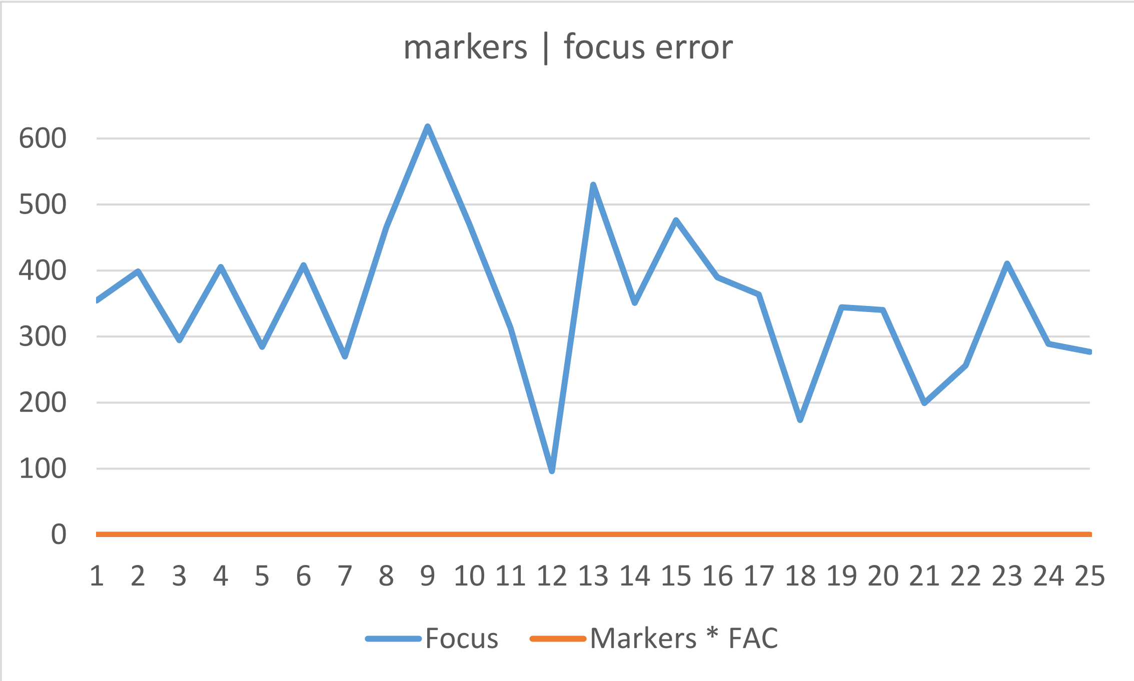

Figure 58. *Focus error (blue) and Markers error*30 (orange) for 25 cases evaluated with a flat localizer.*

An interesting characteristic that appears for this precise localizer is the reduction of the *markers error* by several orders of magnitude. However, this is not correlated with a more precise calculus as it can be seen from the average *focus error*. The existence of several solutions is a sufficient argument to discard a planar localizer as a possible configuration for the design of localizers. In addition, the high average *focus error* of 351.1520 mm, together with a respectively high Standard Deviation of 114.4151 mm, support this statement. It can be, therefore, concluded that a planar localizer does not allow the ApLoFX to accurately localize the focus of X-ray. In addition, the multiplicity of solutions indicate that it is not valid for any methodology.

6.3. Influence of the size

Currently commercialized calibration objects have usually large dimensions and are difficult to operate, (Muharemovic, Gosvig, Troelsen, Thomsen, & Kallemose, 2018). The previously introduced PDS-2 calibration phantom of Siemens presents a cylindrical shape with an outer radius of 72 mm and 206 mm of height (Hoppe, Noo, Dennerlein, & Lauritsch, 2007) and the calibration box suggested in (García Ruesgas, 2014) has a side of 258 mm. One of the objectives of this project consisted in the development of a methodology independent on the characteristics of the localizer. To achieve this, it is interesting to pose the inverse hypothesis. Are there some characteristics of the localizer that influence the performance of the LoFX? One of mots intuitive variables to study is the size of the object. Thanks to the design of the reference localizer, modifications on the geometry and subsequent studies have been successfully carried out. Analogously to the study of the influence of other parameters in the operation of the methodology, the interesting variable (in this case the size of the localizer) has been isolated, keeping the other working conditions stable. For this reason, these tests have been conducted using standardized conditions: RAD of 50 mm, increment of 0.05 mm for the precise calculus and a positioning given by the Table 18. Variations of the size ranging from 100 mm to 300 mm have been assessed.

Positioning			
	X	Y	Z
Localizer	100	-100	1200
Focus	0	0	1500

Table 18 *Positioning for the tests. Coordinates of the localizer are applied to the reference or 0 marker.*

Test results for the localizer 5M-100 mm

For an initial size of 100 mm, the execution of the ApLoFX in 25 different cases brings about the results shown in Table 19.

Case	Range (mm)	eM (mm)	eF (mm)	Time (s)
1	5	0.0033	0.4295	207
2	10	0.0039	0.3896	2650
3	5	0.0033	0.0610	199
4	5	0.0042	0.1385	195
5	8	0.0028	0.1355	1122
6	6	0.0034	0.0213	377
7	5	0.0025	0.0315	200
8	12	0.0024	0.0664	5397
9	8	0.0028	0.3982	1084
10	8	0.0033	0.4352	1094
11	6	0.0039	0.3130	366
12	5	0.0038	0.1741	194
13	5	0.0019	0.1011	199
14	5	0.0033	0.3601	197
15	10	0.0024	0.3350	2699
16	7	0.0022	0.1510	679

17	8	0.0045	0.2947	1144
18	8	0.0043	0.5153	1115
19	5	0.0040	0.2969	203
20	5	0.0024	0.0676	202
21	8	0.0033	0.2251	1149
22	5	0.0027	0.2155	205
23	5	0.0027	0.2422	199
24	5	0.0029	0.4016	200
25	5	0.0038	0.3956	201
Average		0.0032	0.2478	357

***Table 19**. Range, Markers error (eM), Focus error (eF) and calculus time for 25 cases studied with an increment of 0.05 mm and a localizer of size 100 mm.*

With the aim of providing more comprehensive information, the Figure 59 allows to visualize the *focus error* and the *markers error*. This last multiplied by a factor (FAC) of 30.

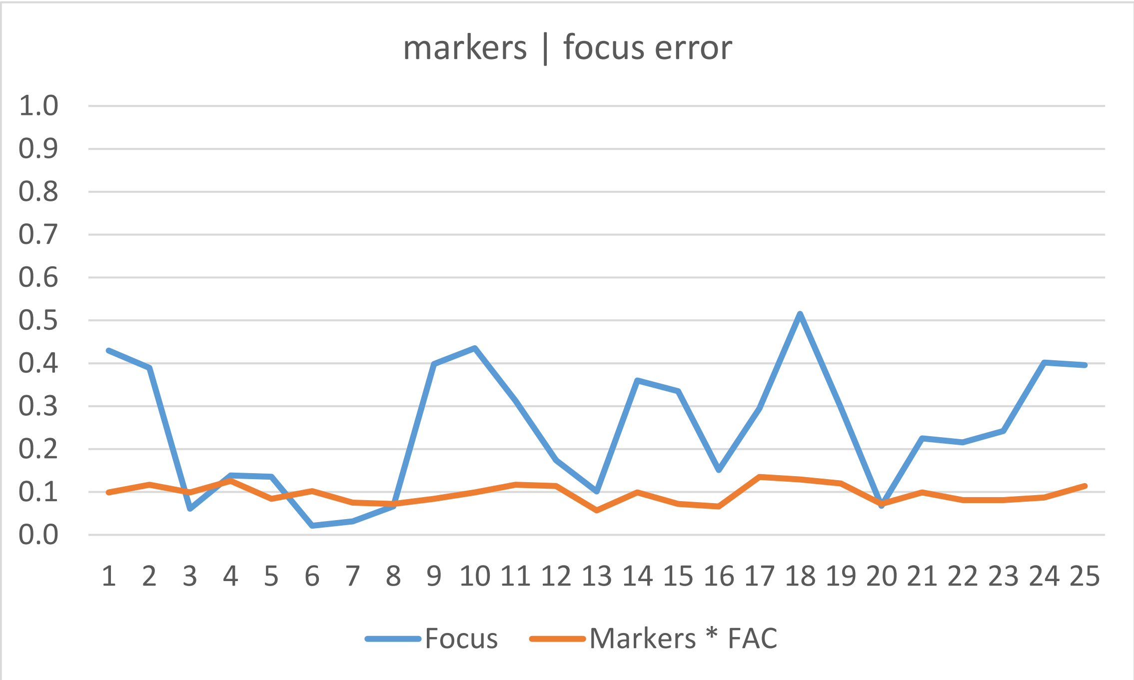

***Figure 59** Focus error (blue) and Markers error*30 (orange) for 25 cases evaluated with an increment of 0.05 mm and a localizer of size 100 mm.*

Test results for the localizer 5M-150 mm

As for the case of the localizer of 100 mm of size. The same tests are executed for an enlarged localizer of 150 mm, showing the results collected in the Table 20.

Case	Range (mm)	eM (mm)	eF (mm)	Time (s)
1	11	0.0039	0.1242	4083
2	6	0.0042	0.1895	367
3	11	0.0060	0.2626	3801
4	5	0.0097	0.3106	42
5	10	0.0082	0.3578	189
6	10	0.0063	0.4503	193
7	5	0.0080	0.3535	42
8	10	0.0166	0.5513	191
9	6	0.0046	0.0881	363
10	5	0.0041	0.3226	201
11	9	0.0065	0.2399	1773
12	5	0.0020	0.0251	218
13	5	0.0053	0.1592	207
14	5	0.0066	0.0254	207
15	9	0.0044	0.0184	1800
16	8	0.0033	0.0536	1143
17	5	0.0013	0.0958	201
18	6	0.0047	0.0626	377
19	7	0.0042	0.2688	674
20	5	0.0061	0.3168	204
21	11	0.0022	0.0386	4367
22	5	0.0071	0.3655	207
23	5	0.0027	0.2173	197
24	5	0.0067	0.2319	200
25	5	0.0025	0.0587	204
Average		0.0055	0.2075	357

***Table 20**. Range, Markers error (eM), Focus error (eF) and calculus time for 25 cases studied with an increment of 0.05 mm and a localizer of size 150 mm.*

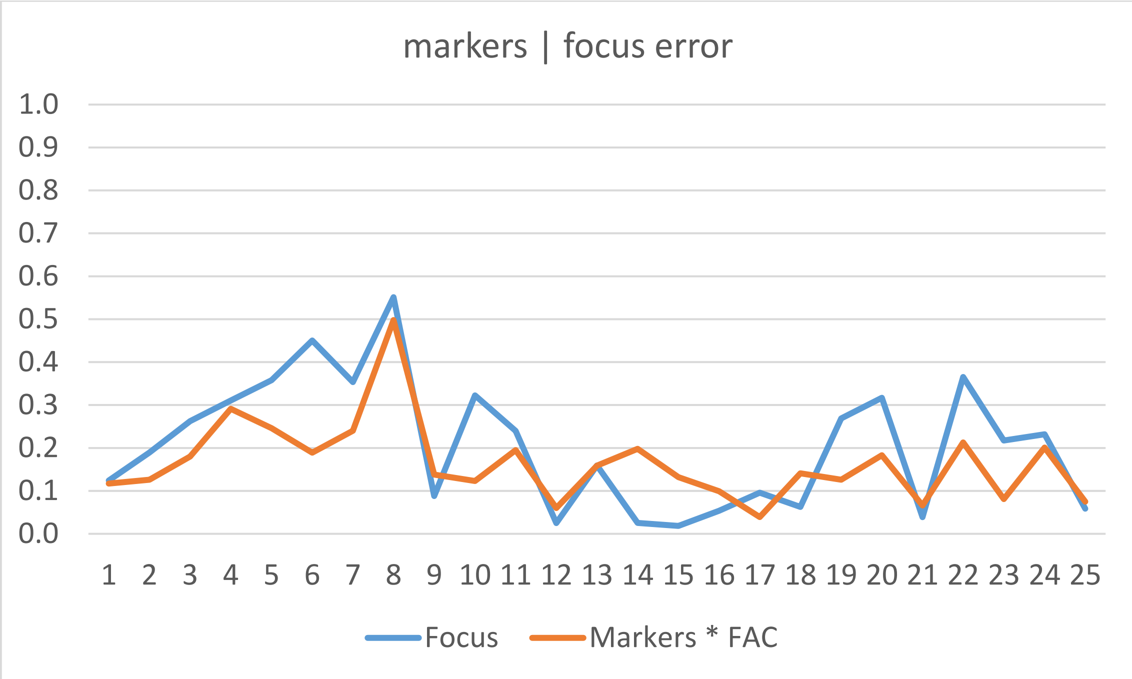

Figure 60 *Focus error (blue) and Markers error*30 (orange) for 25 cases evaluated with an increment of 0.05 mm and a localizer of size 150 mm.*

Test results for the localizer 5M-200 mm

Case	Range (mm)	eM (mm)	eF (mm)	Time (s)
1	9	0.0081	0.2680	1745
2	5	0.0065	0.1842	198
3	5	0.0064	0.2878	198
4	5	0.0073	0.0951	196
5	8	0.0063	0.2594	1086
6	5	0.0072	0.2734	198
7	6	0.0031	0.0286	387
8	10	0.0079	0.1609	2694
9	5	0.0089	0.2024	207
10	5	0.0076	0.2263	201
11	8	0.0051	0.0794	1125
12	5	0.0053	0.1901	217
13	5	0.0062	0.2608	214
14	5	0.0055	0.0564	217
15	11	0.0079	0.1934	4076
16	9	0.0039	0.1288	1862
17	9	0.0084	0.0767	2012
18	5	0.0071	0.1046	208

19	9	0.0078	0.2949	1715
20	5	0.0071	0.2035	240
21	5	0.0041	0.0550	193
22	5	0.0082	0.2036	194
23	6	0.0053	0.0170	363
24	7	0.0062	0.1712	642
25	8	0.0015	0.0252	1152
Average		0.0064	0.1619	359

Table. 21 *Range, Markers error (eM), Focus error (eF) and calculus time for 25 cases studied with an increment of 0.05 mm and a localizer of size 200 mm.*

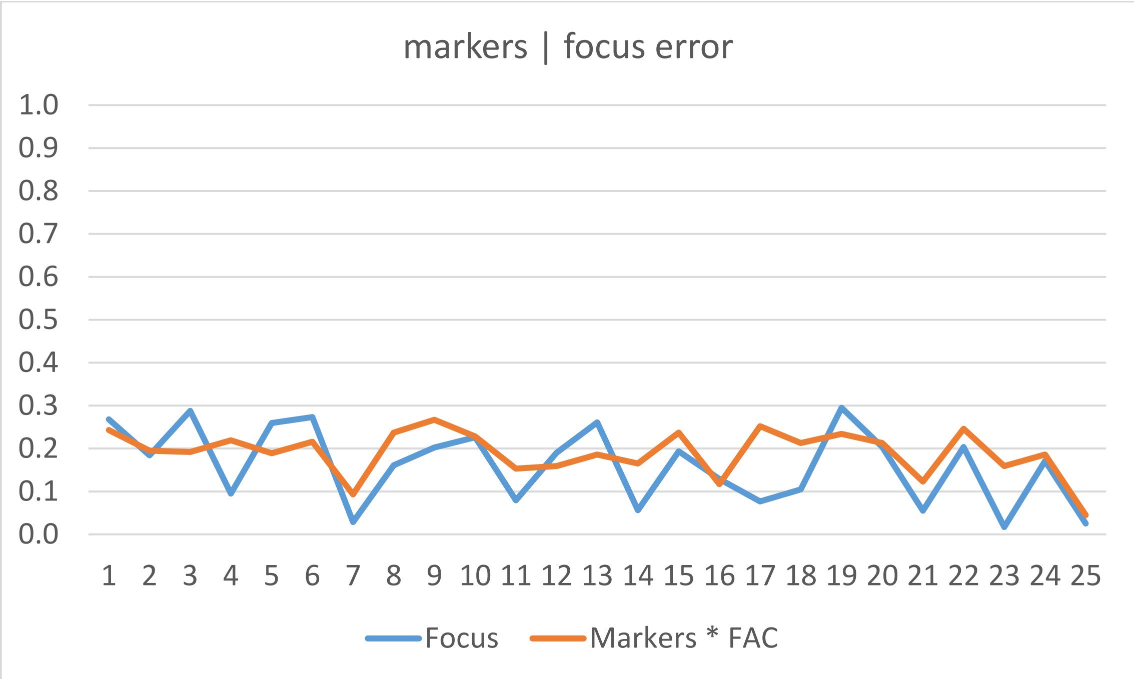

Figure 61 *Focus error (blue) and Markers error*30 (orange) for 25 cases evaluated with an increment of 0.05 mm and a localizer of size 200 mm.*

Test results for the localizer 5M-250 mm

More tests are performed with a localizer of 250 mm, showing the results collected in the Table 22.

Case	Range (mm)	eM (mm)	eF (mm)	Time (s)
1	5	0.0108	0.1588	211
2	6	0.0124	0.1313	390
3	12	0.0082	0.1684	5791
4	5	0.0037	0.0853	199
5	5	0.0054	0.0465	223
6	7	0.0092	0.2056	705
7	5	0.0043	0.1200	215
8	5	0.0106	0.2733	217
9	5	0.0031	0.0309	229
10	9	0.0114	0.2092	1912
11	5	0.0069	0.0806	196
12	7	0.0095	0.2486	676
13	5	0.0120	0.0501	196
14	7	0.0074	0.1437	655
15	5	0.0095	0.2502	197
16	5	0.0066	0.1117	196
17	5	0.0069	0.0553	205
18	5	0.0106	0.2198	197
19	9	0.0100	0.3074	1771
20	5	0.0098	0.0821	198
21	5	0.0087	0.1599	233
22	5	0.0113	0.1376	219
23	8	0.0068	0.1807	1124
24	5	0.0100	0.2797	197
25	8	0.0049	0.0513	1151
Average		0.0084	0.1515	291

***Table 22** Range, Markers error (eM), Focus error (eF) and calculus time for 25 cases studied with an increment of 0.05 mm and a localizer of size 250 mm.*

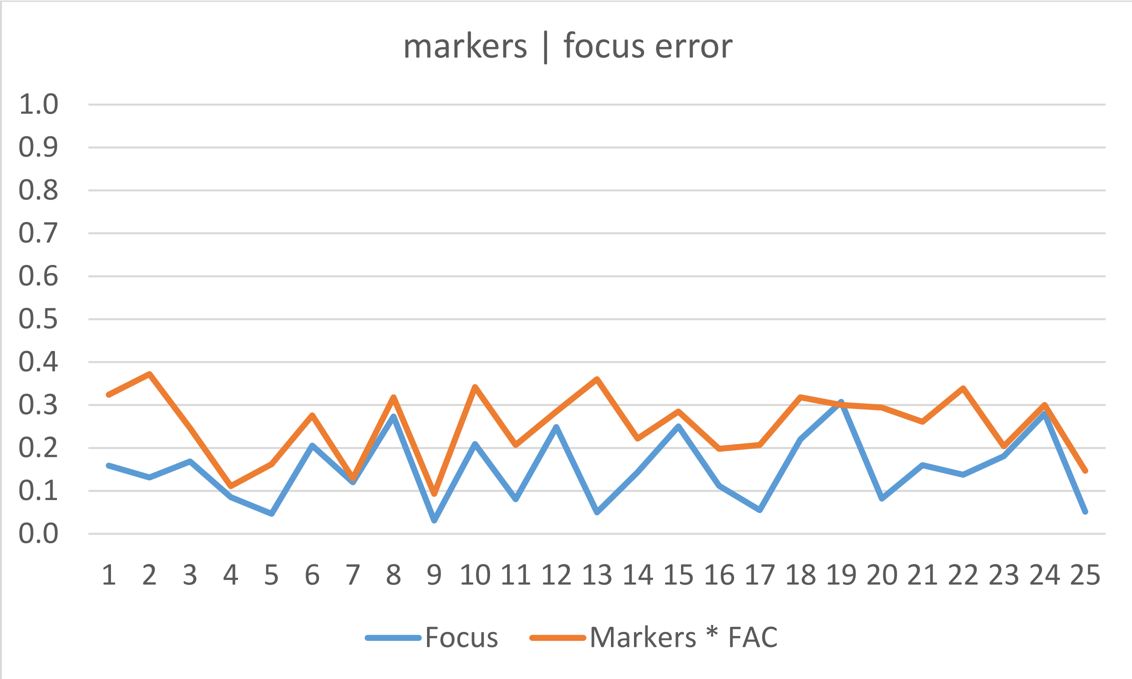

Figure 62 *Focus error (blue) and Markers error*30 (orange) for 25 cases evaluated with an increment of 0.05 mm and a localizer of size 250 mm.*

Test results for the localizer 5M-300 mm

Lastly, a localizer of 300 mm is studied, showing the results collected in the Table 23. Greater sizes showed no interest as their location over the radiographic film presented more difficulties.

Case	Range (mm)	eM (mm)	eF (mm)	Time (s)
1	5	0.0135	0.2733	199
2	8	0.0157	0.1597	1123
3	5	0.0057	0.0388	202
4	5	0.0142	0.2755	195
5	5	0.0079	0.1154	204
6	10	0.0130	0.1901	2699
7	5	0.0020	0.0290	202
8	6	0.0082	0.0225	376
9	5	0.0056	0.0872	199
10	5	0.0068	0.0812	202
11	5	0.0125	0.1198	205
12	5	0.0128	0.2134	200
13	9	0.0136	0.2136	1753
14	5	0.0090	0.0323	195

15	5	0.0051	0.0609	198
16	5	0.0136	0.0449	196
17	6	0.0117	0.2024	376
18	5	0.0101	0.1609	203
19	7	0.0109	0.2361	659
20	5	0.0052	0.0784	196
21	6	0.0145	0.2924	363
22	5	0.0053	0.0175	199
23	7	0.0100	0.1031	667
24	5	0.0092	0.1503	199
25	5	0.0113	0.1513	200
Average		0.0099	0.1340	190.20

Table 23 *Range, Markers error (eM), Focus error (eF) and calculus time for 25 cases studied with an increment of 0.05 mm and a localizer of size 300 mm.*

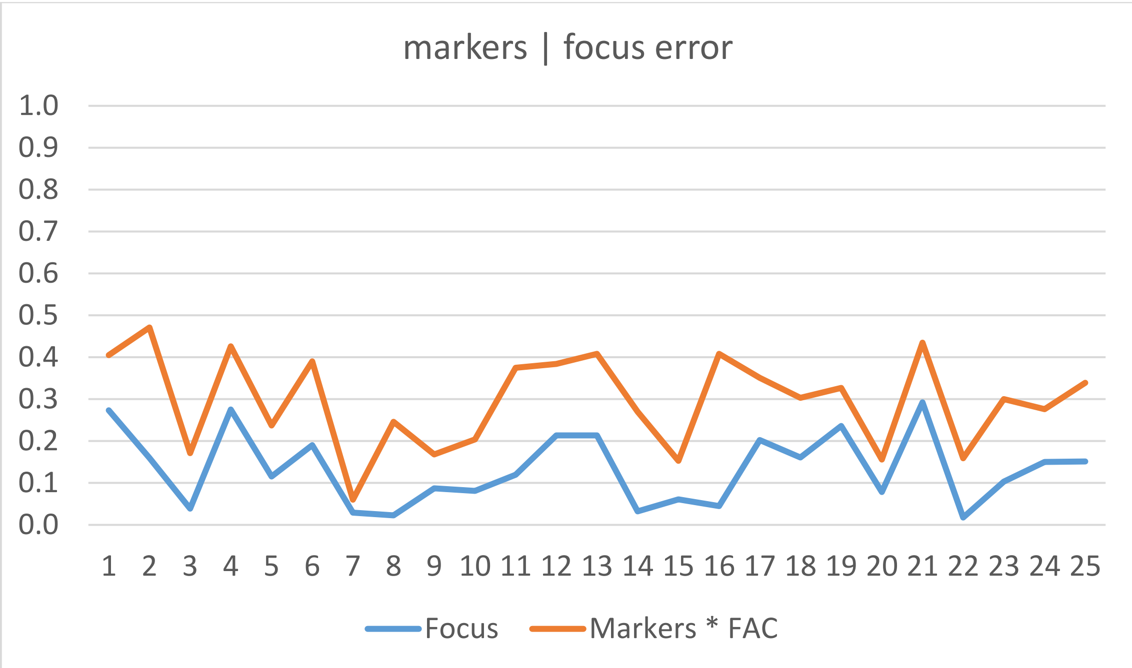

Figure 63. *Focus error (blue) and Markers error*30 (orange) for 25 cases evaluated with an increment of 0.05 mm and a localizer of size 300 mm.*

6.3.1. Analysis

The data obtained for the different sizes of localizer show a tendency in the behaviour of the errors. On the one hand, the *focus error* shows to decrease with increasing sizes, what leads to a higher precision for bigger localizers. On the other hand, the *markers error* acts in the other direction: for greater localizers, it increases. It is interesting to remember the role of the *markers error* and the reason that this increase has no negative effects on the performance of the ApLoFX. As stated in previous sections, *markers error* is used in order to determine whether a solution is the best or not. With this purpose, the different *markers errors* within a test are assessed. The *marker errors* are compared between those generated inside the same case. Consequently, a higher average has no effect in the precision of the methodology. For a deeper and more exhaustive study, relevant data obtained from the 25 *projective cases* for each of the dimensions of the localizer are gathered and shown in the Table 24 and the Figure 64.

Case	100 mm	150 mm	200 mm	250 mm	300 mm
1	0.4295	0.1242	0.2680	0.1588	0.2733
2	0.3896	0.1895	0.1842	0.1313	0.1597
3	0.0610	0.2626	0.2878	0.1684	0.0388
4	0.1385	0.3106	0.0951	0.0853	0.2755
5	0.1355	0.3578	0.2594	0.0465	0.1154
6	0.0213	0.4503	0.2734	0.2056	0.1901
7	0.0315	0.3535	0.0286	0.1200	0.0290
8	0.0664	0.5513	0.1609	0.2733	0.0225
9	0.3982	0.0881	0.2024	0.0309	0.0872
10	0.4352	0.3226	0.2263	0.2092	0.0812
11	0.3130	0.2399	0.0794	0.0806	0.1198
12	0.1741	0.0251	0.1901	0.2486	0.2134
13	0.1011	0.1592	0.2608	0.0501	0.2136
14	0.3601	0.0254	0.0564	0.1437	0.0323
15	0.3350	0.0184	0.1934	0.2502	0.0609
16	0.1510	0.0536	0.1288	0.1117	0.0449
17	0.2947	0.0958	0.0767	0.0553	0.2024
18	0.5153	0.0626	0.1046	0.2198	0.1609
19	0.2969	0.2688	0.2949	0.3074	0.2361
20	0.0676	0.3168	0.2035	0.0821	0.0784
21	0.2251	0.0386	0.0550	0.1599	0.2924
22	0.2155	0.3655	0.2036	0.1376	0.0175
23	0.2422	0.2173	0.0170	0.1807	0.1031
24	0.4016	0.2319	0.1712	0.2797	0.1503
25	0.3956	0.0587	0.0252	0.0513	0.1513
eF (mm)	0.2403	0.2110	0.1574	0.1512	0.1282
S.D (mm)	0.1439	0.1448	0.0874	0.0799	0.0841

Table 24. *Focus error and Standard Deviation evaluated for 25 cases with an increment value of 0.05 mm and localizer sizes of 100 mm, 150 mm, 200 mm, 250 mm and 300 mm.*

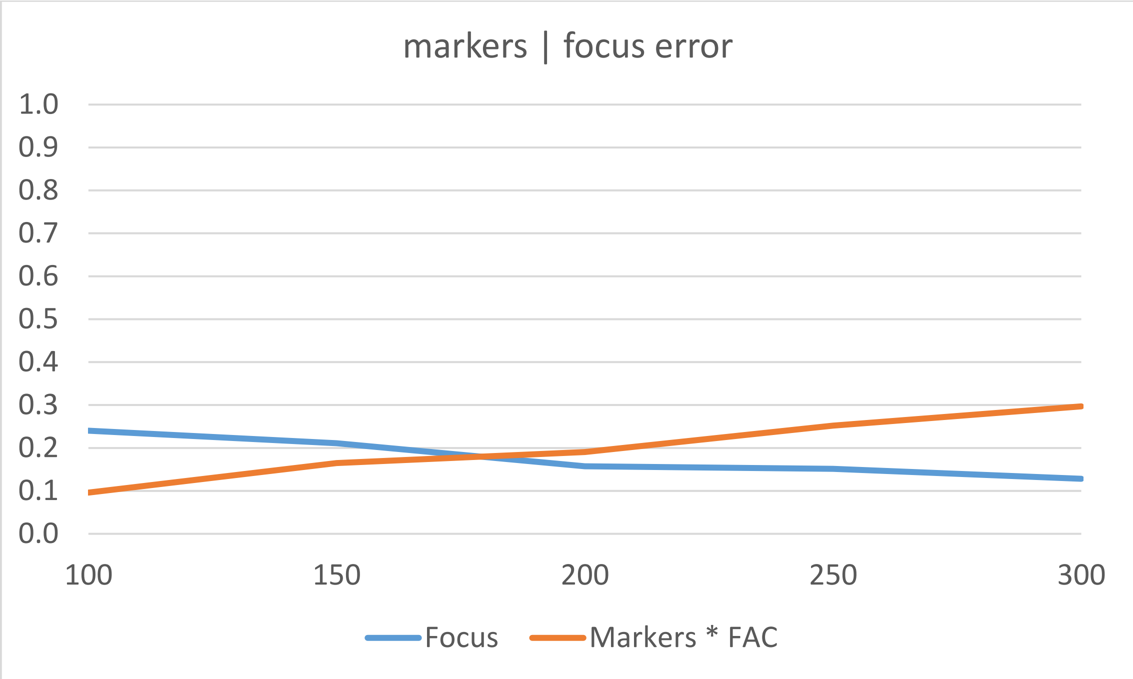

Figure 64. *Correspondence between Focus error (blue) and Markers error*30 (orange) with the size of the localizer.*

Looking at the average errors and the standard deviation it is possible to observe the relevance of the size of the localizer when assessing the performance of the ApLoFX. When reviewing the data, a main conclusion can be drawn: there is a dependency on the size of the localizer and the error obtained by the ApLoFX. Larger localizers show better behaviour with respect to smaller ones. From the application of the methodology with the localizer 5M-100 mm to the use of the localizer 5M-300 mm, the precision in the localization of the focus is doubled. With respect to the reliability of the localization, the standard deviation (SD) of the *focus error*s for the 25 cases shows that the variability of the error decreases with the error itself. Again, comparing the 5M-100 mm localizer with the 5M-300 mm one, the SD is reduced by 40% from the firs to the second.

In conclusion, it can be stated that larger localizers not only provide more accurate calculus but also more reliable, allowing to narrow the error in the application of the methodology.

The Figure 65 shows a boxplot of the *focus error* for the different increment sizes. According to the type of graph, the 25, 50 and 75 percentiles are indicated. In addition, for this particular case, the mean values have been pointed with a red asterisk.

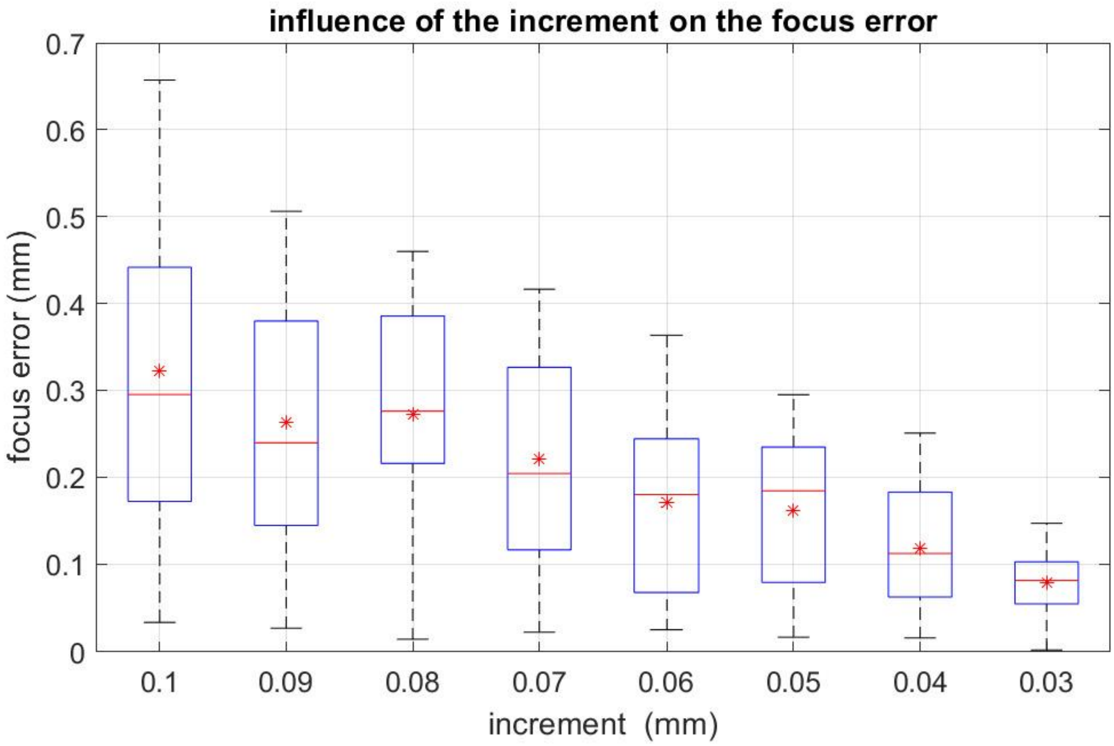

Figure 65 *Boxplot of the focus error for localizer sizes ranging from 100 mm to 300 m. Red asterisks indicate the mean value for each increment.*

6.4. Special case. Thin localizer

In the section 6.2, restrictions to the geometry of the localizer were introduced. To remember: the number of markers that form it must be equal or greater than 4, and they cannot be contained in the same geometrical plane. The later restriction was assessed considering a plane parallel to the radiographic film. It is interesting to explore the "limit case" for which a narrow localizer (with several proximate planes) may be acceptable. This has special interest and has been an objective of the project from the earlier stages. The reason is the multiple possibilities than a narrow localizer may have. To cite one: current calibration boxes used in RSA, and also the one suggested in (García Ruesgas, 2014), have a large size. The possibility to locate them in the radiography at the same time than the patient require from special considerations. In the mentioned work, a hollow shape allows to locate the patient's extremity inside the box. In other cases, the calibration box and the radiographic film have to be placed behind the patient desk, increasing considerably the patient to detector distance and, hence, the blurring of the radiography. The development of a thin localizer could allow new possibilities as, for example, its attachment to the patient's desk without interfering, the normal operation of the system.

In this direction, several trials were performed in initial stages of the project. Localizers of 4 and 5 markers with a different thickness were tested and the performance of the methodology was studied (see Figure 66). These examinations took place before the implementation of the *Application Method* and, consequently, the increment value that could be applied to the study had a minimum value of 0.1 mm. However, the results motivated a deeper study when the whole ApLoFX was completely functional.

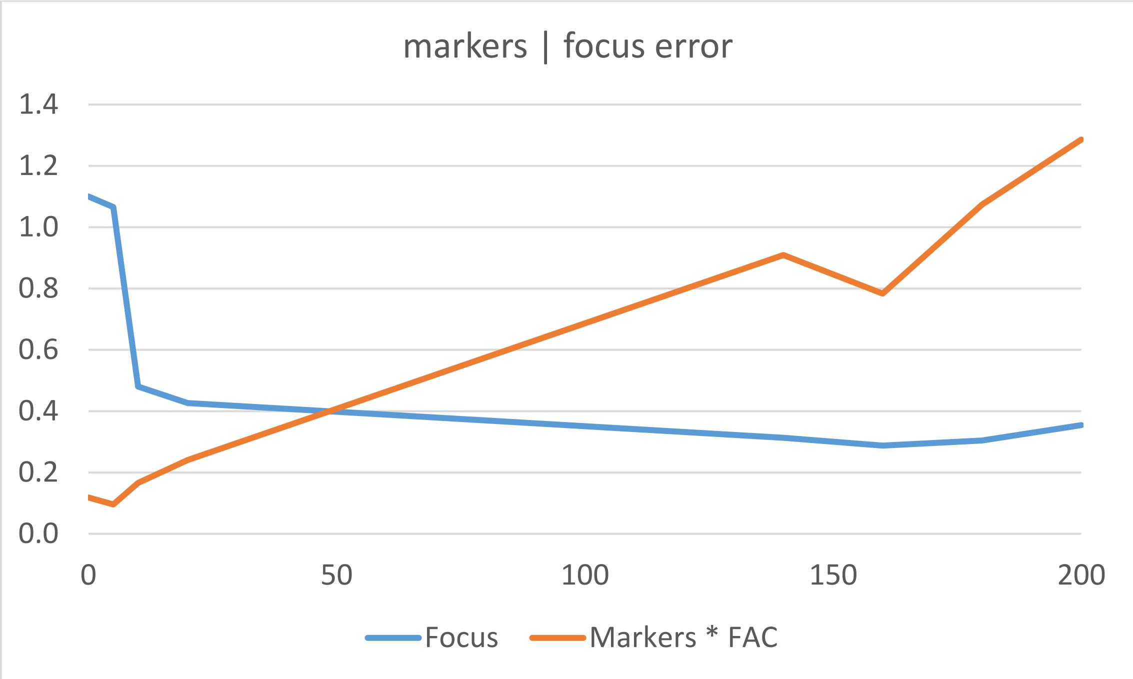

Figure 66. *Focus error (blue) and Markers error*30 (orange) for localizer heights ranging from 4 mm to 200 mm.*

Figure 66 shows excessive error for thickness lower than 20 mm. However, the gradient of improvement falls drastically around this value. The possibility of studying a localizer with thickness in the range of 20-30 mm was, therefore, motivated. With the ApLoFX fully operative, a more precise study could be performed. Using an increment value of 0.05 mm, further studies showed interesting results for a thickness of 30 mm. As in the case of the different sizes experienced for a cubic localizer, the results for a new shape consisting in a hexaedrom of dimensions 200x200x30 mm are assessed. The experimental results for this localizer are shown in Table 25.

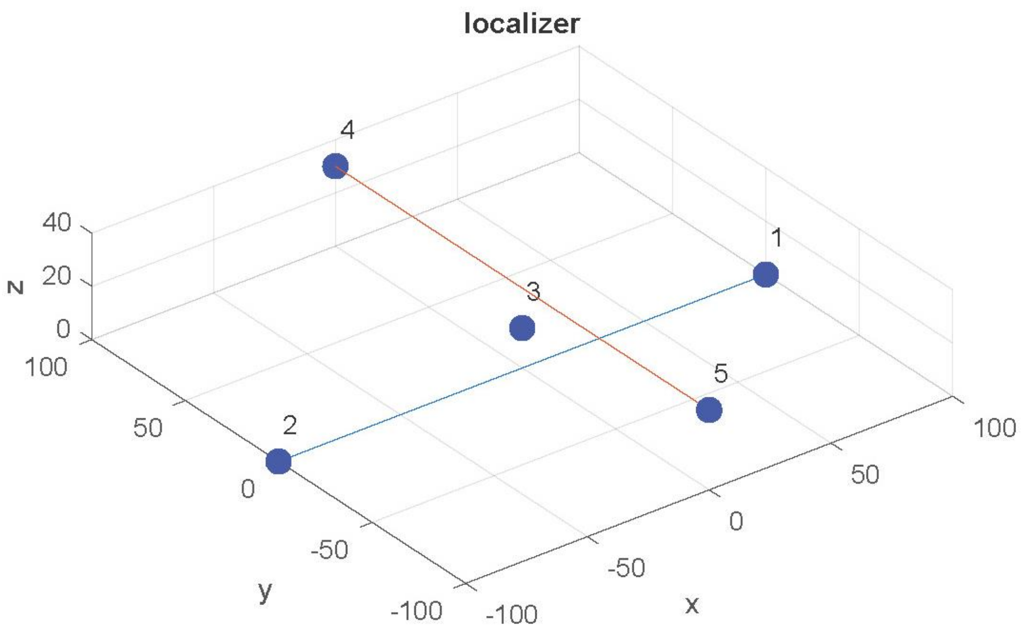

Figure 67 *Localizer 5M-200 mm-30 mm used as special case for a reduced height in perspective.*

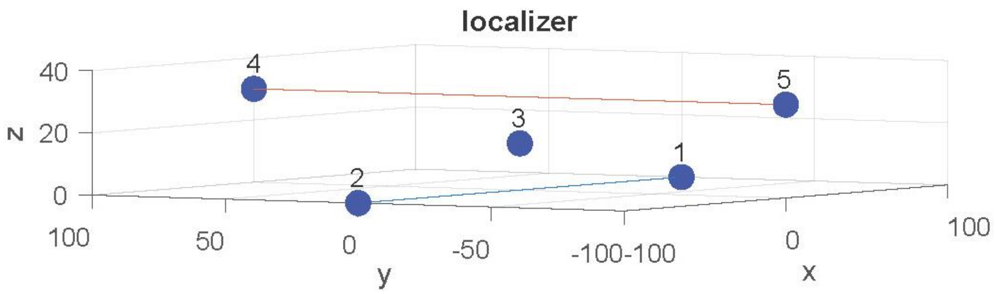

Figure 68. *Localizer 5M-200 mm-30 mm used as special case for a reduced thickness.*

Case	eM (mm)	eF (mm)	Time (s)
1	0.0015	0.2882	229
2	0.0024	0.0531	389
3	0.0012	0.1217	205
4	0.0022	0.1296	203
5	0.0021	0.0851	198
6	0.0014	0.2450	197
7	0.0012	0.1444	199
8	0.0022	0.0926	217
9	0.0018	0.3030	1130
10	0.0011	0.1982	3867
11	0.0019	0.1273	7401
12	0.0013	0.0223	199
13	0.0018	0.4081	199
14	0.0018	0.2739	204
15	0.0012	0.0962	226
16	0.0008	0.0759	1625
17	0.0019	0.2020	6102
18	0.0022	0.3448	572
19	0.0016	0.3217	1811
20	0.0020	0.1812	5350
21	0.0022	0.3086	245
22	0.0017	0.0294	1902
23	0.0012	0.1435	813
24	0.0016	0.2040	571
25	0.0017	0.0833	1402
Average	0.0017	0.1793	1418

Table 25. *Markers error (eM), Focus error (eF) and calculus time for 25 cases studied with an increment of 0.05 mm and a localizer of 30 mm of thickness.*

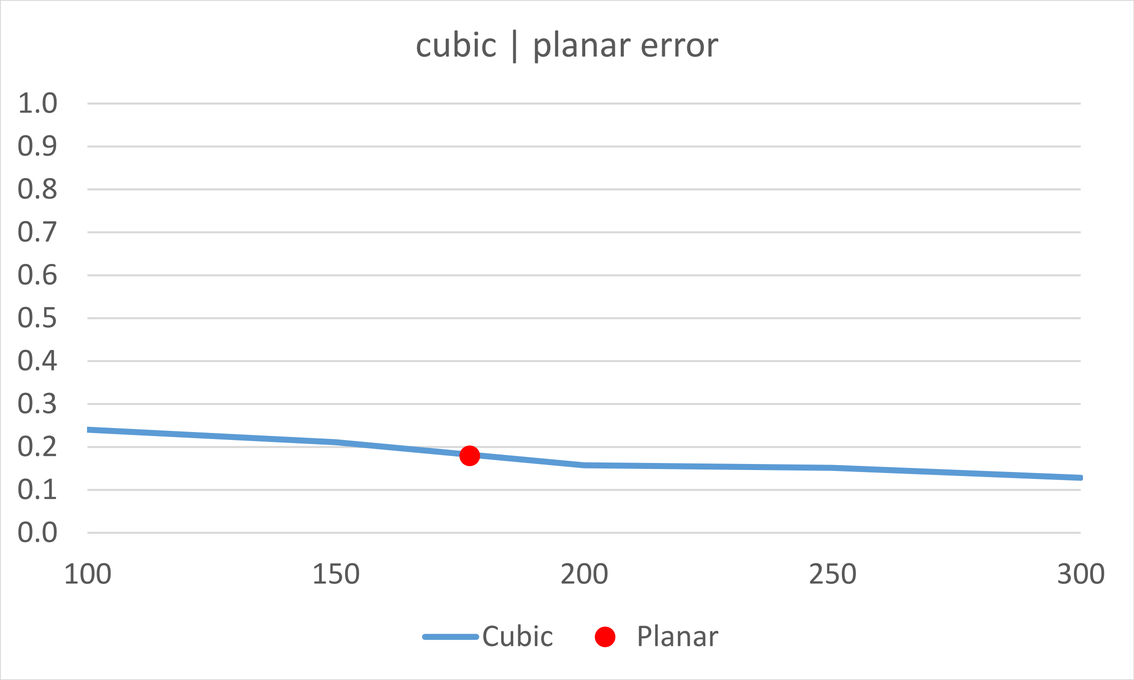

Figure 69. *Focus error of localizer 5M-200 mm-30 mm used as special case for a reduced thickness compared with the errors of the cubic-shaped localizers according to their size.*

Figure 69 presents a comparison between the flat localizer and the standard cubic localizers previously tested. The average *focus error* obtained of 0.193 mm is equivalent to the one expected from a cubic localizer of 173 mm.

The possibility to design an almost flat localizer has, as mentioned before, a wide range of possibilities. Specifically, a relevant fact can be pointed out: Both ApLoFX and the precise calculus stage consider the relative movements of the localizer and the focus with respect to the projection film (this last one is achieved through the movement of the projection film itself). If a sufficiently flat localizer is designed, it could be attached to the radiographic table or surface and remain static for later procedures. In this case, the algorithm could reduce (if not completely remove) the range of iterations corresponding to Z_{loc} reducing significantly the computational time or, if preferred, augmenting the precision of the focus localization.

6.5. Influence of the number of markers

In the previous section, the influence that the localizer's size had on the performance of ApLoFX was assessed. After numerous tests, a correlation between the size and the accuracy in the determination of the focus location was inferred. In addition, the possibility to design an almost flat localizer was introduced with interesting results. These tests were conducted with a 5 markers localizer, based on the reference localizer 5M-200 mm introduced before.

Reviewing the bibliography and current commercial localizers, it can be seen that there is a variable number of markers composing the calibration object. From 36 markers in (García Ruesgas, 2014) to more than 300 in (Yuan, Ryd, & Tanner, 2002).According to these sources, the minimum number of markers needed to achieve the localization of the focus is 4. In the section 6.2, this has been studied. The use of additional markers has, mainly, practical purposes. The application in real situations may cause some of the markers to be superimposed with others or with skeletal structures, affecting to its identification in the radiography, justifying the reduncandy. In addition, (Yuan, Ryd, & Tanner, 2002) suggests that a greater number of markers can achieve less variability in the error committed when localizing the focus, as it is shown in Figure 70.

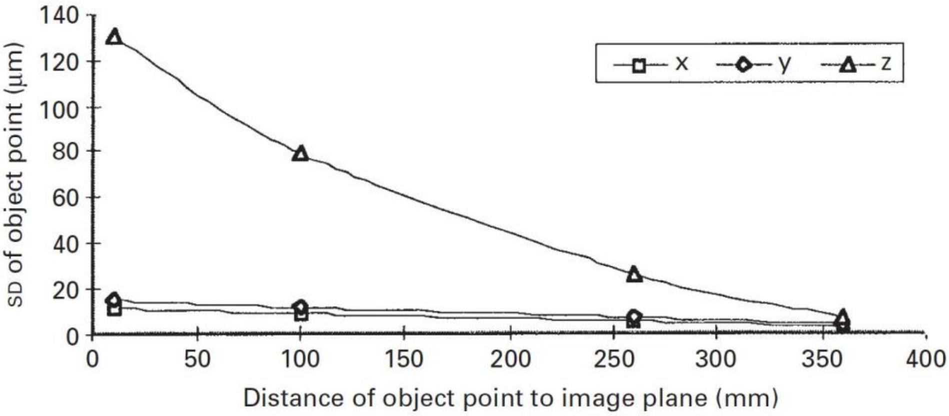

Figure 70. *Variation of the SD in the Focus error according to the number of markers. Extracted from (Yuan, Ryd, & Tanner, 2002).*

The different approach of the analytical methodologies proposed by the mentioned authors, contrasted with the algorithmic methodology in which LoFX is based, requires to be cautious when importing the conclusions stated by their research into the expected performance of the methodology developed in this project. However, it is relevant to study whether number of markers that compose the localizer may have an influence on the performance of the method. Using the same procedure that in previous sections, the interest parameter is isolated. In this case the number of markers. Based in the reference localizer 5M-200 mm (Figure 40) and, without modifying of other features, a series of tests were performed.

Test results for the localizer 4M-200 mm

In the initial stages of the project, based on (García Ruesgas, 2014) and other authors, a localizer of 4 markers was mainly used as a reference for the development of the software. However, it was not until the fully completion of the ApLoFX that a deep study of the significance of this localizer could be performed. The results are shown in the next pages.

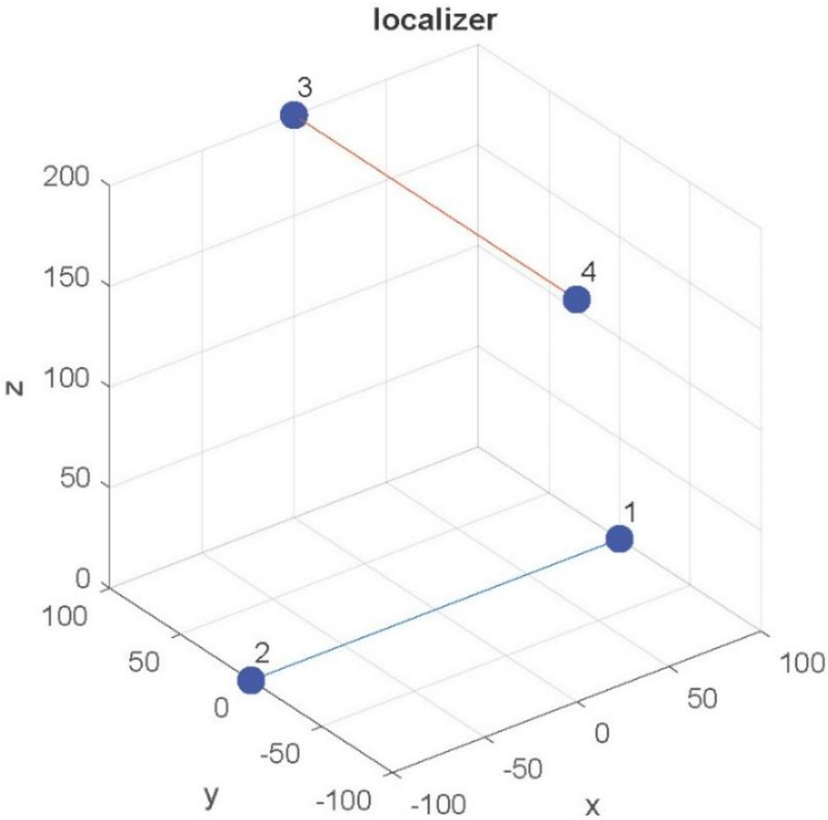

Figure 71. *4 Markers Localizer used for the study of the influence of the number of markers.*

Case	Range (mm)	eM (mm)	eF (mm)	Time (s)
1	5	0.0048	0.1448	164
2	5	0.0049	0.2042	164
3	5	0.0063	0.3113	164
4	5	0.0055	0.1695	164
5	8	0.0072	0.1107	922
6	5	0.0072	0.1808	166
7	5	0.0059	0.2450	167
8	5	0.0056	0.2461	167
9	7	0.0037	0.1315	556
10	5	0.0066	0.0862	165
11	7	0.0043	0.0558	556
12	6	0.0058	0.2346	331
13	5	0.0057	0.2464	176
14	5	0.0055	0.1555	171
15	9	0.0076	0.3184	1459
16	5	0.0078	0.0463	170
17	5	0.0055	0.1905	173

18	5	0.0070	0.2799	174
19	6	0.0064	0.2641	317
20	5	0.0077	0.2391	201
21	5	0.0041	0.1485	165
22	7	0.0062	0.2836	547
23	5	0.0033	0.0622	164
24	7	0.0037	0.0118	541
25	8	0.0056	0.0180	904
Average		0.0058	0.1754	147

Table 26. *Range, Markers error (eM), Focus error (eF) and calculus time for 25 cases studied with an increment of 0.05 mm and a localizer of 4 markers.*

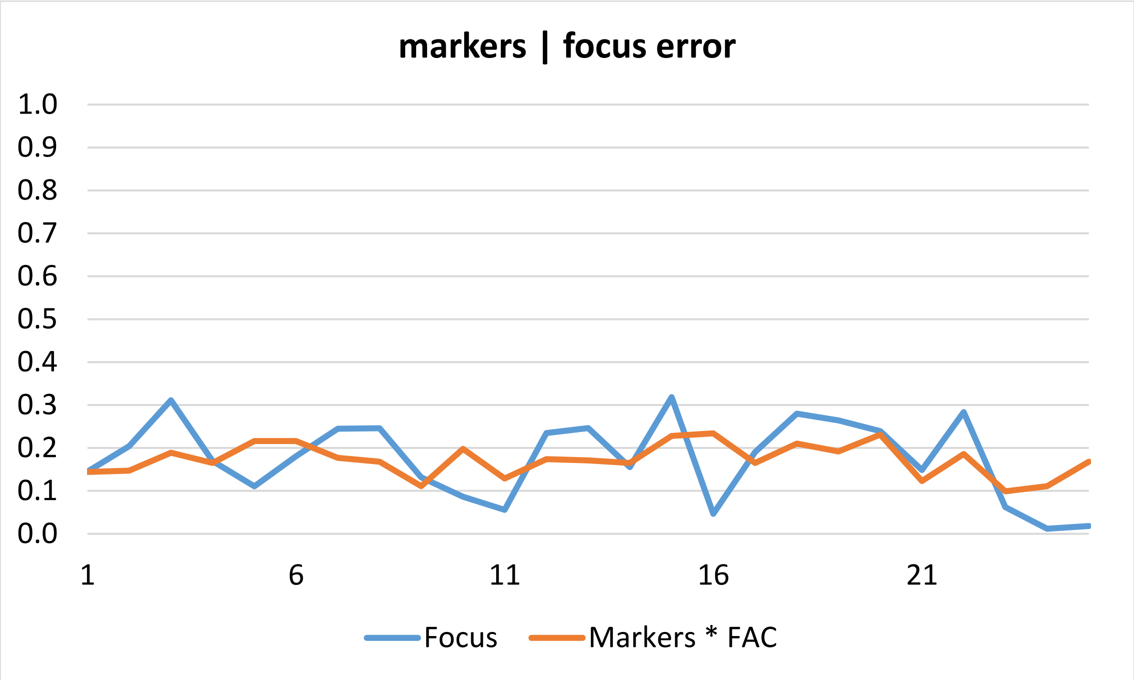

Figure 72. *Focus error (blue) and Markers error*30 (orange) for 25 cases evaluated with an increment of 0.05 mm and the localizer 4M-200 mm.*

Test results for the localizer 5M-200 mm

These tests were presented in when studying the influence of the size of the localizer. The results are collected in the Table. 21 and Figure 61.

Test results for the localizer 6M-200 mm

Based in the same geometry defined by the reference localizer, an extra marker is added to the geometry. Due to the even number of markers, the centre of the volume is kept empty.

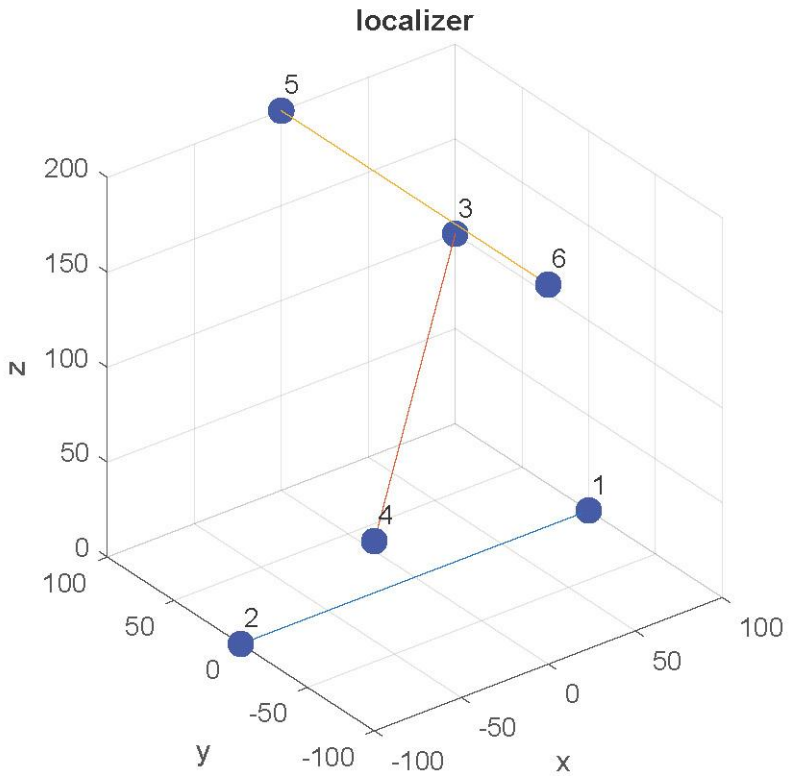

Figure 73. *6 Markers Localizer used for the study of the influence of the number of markers.*

Case	Range (mm)	eM (mm)	eF (mm)	Time (s)
1	5	0.0067	0.0852	230
2	5	0.0069	0.0847	233
3	5	0.0091	0.1402	229
4	5	0.0087	0.2357	234
5	8	0.0082	0.1541	1343
6	5	0.0108	0.0486	236
7	10	0.0094	0.0247	3187
8	10	0.0081	0.1960	3153
9	5	0.0078	0.2531	243
10	10	0.0082	0.0210	3137
11	9	0.0083	0.1918	2088
12	5	0.0094	0.0812	252
13	5	0.0068	0.1624	239

14	5	0.0052	0.0466	238
15	8	0.0049	0.0853	1391
16	10	0.0070	0.1647	3161
17	5	0.0063	0.1104	231
18	5	0.0098	0.2277	233
19	5	0.0068	0.0582	240
20	5	0.0066	0.1606	236
21	5	0.0091	0.0738	276
22	5	0.0093	0.1643	250
23	5	0.0105	0.2702	239
24	5	0.0103	0.0236	240
25	5	0.0083	0.0428	226
Average		0.0081	0.1243	362

Table 27. *Range, Markers error (eM), Focus error (eF) and calculus time for 25 cases studied with an increment of 0.05 mm and a localizer of 6 markers.*

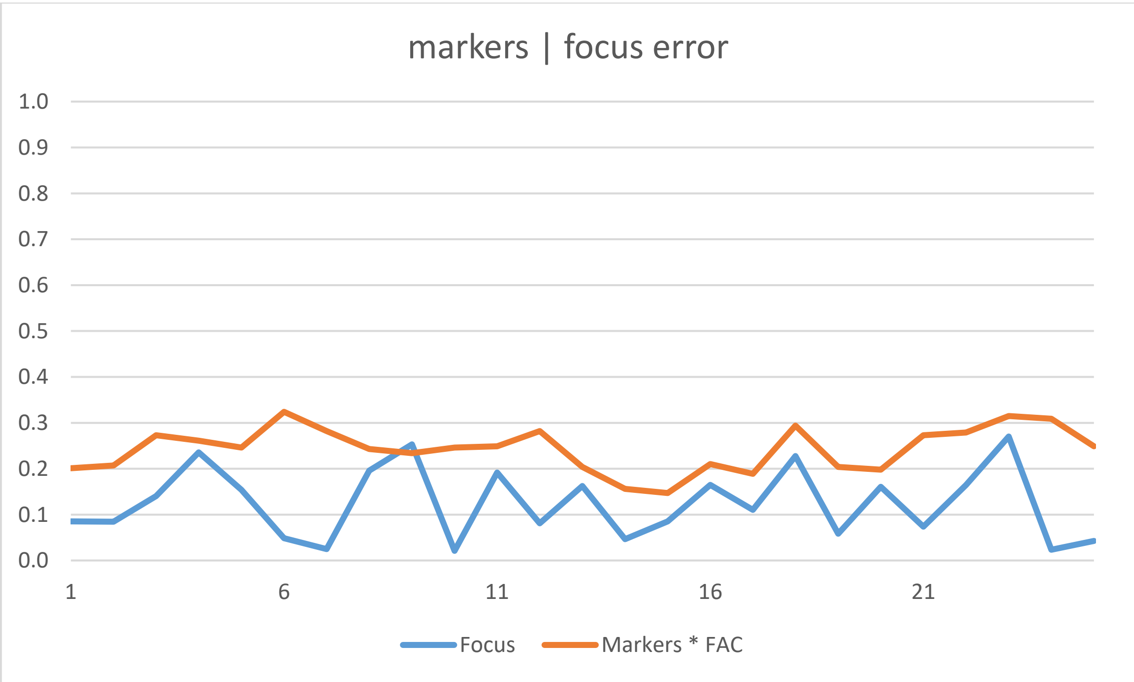

Figure 74. *Focus error (blue) and Markers error*30 (orange) for 25 cases evaluated with an increment of 0.05 mm and the localizer 6M-200 mm.*

Test results for the localizer 7M-200 mm

Again, the geometry of the reference localizer is recovered. In this case, the odd number of markers allows to retake the 6 Markers localizer and add an extra one in the centre of the volume.

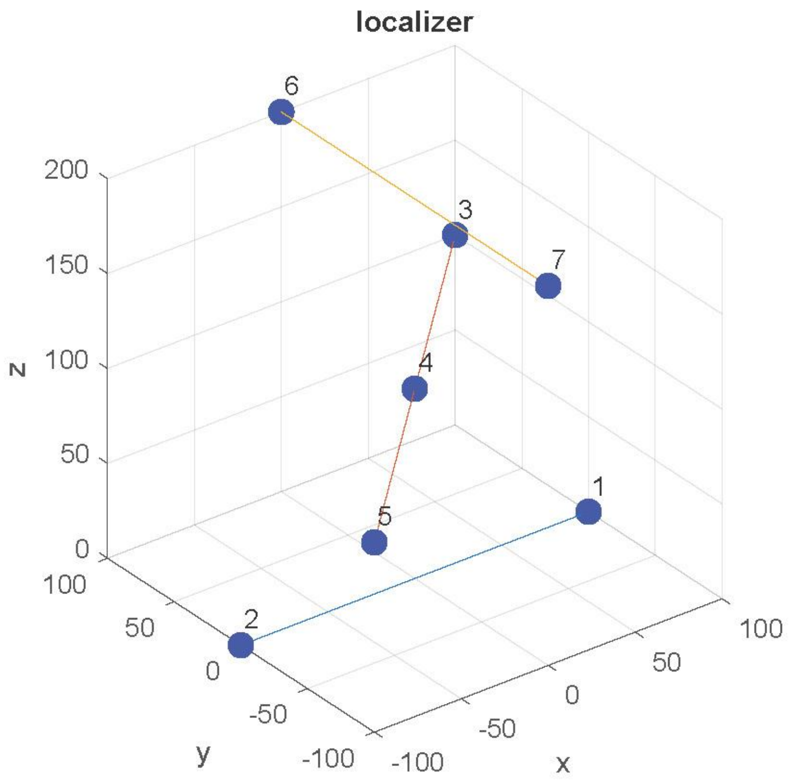

Figure 75. *7 Markers Localizer used for the study of the influence of the number of markers.*

Case	Range (mm)	eM (mm)	eF (mm)	Time (s)
1	5	0.0096	0.0573	291
2	5	0.0081	0.1257	325
3	8	0.0102	0.0191	1696
4	5	0.0094	0.2916	292
5	5	0.0069	0.1399	332
6	5	0.0085	0.1893	324
7	6	0.0112	0.3505	545
8	5	0.0072	0.1220	282
9	5	0.0124	0.0538	289
10	13	0.0088	0.1901	10659
11	10	0.0081	0.1395	3732
12	5	0.0090	0.1499	284

13	5	0.0112	0.2365	287
14	5	0.0091	0.2636	267
15	5	0.0106	0.1201	265
16	5	0.0116	0.2750	263
17	5	0.0093	0.0248	270
18	5	0.0095	0.1685	266
19	6	0.0073	0.1955	200
20	7	0.0102	0.1334	906
21	5	0.0112	0.0230	271
22	5	0.0113	0.1490	263
23	5	0.0102	0.2378	265
24	7	0.0097	0.0967	921
25	5	0.0078	0.1577	264
Average		0.0095	0.1564	395

Table 28. Range, Markers error (eM), Focus error (eF) and calculus time for 25 cases studied with an increment of 0.05 mm and a localizer of 7 markers.

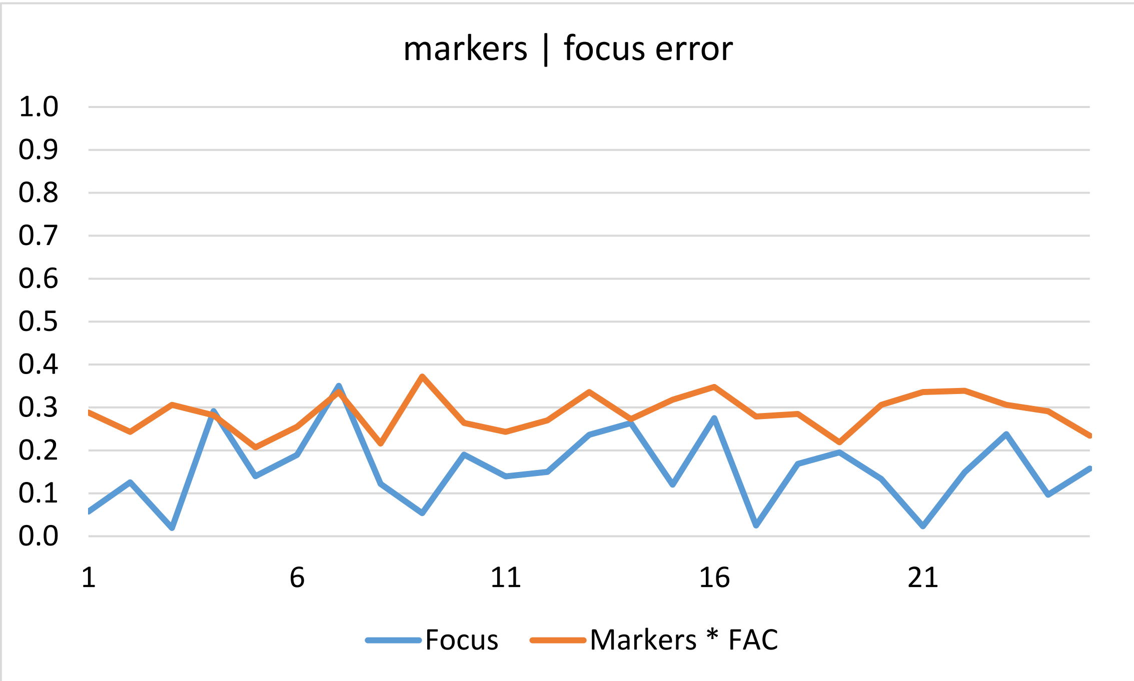

Figure 76. *Focus error (blue) and Markers error*30 (orange) for 25 cases evaluated with an increment of 0.05 mm and the localizer 7M-200 mm.*

Test results for the localizer 8M-200 mm

Two extra markers are added to the 6M-200 mm localizer in the opposite diagonal to the first. All the additional markers meet the restriction of no superimposing each other in a top view.

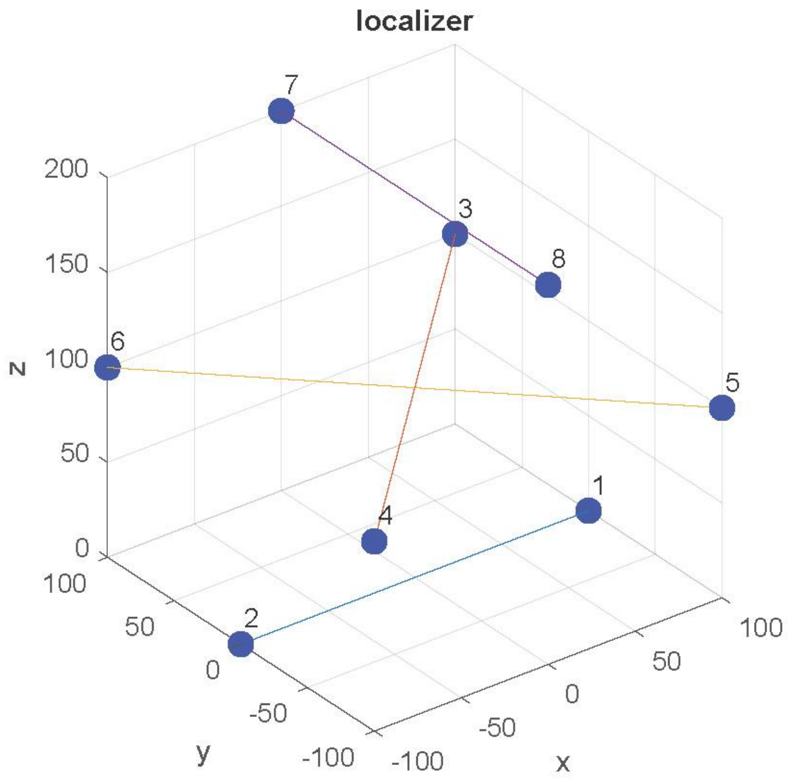

Figure 77. *8 Markers localizer used for the study of the influence of the number of markers.*

Case	Range (mm)	eM (mm)	eF (mm)	Time (s)
1	8	0.0058	0.0463	1956
2	5	0.0125	0.3388	330
3	7	0.0067	0.0513	1262
4	6	0.0087	0.0179	1338
5	5	0.0083	0.2027	703
6	7	0.0067	0.0425	1356
7	5	0.0079	0.1413	394
8	5	0.0086	0.2263	408
9	5	0.0114	0.1704	520
10	5	0.0145	0.2201	514
11	5	0.0063	0.1281	498
12	5	0.0117	0.2320	498
13	5	0.0117	0.2612	344

14	6	0.0113	0.1332	620
15	5	0.0113	0.1800	334
16	5	0.0089	0.1846	334
17	7	0.0084	0.1854	1133
18	5	0.0101	0.1439	320
19	7	0.0107	0.2084	1044
20	15	0.0046	0.1057	20794
21	12	0.0128	0.0939	8773
22	11	0.0082	0.2112	6606
23	5	0.0114	0.1376	307
24	5	0.0103	0.1562	322
25	5	0.0105	0.0197	321
Average		0.0096	0.1535	850.50

Table 29. *Range, Markers error (eM), Focus error (eF) and calculus time for 25 cases studied with an increment of 0.05 mm and a localizer of 8 markers.*

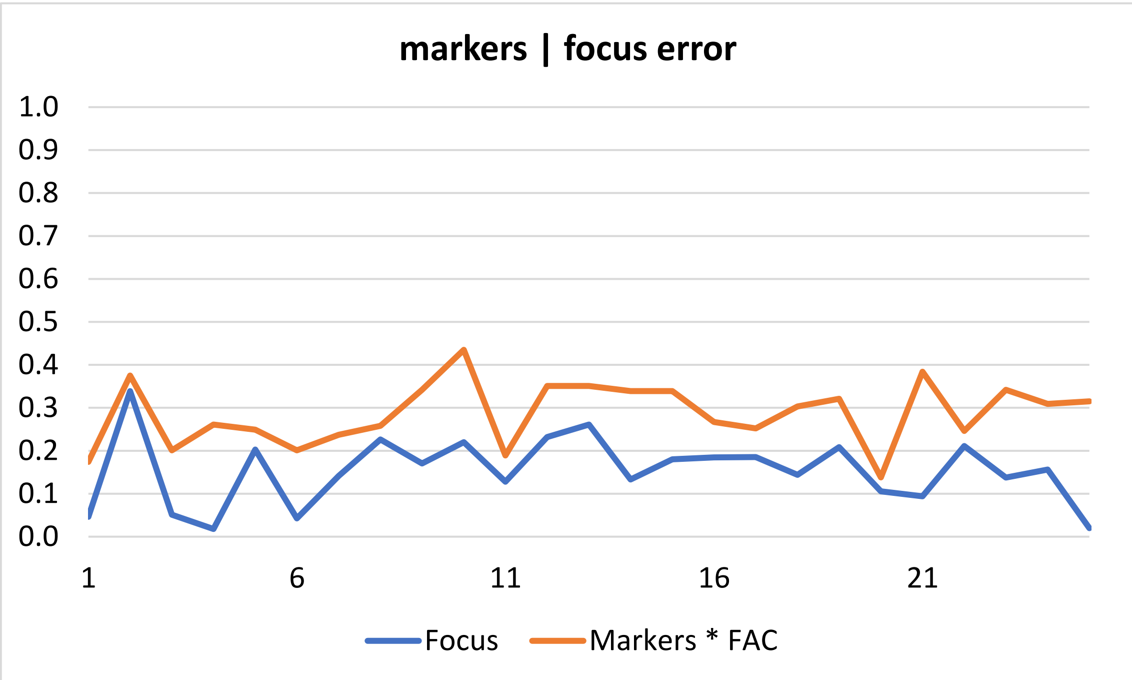

Figure 78. *Focus error (blue) and Markers error*30 (orange) for 25 cases evaluated with an increment of 0.05 mm and the localizer 8M-200 mm.*

Test results for the localizer 9M-200 mm

A new localizer of 9 markers, based in the reference localizer is used for the next tests.

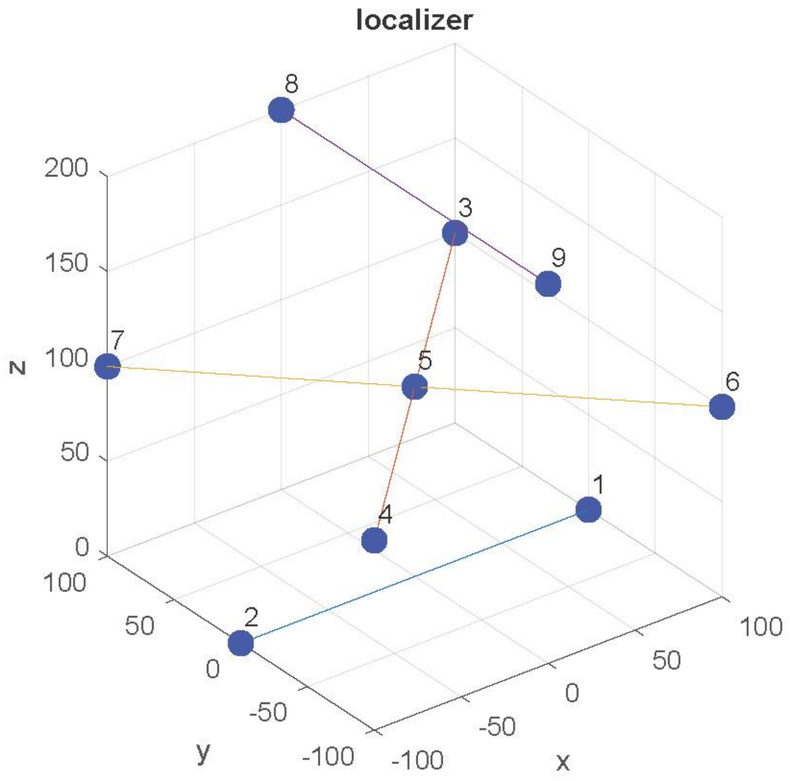

Figure 79 *9 Markers Localizer used for the study of the influence of the number of markers.*

Case	Range (mm)	eM (mm)	eF (mm)	Time (s)
1	6	0.0117	0.1800	696
2	10	0.0099	0.2270	4644
3	5	0.0155	0.3589	350
4	5	0.0125	0.3186	351
5	5	0.0141	0.3257	351
6	5	0.0052	0.1011	337
7	5	0.0143	0.3441	389
8	6	0.0118	0.2074	735
9	5	0.0105	0.1582	400
10	8	0.0107	0.2273	2050
11	5	0.0129	0.3562	364
12	5	0.0103	0.0160	366
13	5	0.0198	0.5973	344
14	5	0.0092	0.2088	343

15	5	0.0149	0.1544	351
16	5	0.0074	0.1141	351
17	8	0.0142	0.0314	2275
18	6	0.0131	0.0682	676
19	9	0.0132	0.0782	3119
20	10	0.0108	0.2028	4667
21	5	0.0095	0.2079	334
22	12	0.0101	0.2201	7355
23	5	0.0101	0.0949	337
24	5	0.0076	0.1313	331
25	10	0.0136	0.1502	4551
Average		0.0117	0.2032	601

Table 30 *Range, Markers error (eM), Focus error (eF) and calculus time for 25 cases studied with an increment of 0.05 mm and a localizer of 9 markers.*

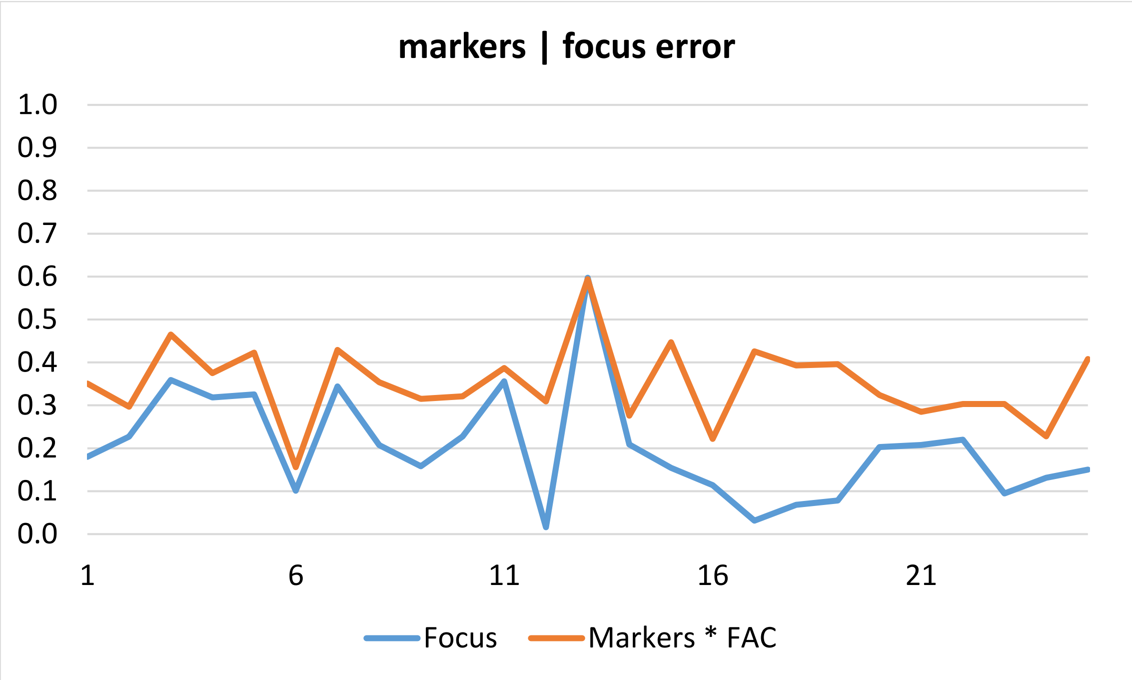

Figure 80 *Focus error (blue) and Markers error*30 (orange) for 25 cases evaluated with an increment of 0.05 mm and the localizer 9M-200 mm.*

6.5.1.Analysis

Continuing with the system used to extract conclusions about the influence that a certain parameter has on the performance of the ApLoFX, a table that collects the *focus error*s for the different configurations is showed below. In addition to the localizers with 4, 5, 6, 7, 8 and 9 markers, a column with the results obtained for a localizer of 3 markers (3M-200 mm) is shown in order to highlight the importance of a minimum of 4 markers for the obtaining of acceptable results in the application of the methodology.

Case	3 M	4 M	5 M	6 M	7 M	8 M	9 M
1	15.4524	0.1448	0.2680	0.0852	0.0573	0.0463	0.1800
2	28.9819	0.2042	0.1842	0.0847	0.1257	0.3388	0.2270
3	19.5687	0.3113	0.2878	0.1402	0.0191	0.0513	0.3589
4	42.2339	0.1695	0.0951	0.2357	0.2916	0.0179	0.3186
5	15.0563	0.1107	0.2594	0.1541	0.1399	0.2027	0.3257
6	58.7035	0.1808	0.2734	0.0486	0.1893	0.0425	0.1011
7	10.5196	0.2450	0.0286	0.0247	0.3505	0.1413	0.3441
8	8.3079	0.2461	0.1609	0.1960	0.1220	0.2263	0.2074
9	7.4652	0.1315	0.2024	0.2531	0.0538	0.1704	0.1582
10	17.0440	0.0862	0.2263	0.0210	0.1901	0.2201	0.2273
11	4.7862	0.0558	0.0794	0.1918	0.1395	0.1281	0.3562
12	10.4858	0.2346	0.1901	0.0812	0.1499	0.2320	0.0160
13	42.0053	0.2464	0.2608	0.1624	0.2365	0.2612	0.5973
14	6.9819	0.1555	0.0564	0.0466	0.2636	0.1332	0.2088
15	0.4287	0.3184	0.1934	0.0853	0.1201	0.1800	0.1544
16	31.2077	0.0463	0.1288	0.1647	0.2750	0.1846	0.1141
17	0.3103	0.1905	0.0767	0.1104	0.0248	0.1854	0.0314
18	6.4061	0.2799	0.1046	0.2277	0.1685	0.1439	0.0682
19	36.8775	0.2641	0.2949	0.0582	0.1955	0.2084	0.0782
20	28.4746	0.2391	0.2035	0.1606	0.1334	0.1057	0.2028
21	31.3303	0.1485	0.0550	0.0738	0.0230	0.0939	0.2079
22	32.0650	0.2836	0.2036	0.1643	0.1490	0.2112	0.2201
23	12.7203	0.0622	0.0170	0.2702	0.2378	0.1376	0.0949
24	38.8986	0.0118	0.1712	0.0236	0.0967	0.1562	0.1313
25	55.0438	0.0180	0.0252	0.0428	0.1577	0.0197	0.1502
eF (mm)	22.4542	0.1754	0.1619	0.1243	0.1564	0.1535	0.2032
S.D. (mm)	16.3533	0.0904	0.0874	0.0750	0.0851	0.0778	0.1256

Table 31. *Results of the application of ApLoFX to 25 Projective cases with an increment of 0.05 mm and different number of markers ranging from 3 to 9.*

.

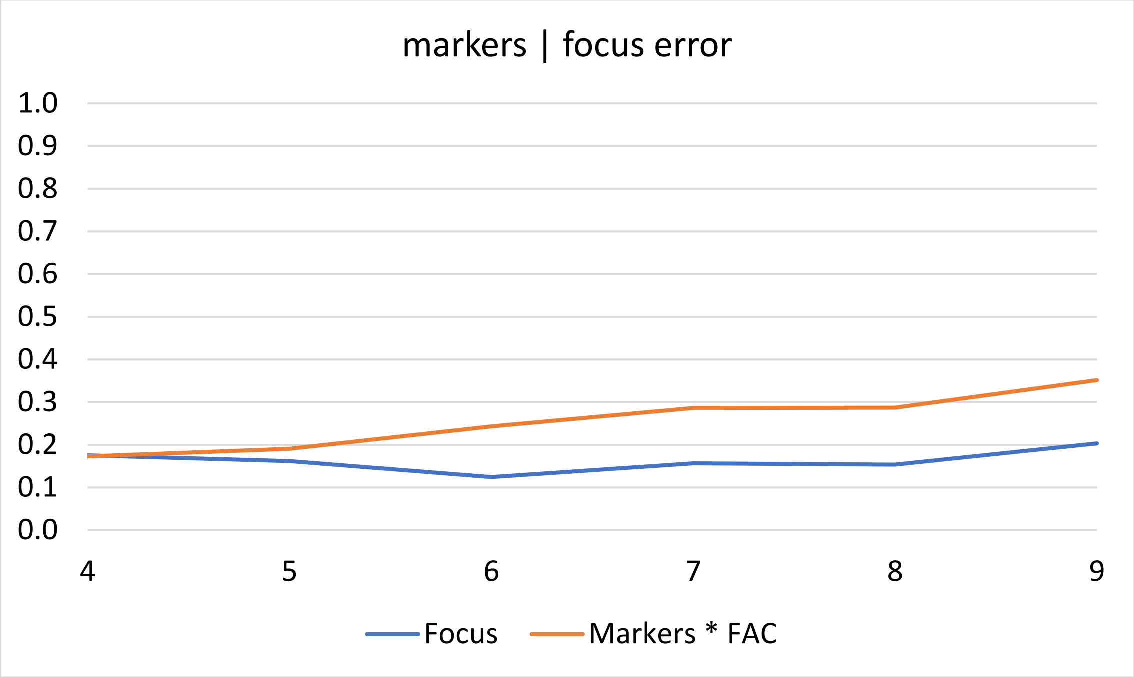

Figure 81 *Focus error (blue) and Markers error*30 (orange). Increment of 0.05 mm and 25 projective cases for localizers of 4,5,6,7,8 and 9 markers respectively.*

As it was previously done with the assessment of the influence of the size of the localizer in the performance of the methodology, it is possible to study the relevance of the number of markers through the study of the *focus error* and its standard deviation. The Figure 81 shows both the *focus error* and the *markers error* (multiplied by a factor of 30) obtained after the execution of the methodology with localizers of 4,5,6,7,8 and 9 markers. The use of the same value for the multiplication factor as well as the axis may affect to the clarity of the graph, leading to erroneous interpretations of the information. For this reason, an extra explanation as well as interpretation is introduced. It is important to remark that the initial intersection between the *focus error* and the *markers error* is just an apparent feature, result of the multiplication factor applied to the *markers error*. A factor of 15, instead, would not present such phenomenon. Additionally, the increasing tendency observed in the *markers error* for higher number or markers has an explanation, related to the nature of this variable. As it was mentioned in previous chapters, the *markers error* corresponds to the sum of the linear distances between the real Projected Markers (introduced as Radiographic Data) and those generated for each virtual projection. The addition of more markers implies the presence of more factors in this sum and, hence, a higher *markers error*.

With respect to the influence of the number of markers in the *focus error*, it cannot be stated that there is any correlation. For the tested cases, no appreciable tendency has been shown. In addition, the standard deviation of the *focus error* for the 25 cases in the 9 localizers configurations shows no significant correspondence with the number of markers. Although not presented in these graphs, section 6.2 demonstrates that a localizer of 3 markers does not provide reliable results if employed by the methodology. This was considered as a geometric restriction, reason why it lies outside the analysis of the influence of the number of markers.

The Figure 82 shows a boxplot of the *focus error* for localizers with different number of markers. According to the type of graph, the 25, 50 and 75 percentiles are indicated. In addition, for this specific case, the mean values have been indicated with a red asterisk.

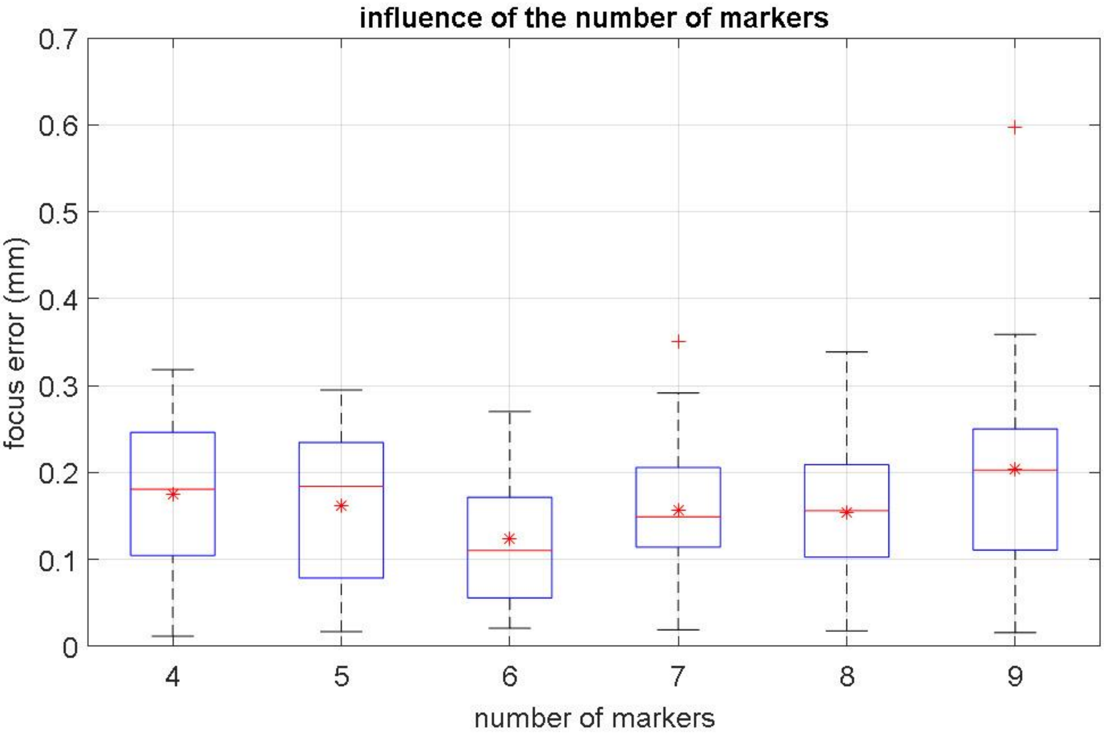

Figure 82. *Boxplot of the focus error for localizers with 4, 5, 6, 7, 8 and 9 markers. Red asterisks indicate the mean value for each increment.*

7. Implementation

In this section, aspects about the implementation of the methodology in a programming language are presented. The previously introduced LoFX and ApLoFX correspond to algorithmic methodologies. In order to test their performance and validity, it is necessary to implement them in a programming language that can be executed and evaluated.

7.1. Software

This project has been implemented in VisualBasic.NET, .NET framework 4.0. and programmed using the IDE of Microsoft Visual Studio 2010. This version of .NET allows its execution in Operative Systems starting from XP and more recent. VB.NET is the programming language used by Microsoft for the development of its applications. Particularly, the .NET framework, initially released in 2000, forms part of the so-called *.NET strategy*, which involved a series of changes in all Microsoft products with the aim of improving the ease of use and the interoperability between different systems. This is one of the main features of the .NET, which includes the *Framework Class Library* that incorporates different packages for the interaction with other programming languages.

The motivation for the use of VisualBasic relies on several aspects. First, its structure is simple and allows the creation of an .exe file that does not require from any installation to run it and can be executed in most of the PCs. Secondly, it incorporates a highly optimized IDE that allows what is called *Rapid Application Development* or RAD, which permits to easily develop graphical user interfaces perfectly connected with the different elements of the code.

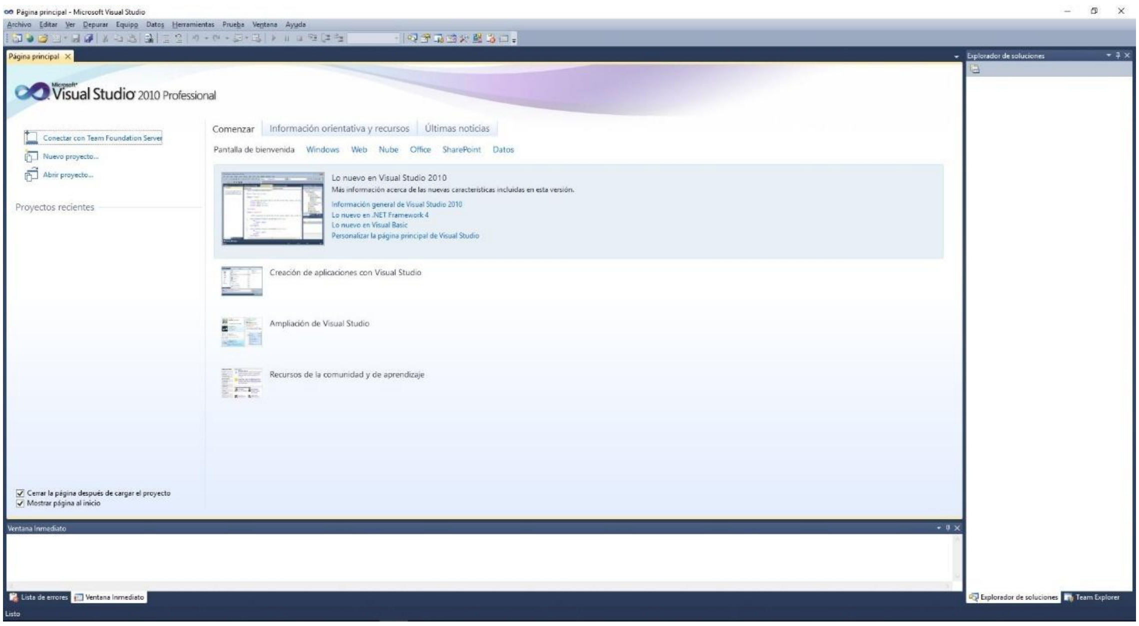

Figure 83. *Microsoft Visual Studio 2010 IDE.*

7.2. System Structure

In this section, the structure of the overall program is described, illustrating this way, the logical implementation of the methodology developed in this project. The software is divided in two modules. The **first module** is in charge of the control of the calculus routines of the methodology and the data structure. The main calculus routine and the two auxiliary ones are presented next.

CalculateFocus. This is the main routine and implements the methodology. It receives two input parameters: p_ADT, as the path for the file where the iteration variables want to be stored (if it is omitted no file is generated); and p_RES, as a boolean variable that determines whether the results (*focus error*, *markers error*) are presented through the interface. This routine defines the LoFX methodology. The function is of type boolean and returns true in case the focus has been successfully determined and false otherwise. During its execution the auxiliary routines are called, and public variables associated to the position of the focus are adjusted with the calculated values.

ProjectPoint. This routine takes two input variables: the coordinates of a point and the $\boldsymbol{Z_{focus}}$ distance between radiography and emitter focus. As output, it brings the coordinates of the projection of the point.

DisplacePoint. This routine takes as an input two variables: the coordinates of a point and the displacement that wants to be applied. As output, it gives the coordinates of the displaced point.

A **second module** manages the control of the interface and the application method. This module is divided in 5 blocks:

Initialization. Presents routines associated to the initialization of the program and the interface.

Sections. It contains routines associated to the behaviour of each of the sections and the change between them.

Parameter Modification. Comprehends routines in charge of the modification of parameters such as the number of markers and other definitions.

Buttons. Gathers the routines related to the administration of the buttons. In addition, the application method is defined in this block.

System routines. Standard "lecture" and "save" routines of the system.

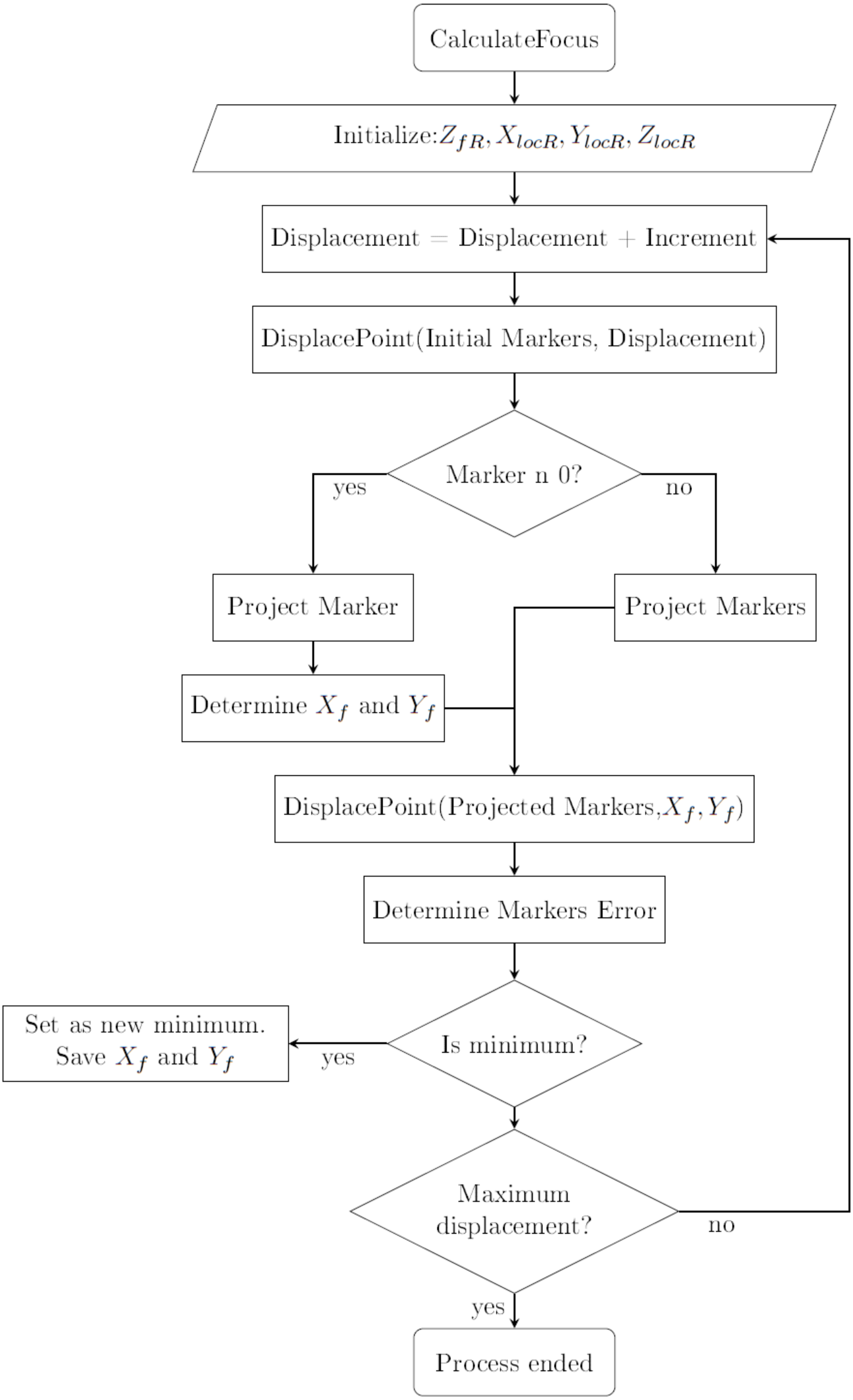

Figure 84. *Flowchart of the CalculateFocus procedure associated to LoFX.*

7.3. Graphical User Interface

In previous sections, the methodology of the ApLoFX was presented. Additionally, the implementation of this methodology in a computational language, Visual Basic NET, and the program structure were explained. To allow a more comprehensive and friendly management of the program, a Graphical User Interface has been implemented. It is imperative to point out that this GUI is designed to meet the requirements of a researcher profile and not those for a clinical use. In the following pages, an introduction guide to explain the features and functionalities of the software is presented. Thanks to the possibilities of Visual Basic NET, the program can be launched by executing the application file "focoRX.exe". Initially, an almost empty window appears (Figure 85). This corresponds to the section "CALCULUS", linked to the "focus" button. From this point there are three possibilities:

- By clicking the button "model", the software conduces to the "MODEL" section, in which it is possible to define and save a new localizer.
- Clicking the button "position", the software enters into "POSITION", where the positioning of both the localizer and the focus can be set.
- If a "case file" has been previously defined, clicking the button "read" it is possible to load its data.

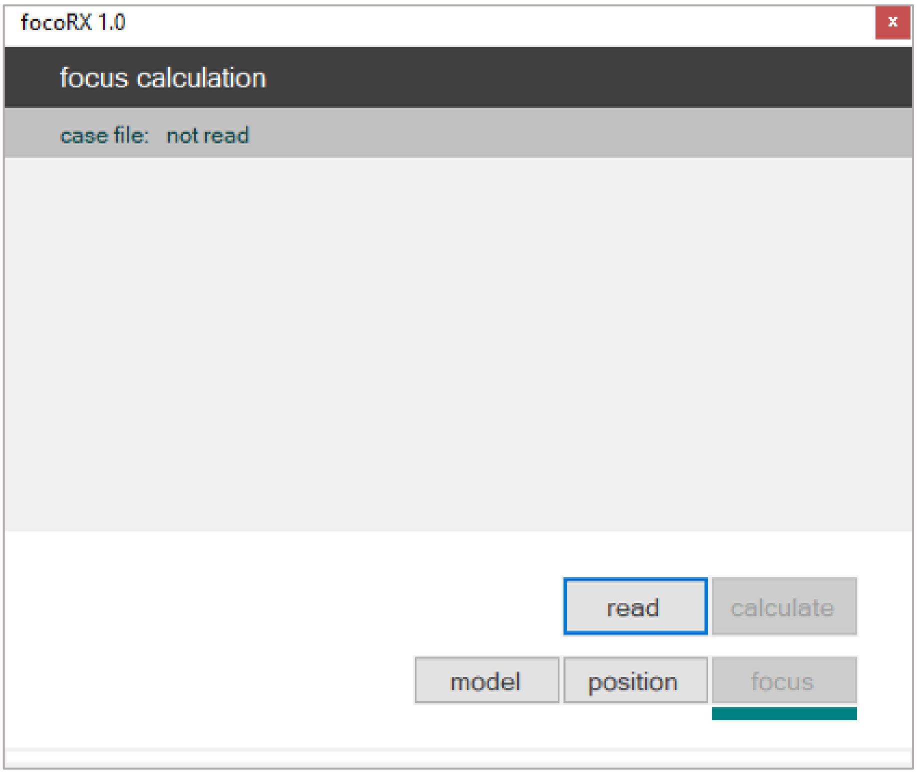

Figure 85. *GUI windows in the focus section without any case file loaded.*

If a "case file" has not been previously saved, the user can opt for the design of a localizer. Pressing the button "model", the software redirects the user to a window for this aim

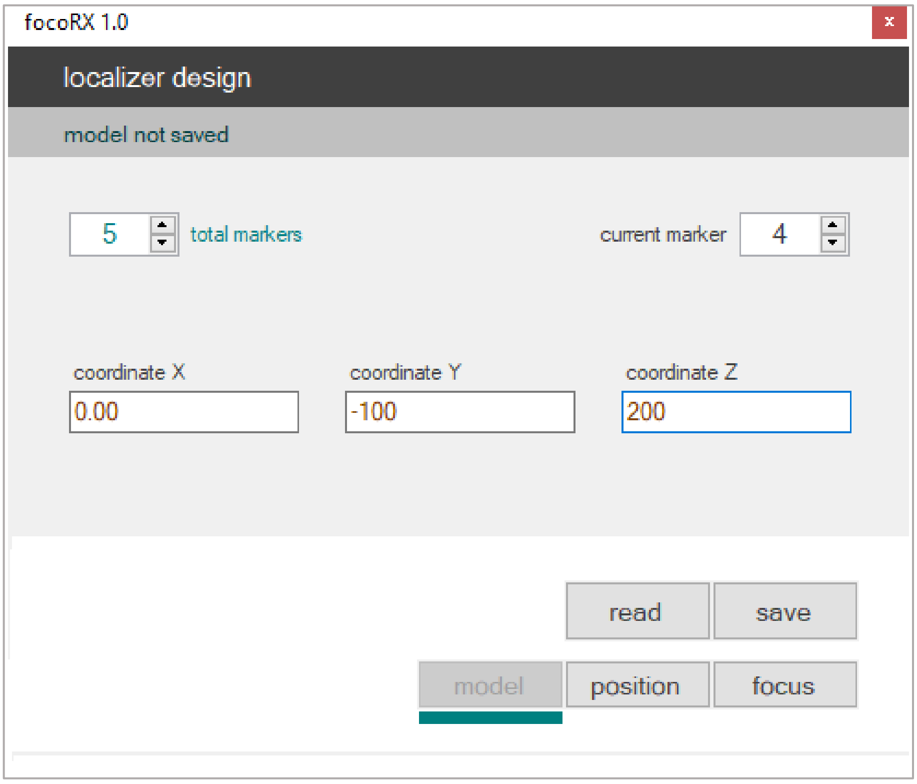

Figure 86. *GUI windows in the model section.*

At the top of the window, a message shows that the localizer design has not been saved. The user can opt, either for the design of a new localizer or for the read of an existing one. Two spinners below include the following functionalities:

- The left spinner determines the number of markers of the localizer that wants to be designed. This value can be selected between a minimum of 3 and a maximum of 50.
- The right spinner specifies the current marker whose coordinates are being modified. Keeping the criterion of most of programming languages, the list starts in 0 up to n-1; consequently, if a localizer of 5 markers is defined, the *current marker* maximum value corresponds to 4.

An example is given to illustrate the design. The reference localizer 5M-200 mm with 5 markers, inscribed in a cube of side 200 mm is created. The coordinates for the markers are given in a local reference system that, for this case, is considered in the centre of the base of the cube. The software allows to redefine any of the markers during the design process by just selecting in the right spinner its corresponding index. After all the markers have been defined, the model can be saved pressing the "save" button. Immediately, the software conduces to a window for saving the file. By default, the destination folder is C:\\Temp. Here, the name of the object localizer file can be defined and the *.olr* extension is added.

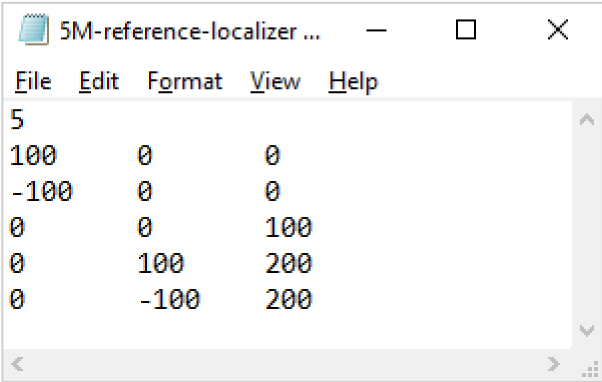

Figure 87. *File containing the information about the localizer.*

The information contained in the file (Figure 87) corresponds to the number of markers (first line) and the respective x, y and z coordinates of each of the markers. If instead of designing a new localizer, a previously existing localizer file wants to be loaded, pressing the button "read" would direct to C:\\Temp allowing to open it.

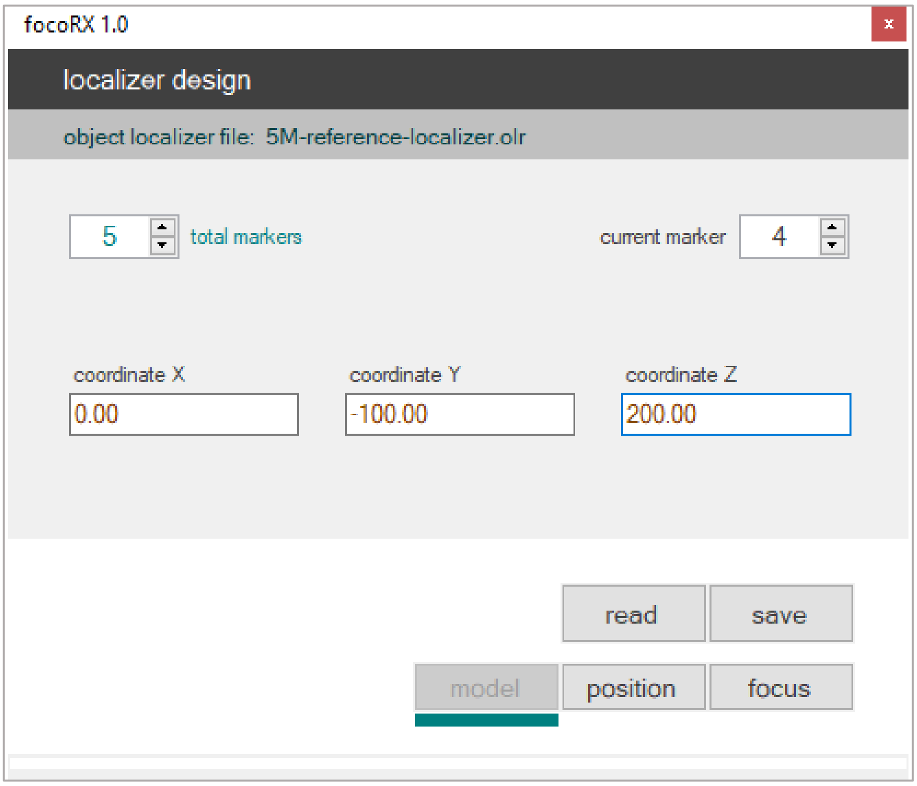

Figure 88*. GUI windows in the model section after saving the localizer.*

Once the object localizer file is loaded into the software, the next step is to define the positioning by clicking the button "position".

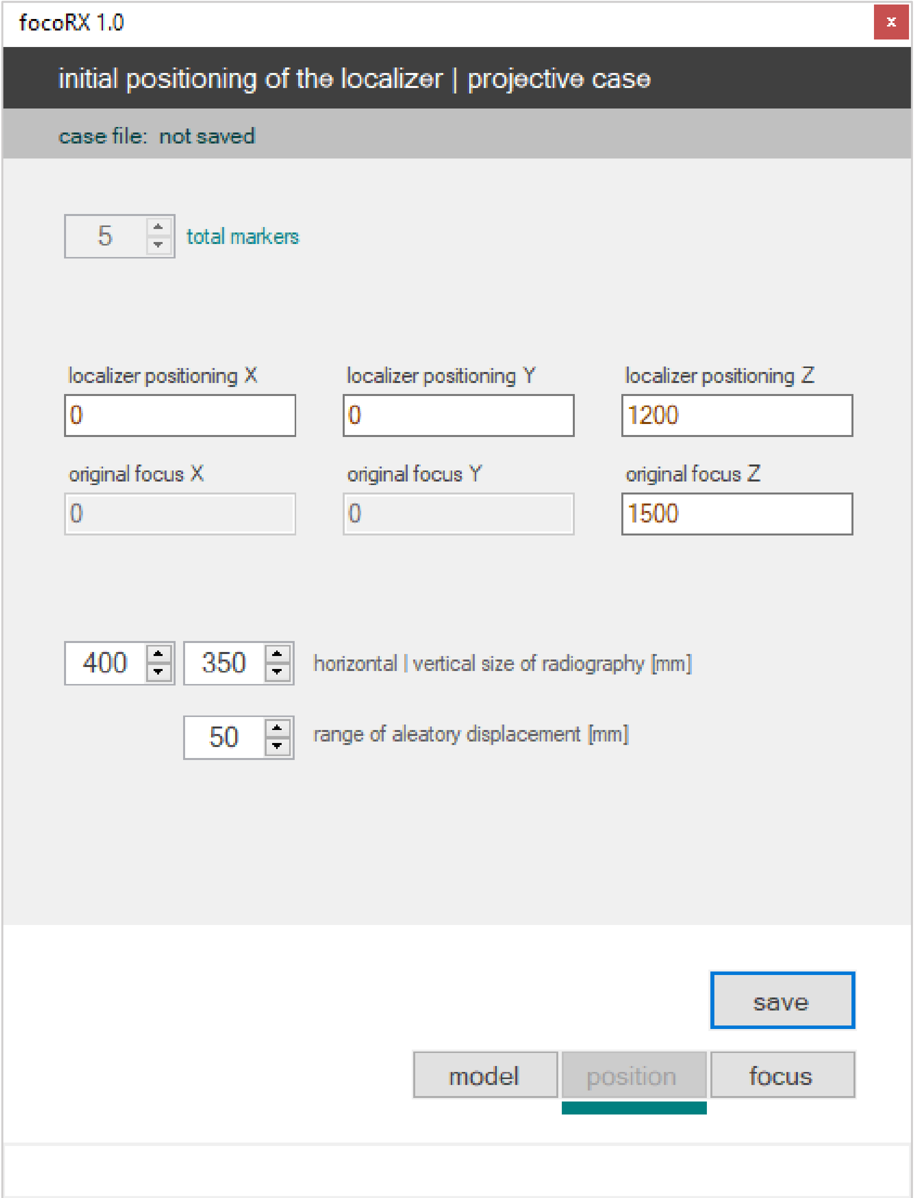

Figure 89. *GUI windows in the position section.*

In this window, the *positioning* is defined and the parameters for the *projective cases* are set. Three "EditText" widgets allow to define the positioning of the localizer. This positioning is applied to the origin of the local reference frame of the localizer, for this example, the centre of the base of the cube. By default, the localizer is centred and placed at 1200 mm from the focus. In addition, analogous EditText widgets are set for the localization of the so-called *original focus*. The focus coordinates are given with respect to the centre of the radiography, attending to the criteria introduced in previous sections of this project. Three more "spinners" are shown in the window. Two of them define the size of the radiography and the last one defines the random displacement range (RAD). It is important to remember that the *projective cases* are created from the "positioning" and modified adding a random displacement to both localizer and focus. The maximum range of this random displacement is defined by the RAD.

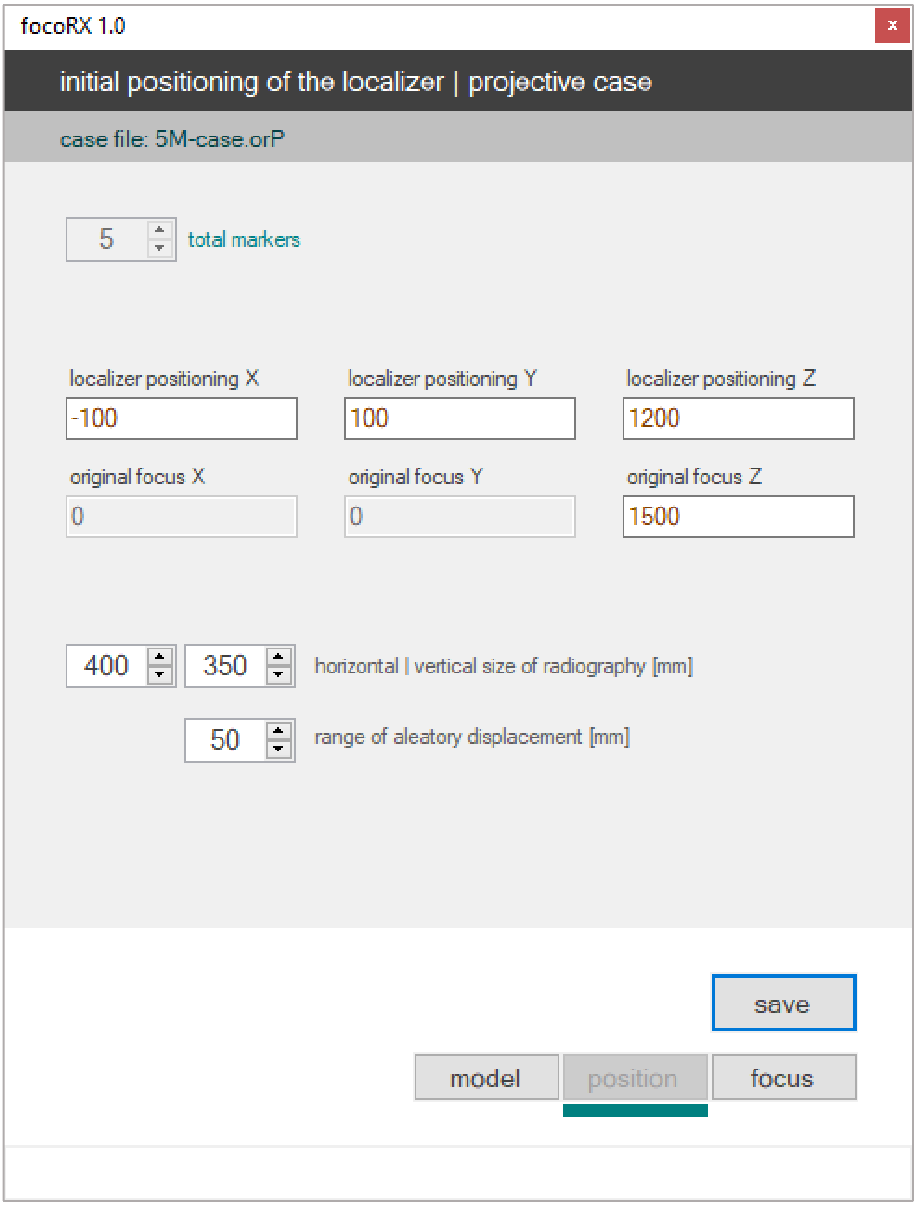

Figure 90. *GUI windows in the position section after defining the positioning.*

For this example, the positioning is set according to the Table 1 and with a RDA of 50 mm. By pressing the "save" button, the software conduces again to the C:\\Temp directory where, by default, the files are stored. Here a new case file can be created with the .orP extension (object localizer positioning). As it can be seen, once returned to the software interface the top of the window shows the saved case file. The data corresponding to the case file: 5M-case is arranged in the following way, indicating the number of the lines and the information presented:

- 1 Total number of markers of the localizer.
- 2-6 Coordinates of the positioned markers for the *projective case* [X, Y, Z].
- 7-11 Coordinates of the randomized markers, displaced according to the RDA [X, Y, Z].
- 12 Original focus coordinates. Centred in with respect to the radiography and defining Z_{focus} [X, Y, Z].
- 13 Coordinates of the randomized focus, corresponding to the searched solution [X, Y, Z].

- 14 Dimensions of the radiography in mm [HORIZONTAL, VERTICAL].
- 15 RAD.
- 16-20 Projections of the displaced markers in the radiography or "Projective Data" as named in previous sections [X, Y, Z].

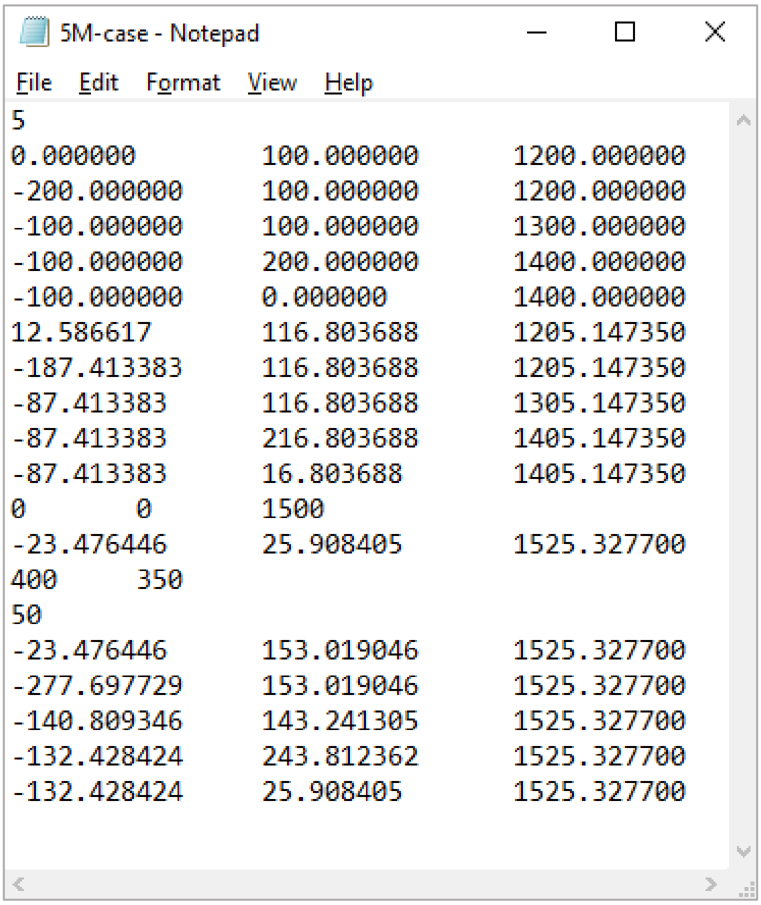


```
5
0.000000        100.000000      1200.000000
-200.000000     100.000000      1200.000000
-100.000000     100.000000      1300.000000
-100.000000     200.000000      1400.000000
-100.000000     0.000000        1400.000000
12.586617       116.803688      1205.147350
-187.413383     116.803688      1205.147350
-87.413383      116.803688      1305.147350
-87.413383      216.803688      1405.147350
-87.413383      16.803688       1405.147350
0       0       1500
-23.476446      25.908405       1525.327700
400     350
50
-23.476446      153.019046      1525.327700
-277.697729     153.019046      1525.327700
-140.809346     143.241305      1525.327700
-132.428424     243.812362      1525.327700
-132.428424     25.908405       1525.327700
```

Figure 91. *File with information about the case.*

Pressing the “focus” button, the interface recovers the initial appearance. Here, the previously saved case can be loaded showing its information in the window (Figure 92).

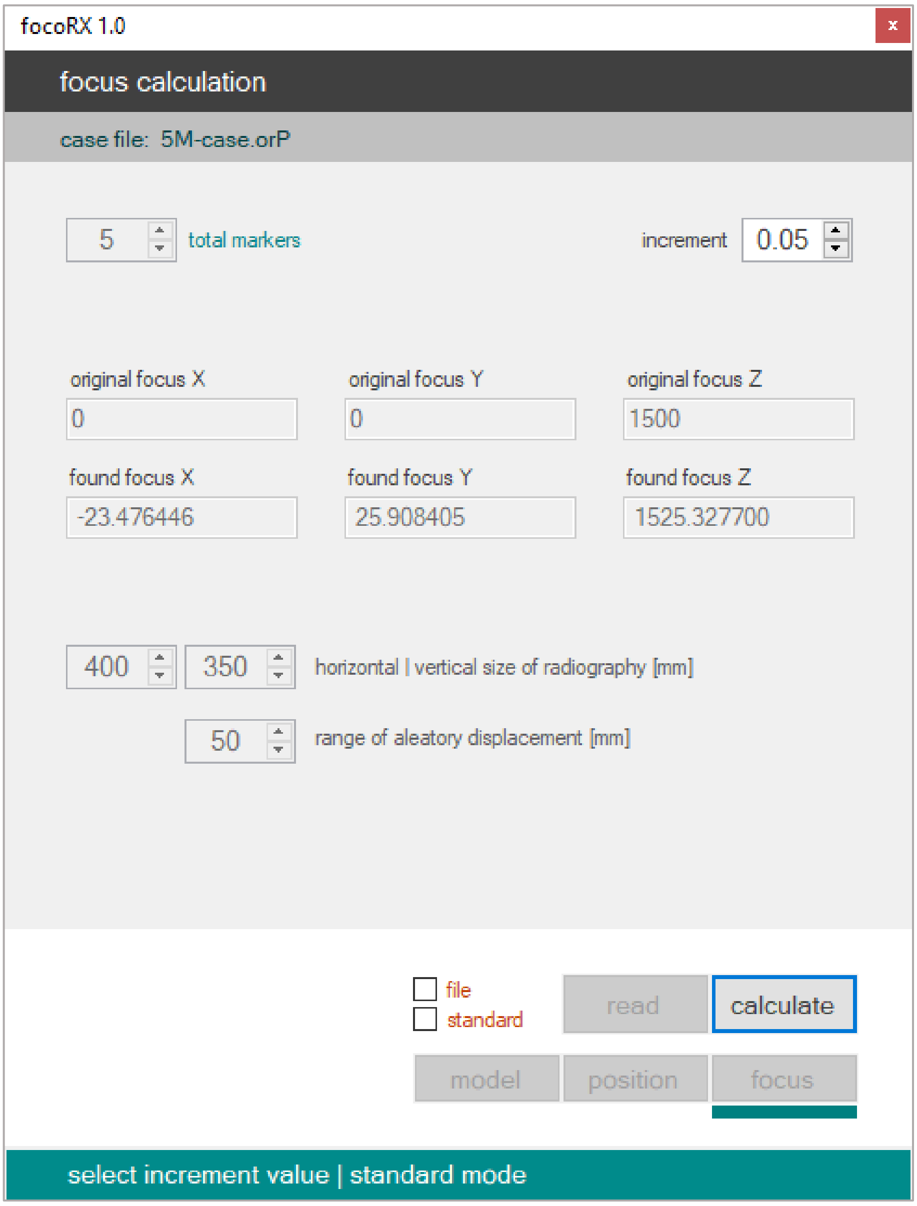

Figure 92. *GUI windows in the focus section ready for calculation.*

Several elements can be pointed in this window: At the top, the loaded case file is shown. Below, information about the corresponding case file is presented:

- Number of markers of the localizer.
- Coordinates of the focus defined during the positioning phase.
- Coordinates of the focus to be found. These coordinates are generated after applying the RDA to the previously presented coordinates.

In addition, elements that can be modified by the user are included: Two CheckBoxes and a spinner:

file checkbox. If this checkbox is selected, the software generates a file with the values of the different variables at each iteration of the process. This kind of file has the extension .rsc, corresponding to "result of the case". Note that this slows down the program considerably.

standard checkbox. This checkbox establishes the application of the LoFX in the area previously indicated by the RAD without a previous execution of the Application Method, ApLoFX. This means that the precise calculus phase with the selected increment will be applied without a prior narrowing of the search area. Consequently, the calculation time can rise exponentially.

increment spinner. Corresponds to the value of the increment that is used for the precise calculus. If the “standard” checkbox is selected, this value is used in all the space defined by the range.

Finally, by pressing the “calculate” button, the software is executed attending to the introduced parameters.

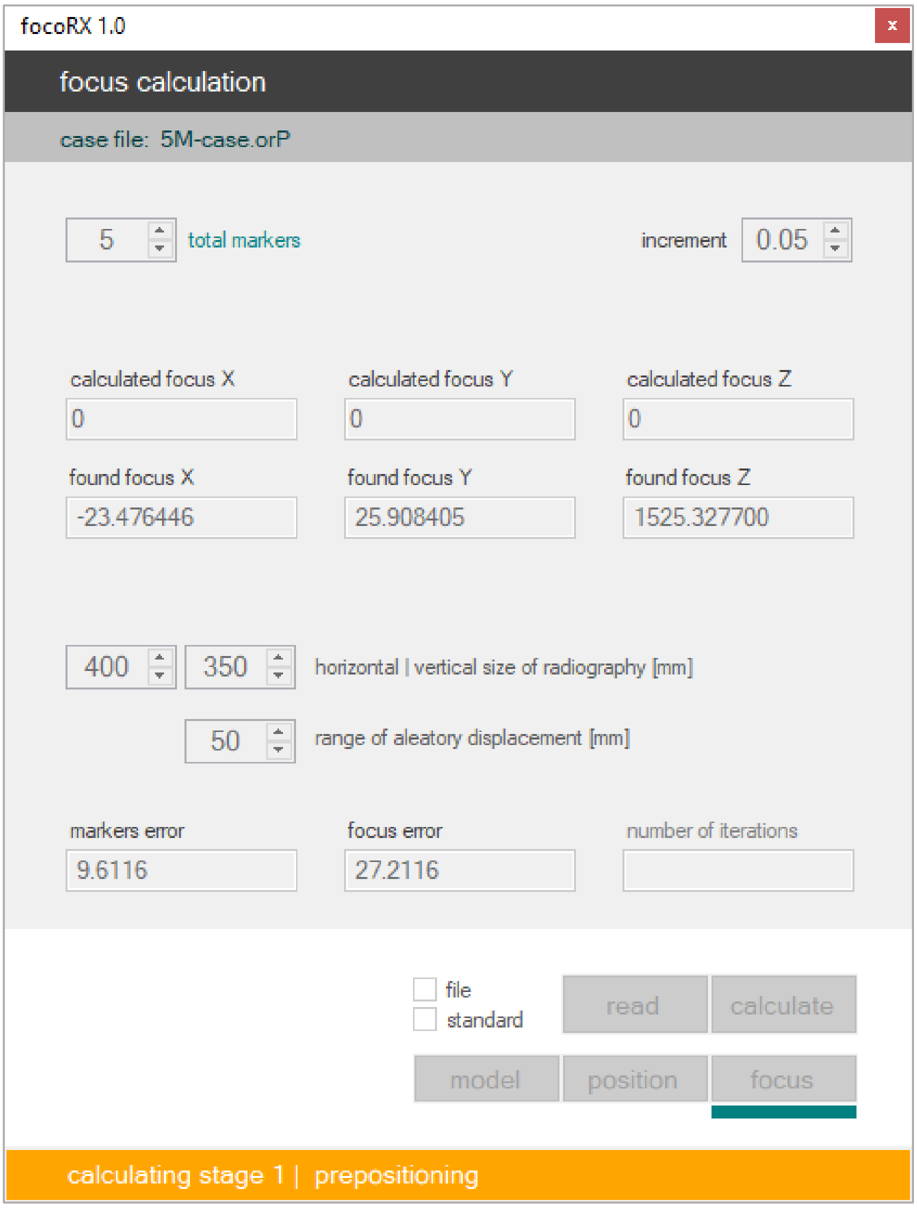

Figure 93. *GUI windows calculating. prepositioning.*

Several new features appear in the window during the calculus. First, the TextBoxes corresponding to the "calculated focus" and the "found focus". As previously stated, calculated focus corresponds to the "real focus to be found". Found focus refers to the position of the focus determined in the last stage executed that met the minimal *markers error* criterion. In addition, on the bottom of the window, the current stage of the application is shown. First, prepositioning. This phase is the quickest and, consequently, only appears for a few instants. Secondly, the "proximate positioning" stage is run. More information appears in the window during this phase. In addition, behind each of the "found focus" boxes, the absolute and the relative error with respect to the real solution are indicated. Below, three TextBoxes with the *markers error*, *focus error* and number of iterations performed at the end of the previous stage are presented.

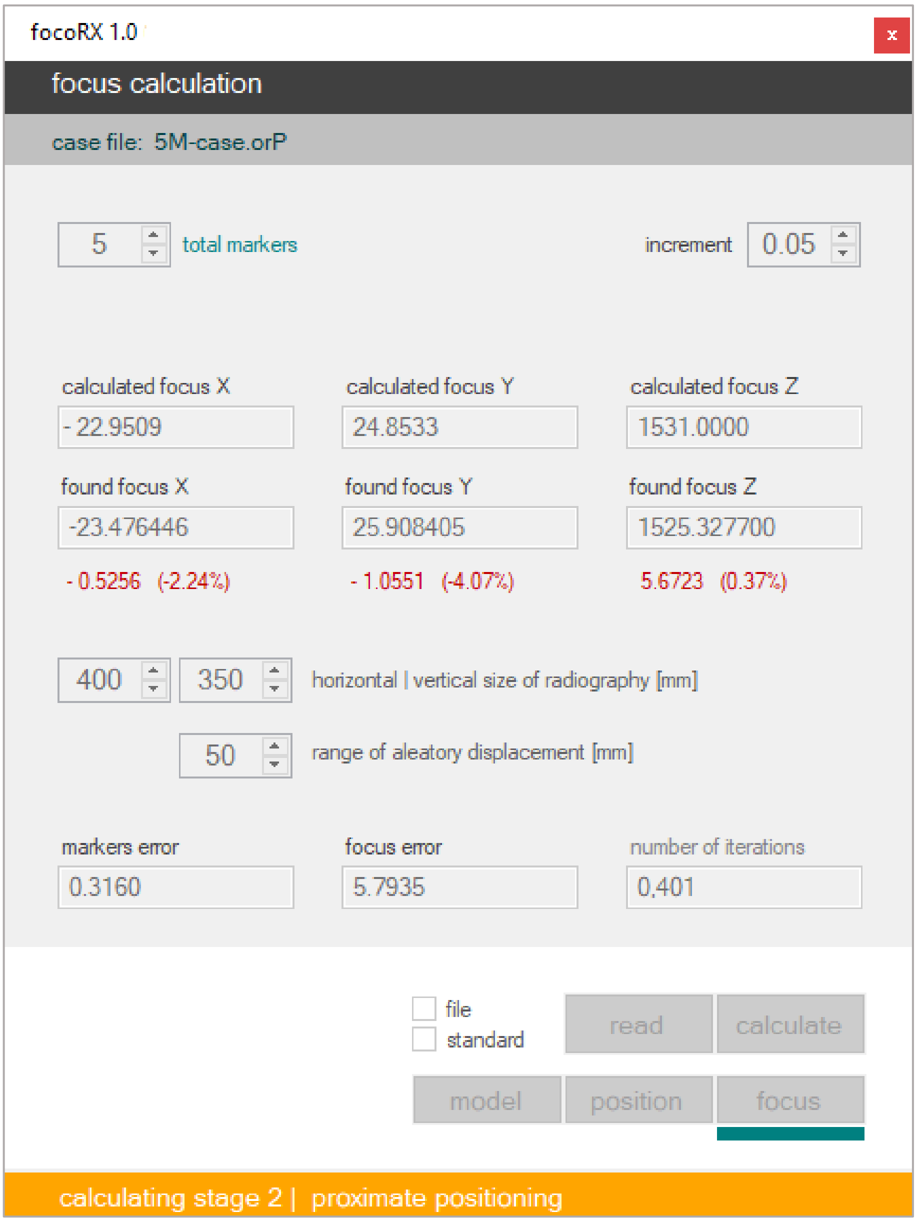

Figure 94. *GUI windows calculating. proximate positioning.*

Afterwards, "minimal opening" stage. Additionally, at the right of the phase, the range that the software is currently exploring is shown.

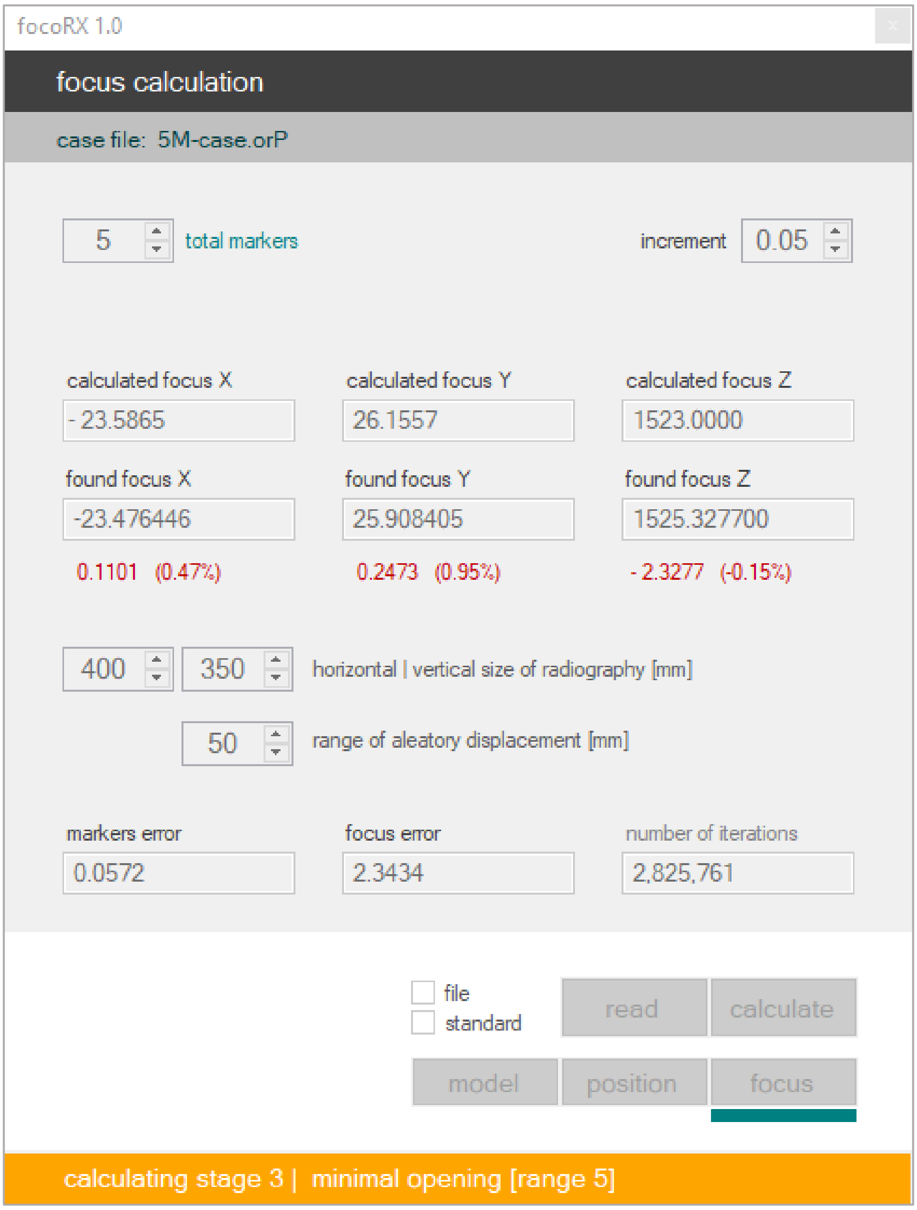

Figure 95. *GUI windows calculating. minimal opening.*

Finally, precise calculus. This phase uses the previously set increment value in the range determined by the "minimal opening" stage.

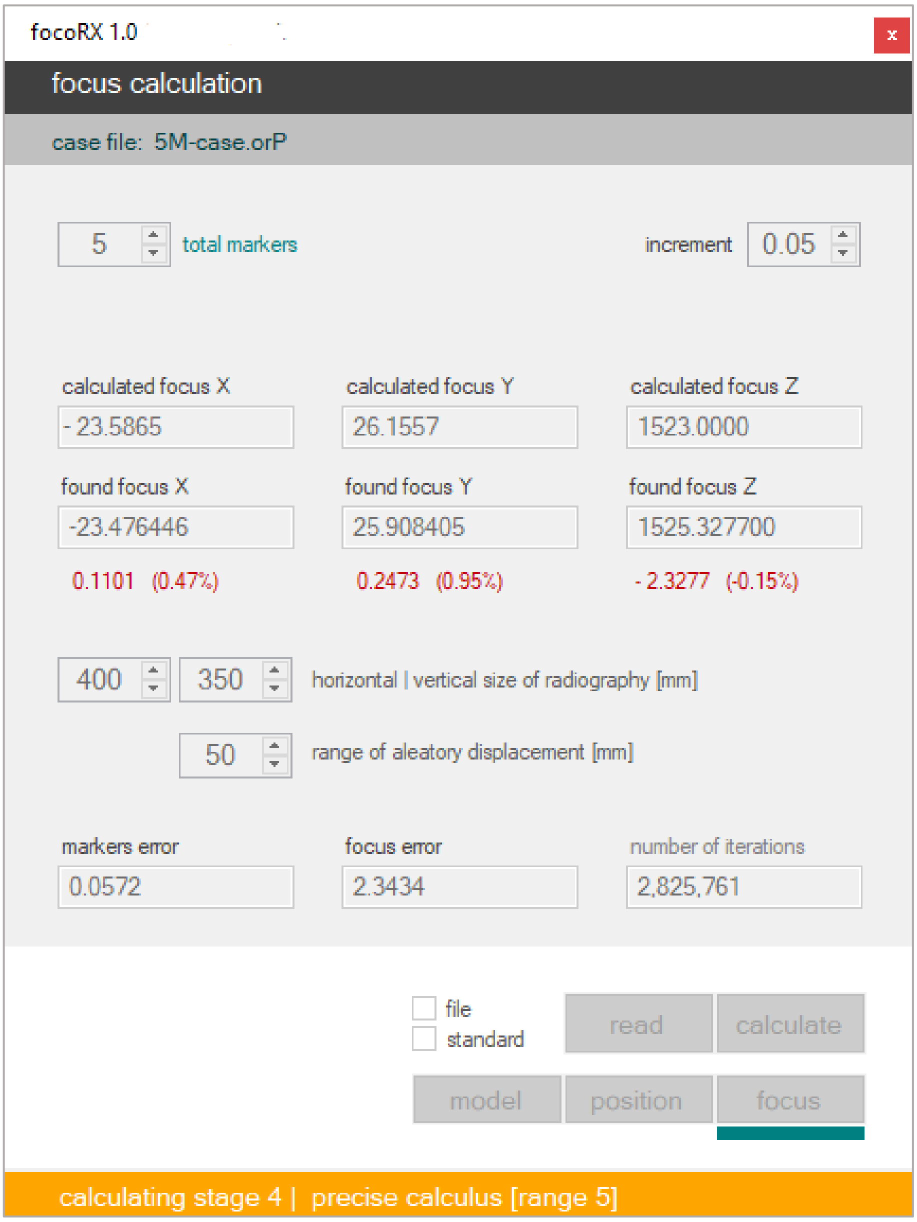

Figure 96. *GUI windows calculating. precise calculus.*

At the end of the procedure, when the solution is found, information about the "calculated focus" coordinates as well as the corresponding errors: both of the markers and the focus, are updated.

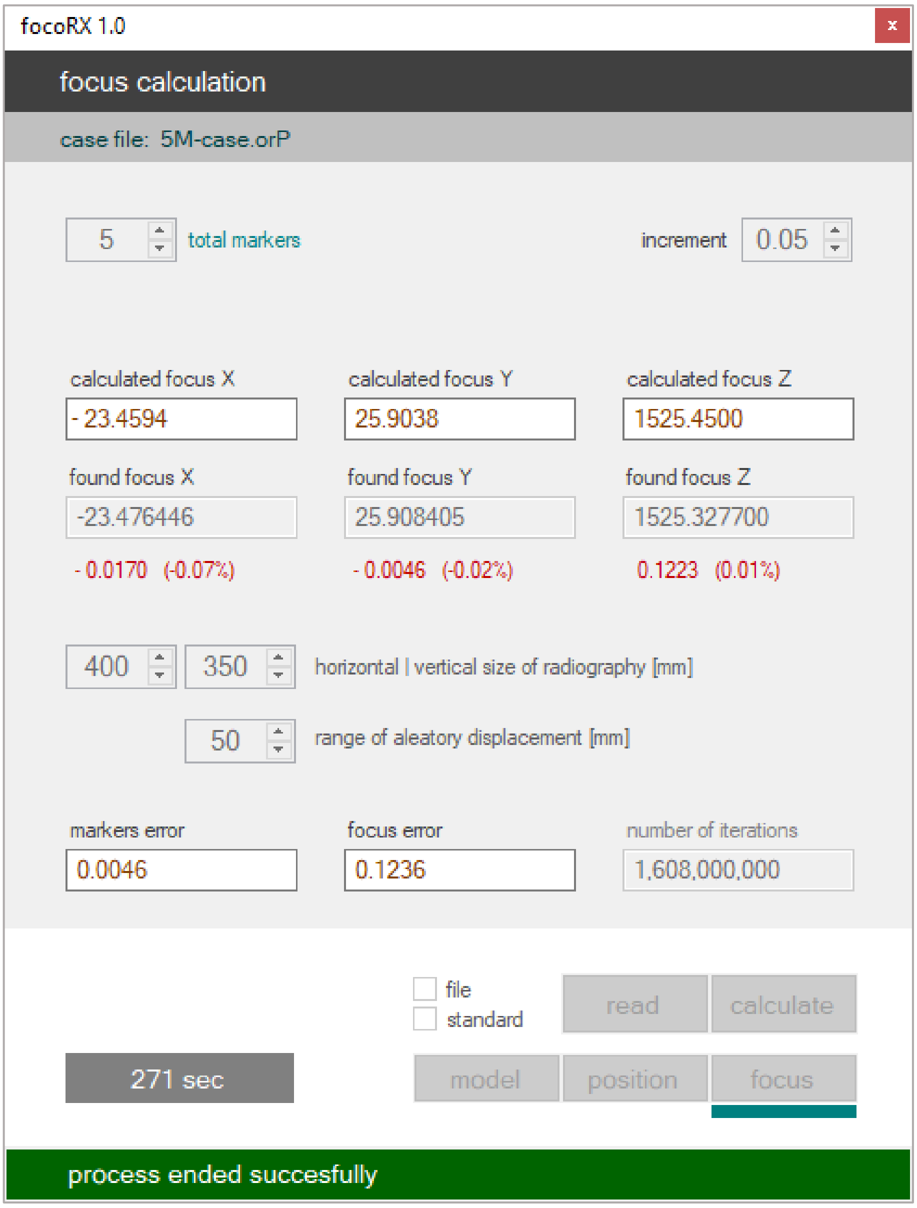

Figure 97. *GUI windows after process successfully completed.*

In addition, the total processing time is presented in the bottom of the window.

8. Conclusions and future lines of research

This chapter summarizes the results and conclusions extracted from the work and studies performed along the research, pointing out the accomplishment of objectives and highlighting significant achievements. In addition, a brief insight into the future lines of research for which the current work serves as a basis is introduced.

8.1. Conclusions

The first and main conclusion of this research is that it has been possible to demonstrate experimentally that the proposed methodology, directly applied, can accurately determine the spatial position of the X-ray emitter focus. Specifically, it has been possible to determine the position of the focus with a minimum average error of 0.0811 millimeters, in the linear distance to the exact position of the focus, in an average time of 108 minutes. Admitting an average position error of the focus of 0.3 millimeters, the calculation is carried out in an average time of just 86 seconds. These error values have been obtained with the reference localizer object of 5 markers, but it has also been shown that the number of markers composing the object hardly influences the average error obtained.

Secondly, it has been shown that the proposed methodology can be computer-implemented. This has been done, in order to carry out the tests that have allowed to demonstrate the validity of the proposed methodology. The implementation can be executed on a medium-power commercial computer. The demonstrated ease of implementation will allow research or technological development groups that need it, to determine the position of the X-ray emitter focus in an economical way, without the need to resort to systems not specifically dedicated to this task.

Thirdly, it has been noted that the direct application of the proposed methodology is not feasible in practical applications, due to excessive calculation times. As an example, there are required 41.823 seconds to calculate the focus position with an average error of the order of 0.08 millimeters. To solve this problem, which for practical purposes would prevent the application of the methodology, it has been developed and validated experimentally an application method. This method of application allows to abbreviate the calculations in an average of 4 times. Thus, for the case of a low profile localizer object (the special case localizer introduced 6.4 6.4), it has been possible to measure calculation times of 94 minutes, for direct application, reduced to 23 minutes using the developed method.

Fourthly, it has been shown that the localizer object does not condition the calculation methodology of the focus position rather than including the condition that it should have more than three markers, and these should not be disposed in a single geometric plane. It is to be noted that it has been possible to show that a localized object with just 5 markers and a thickness of 30 mm generates position errors of the focus of 0.18 mm, which opens the possibility to design in the future, boxes of markers that hardly interfere with the radiographic process in presence of the patient.

8.2. Future lines of research

The necessity to validate the methodology in the available time frame as well as the unpredictable evolution of the work make it necessary to omit some labour, opening the door to future research. Some interesting ideas are considered here:

Although the good results obtained by the current application method, which reduces the calculus time several times with respect to the "direct application" of the methodology, a more efficient software would require the exploration of better ways to boost the process. An ongoing idea considers the use of an adaptive increment value for the discretization. This would be absolutely necessary if the implementation of rotations applied to the localizer object wants to be considered in addition to the already applied translations.

Currently, the projection of the markers of the localizers must be identified and matched with the corresponding marker. The development of a method that eliminates this dependence, which difficulties the performance of the methodology in practical applications, would be a valuable implementation.

As mentioned in previous chapters, current localizer objects require a high precision in its manufacture. A method not dependent on this precision would allow a significant reduction of the overall price of the process. The possibility of using radiographic images for the definition of the localizer is currently being considered.

Lastly, the development of a commercial software that implements the methodology for its commercialization is an interesting possibility.

Pseudocode

```
PROCEDURE CalculateFocus (BOOLEAN) // Function for the calculus of the position of the focus.
(LoFX)


CalculateFocus=FALSE

Zfocus=ZfocusREF+Zfocus_INI
DO
  Xlocalizer=Xlocalizer_INI
  DO
    Ylocalizer=Ylocalizer_INI
    DO
      Zlocalizer=Zlocalizer_INI
      DO

        MarkersDisplacement.X=Xlocalizer
        MarkersDisplacement.Y=Ylocalizer
        MarkersDisplacement.Z=Zlocalizer

        MarkersError=0
        IterationNumber=IterationNumber+1

        MobileMarkerI(0)= DisplacePoint (InitialMarker(0),MarkersDisplacement
        ProjectedMarker(0)= ProjectPoint (MobileMarker(0),Zfocus)

        Xfocus=RadiographMarker(0).X-ProjectedMarker(0).X
        Yfocus=RadiographMarker(0).Y-ProjectedMarker(0).Y

        FOR nM=1 TO TotalMarkers-1

          MobileMarker(nM)=DisplacePoint (InitialMarkerI(nM),MarkersDisplacement)
          ProjectedMarker(nM)=ProjectPoint(MobileMarker(nM),Zfocus)

          ProjectionDisplacement.X=Xfocus
          ProjectionDisplacement.Y=Yfocus
          ProjectionDisplacement.Z=0

          ProjectedMarker(nM)=DisplacePoint (ProjectedMarker(nM),ProjectionDisplacement)

          MarkerErrorX=RadiographMarker(nM).X-ProjectedMarker(nM).X
          MarkerErrorY=RadiographMarker(nM).Y-ProjectedMarker(nM).Y
          MarkersError=MarkersError+SQRT(MarkerErrorX^2+MarkerErrorY^2)

        NEXT

        If MarkersError<=MinimumMarkersError Then

          If MinimumMarkersError=MarkersError Then
```

```
            SolutionNumber = SolutionNumber+1
          END IF

          MinimumMarkersError=MarkersError
          SolutionFocus.X=Xfocus
          SolutionFocus.Y=Yfocus
          SolutionFocus.Z=Zfocus
          ExternalMarkersError=MarkersError

          CalculateFocus=TRUE

        END IF

        Zlocalizer=Zlocalizer+Zlocalizer_INC
      LOOP UNTIL Zlocalizer>Zlocalizer_FIN

      Ylocalizer=Ylocalizer+Ylocalizer_INC
    LOOP UNTIL Ylocalizer>Ylocalizer_FIN

    Xlocalizer=Xlocalizer+Xlocalizer_INC
  LOOP UNTIL Xlocalizer>Xlocalizer_FIN

  Zfocus=Zfocus+Zfocus_INC
LOOP UNTIL Zfocus>(ZfocusREF+Zfocus_FIN)


PROCEDURE END
```

```
PROCEDURE ProjectPoint [p_PT,p_ZFR] (PT) // Function for the calculus of the projected point

// p_PT: point to project
// p_ZFR: Z coordinate of the focus with respect to the radiography


ProjectPoint.X=(p_PT.X*p_ZFR)/p_PT.Z

ProjectPoint.Y=(p_PT.Y*p_ZFR)/p_PT.Z

ProjectPoint.Z=p_ZFR


PROCEDURE END



PROCEDURE DisplacePoint [p_PT,p_DIS] (PT) // Function for the calculus of the displacement of
a point

// p_PT: point to displace
// p_DIS: XYZ components of the displacement (with sign)


DisplacePoint.X=p_PT.X+p_DIS.X

DisplacePoint.Y=p_PT.Y+p_DIS.Y

DisplacePoint.Z=p_PT.Z+p_DIS.Z


PROCEDURE END
```

```
PROCEDURE CalculateFocusAbbreviated () // Application Method (ApLoFX)


// stage 1: PREPOSITIONING of the focus

Range=200
Increment = 1

Zfocus_INI=-Range
Zfocu_FIN=Range
Zfocus_INC=Increment

Xlocalizer_INI=0
Xlocalizer_FIN=0
Xlocalizer_INC=1

Ylocalizer_INI=0
Ylocalizer_FIN=0
Ylocalizer_INC=1

Zlocalizer_INI=0
Zlocalizer_FIN=0
Zlocalizer_INC=1

IF CalculateFocus=FALSE THEN END // prepositioning of the focus Z coordinate

Zfocus_PREPOSITIONED=Zfocus_PRE
ZfocusREF=Zfocus_PRE

Zfocus_INI=0
Zfocus_FIN=0
Zfocus_INC=1

Xlocalizer_INI=-Range
Xlocalizer_FIN=Range
Xlocalizer_INC=Increment

Ylocalizer_INI=0
Ylocalizer_FIN=0
Ylocalizer_INC=1

Zlocalizer_INI=0
Zlocalizer_FIN=0
Zlocalizer_INC=1

IF CalculateFocus=FALSE THEN END // prepositioning of the localizer X coordinate

Xlocalizer_PREPOSITIONED=Xlocalizer_PRE

Zfocus_INI=0
Zfocus_FIN=0
```

```
Zfocus_INC=1

Xlocalizer_INI=Xlocalizer_PREPOSITIONED
Xlocalizer_FIN=Xlocalizer_PREPOSITIONED
Xlocalizer_INC=1

Ylocalizer_INI=-Range
Ylocalizer_FIN=Range
Ylocalizer_INC=Increment

Zlocalizer_INI=0
Zlocalizer_FIN=0
Zlocalizer_INC=1

IF CalculateFocus=FALSE THEN END // prepositioning of the localizer Y coordinate

Ylocalizer_PREPOSITIONED=Ylocalizer_PRE

Zfocus_INI=0
Zfocus_FIN=0
Zfocus_INC=1

Xlocalizer_INI=Xlocalizer_PREPOSITIONED
Xlocalizer_FIN=Xlocalizer_PREPOSITIONED
Xlocalizer_INC=1

Ylocalizer_INI=Ylocalizer_PREPOSITIONED
Ylocalizer_FIN=Ylocalizer_PREPOSTIONED
Ylocalizer_INC=1

Zlocalizer_INI=-Range
Zlocalizer_FIN=Range
Zlocalizer_INC=Increment

IF CalculateFocus=FALSE THEN END // prepositioning of the localizer Z coordinate

Zlocalizer_PREPOSITIONED=Zlocalizer_PRE


// stage 2 PROXIMATE POSITIONING of the focus position

Range=100
Increment=1.5

ZfocusREF=Zfocus_PRE

Zfocus_INI=-Range
Zfocus_FIN=Range
Zfocus_INC=Increment

Xlocalizer_INI=Xlocalizer_PREPOSITIONED-Rang6
```

```
Xlocalizer_FIN=Xlocalizer_PREPOSITIONED+Range
Xlocalizer_INC=Increment

Ylocalizer_INI=Ylocalizer_PREPOSITIONED-Range
Ylocalizer_FIN=Ylocalizer_PREPOSITIONED+Range
Ylocalizer_INC=Increment

Zlocalizer_INI=Zlocalizer_PREPOSITIONED-Range
Zlocalizer_FIN=Zlocalizer_PREPOSITIONED+Range
Zlocalizer_INC=Increment

IF CalculateFocus=FALSE THEN END


// stage 3 MINIMAL OPENING of the range of exploration

Range=4
Increment=0.5

Condition=False
PreviousMarkersError=0
MinimalOpening=0
CoincidenceCounter=0

ZfocusREF=Zfocus_PRE

DO

  Range=Range+1

  Zfocus_INI=-Range
  Zfocus_FIN=Range
  Zfocus_INC=Increment

  Xlocalizer_INI=Xlocalizer_PRE-Range
  Xlocalizer_FIN=Xlocalizer_PRE+Range
  Xlocalizer_INC=Incremento

  Ylocalizer_INI=Ylocalizer_PRE-Range
  Ylocalizer_FIN=Ylocalizer_PRE+Range
  Ylocalizer_INC=Increment

  Zlocalizer_INI=Zlocalizer_PRE-Range
  Zlocalizer_FIN=Zlocalizer_PRE+Range
  Zlocalizer_INC=Increment

  IF CalculateFocus=FALSE THEN END

    IF PreviousMarkersError=ExternalMarkersError THEN

      CoincidenceCounter=CoincidendeCounter+1
```

```
        IF CoincidenceCounter=5 THEN Condition=TRUE

          ELSE

          MinimalOpening=Range
          CoincidenceCounter=0

        END IF

LOOP UNTIL Condition=True


// stage 4 PRECISE CALCULUS of the coordinate of the focus

Range=MinimalOpening
Increment = READ(Value)

ZfocusREF=Zfocus_PRE

Zfocus_INI=-Range
Zfocus_FIN=Range
Zfocus_INC=Increment

Xlocalizer_INI=Xlocalizer_PRE-Range
Xlocalizer_FIN=Xlocalizer_PRE+Range
Xlocalizer_INC=Increment

Ylocalizer_INI=Ylocalizer_PRE-Range
Ylocalizer_FIN=Ylocalizer_PRE+Range
Ylocalizer_INC=Increment

Zlocalizer_INI=Zlocalizer_PRE-Range
Zlocalizer_FIN=Zlocalizer_PRE+Range
Zlocalizer_INC=Increment

IF CalculateFocus=FALSE THEN END


PROCEDURE END
```

References

Börlin, N., Röhrl, S. M., & Bragdon, C. R. (2006). RSA wear measurements with or without markers in total hip arthoplasty. *Journal of Biomechanics, 39*(9), 1641-1650. doi:10.1016/j.jbiomech.2005.05.004

Bottner, F., Su, E., Nestor, B., Azzis, B., Sculco, T., & Bostrom, M. (2005). Radiostereometric Analysis: The Hip. *HSS Journal,* 94-99. doi:10.1007/s11420-005-0114-2

Cai, R., Yuan, X., Rorabeck, C., Bourne, R. B., & Holdsworth, D. W. (2008). Development of an RSA calibration system with improved accuracy and precision. *Journal of Biomechanics*, 907-911. doi:10.1016/j.jbiomech.2007.11.012

Calabrò, C. (2004). *Calibrazione di un C-Arm per la Riconstruzione Tridimensionale in Neuroangiografia e Coronografia.* Master Thesis, Politecnico di Milano, Milano.

Cappozzo, A., Della Croce, U., Leardini, A., & Chiari, L. (2005). Human movement analysis using sterephotogrammetry. *Gait & Posture, 21*(2), 186-196. doi:10.1016/j.gaitpost.2004.01.010

Chabbal, J., Chaussat, C., Ducourant, T., Fritsch, L., Michailos, J., Spinnler, V., . . . Spahn, M. (1996). Amorphous silicon X-ray image sensor. *Proceedings of SPIE*. doi:10.1117/12.237812

Choo, A. M., & Oxland, T. R. (2003). Improved RSA accuracy with DLT and balanced calibration marker distributions with an assessment of initial-calibration. *Journal of Biomechanics*, 259-264. doi:10.1016/s0021-9290(02)00361-5

Compagnone, G., Baleni, M. C., Pagan, L., Calzolaio, F., Barozzi, L., & Bergamini, C. (2006). Comparison of radiation doses to patients undergoing standard radiographic examinations with conventional screen–film radiography, computed radiography and direct digital radiography. *The British Journal of Radiology, 79*(947), 899-904. doi:10.1259/bjr/57138583

de Bruin, P., Kaptein, B., Stoel, B., Reiber, J., Rozing, R., & Valstar, E. (2008, August). Image-based RSA: Roentgen stereophotogrammetric analysis based on 2D-3D image registration. *Journal of Biomechanics, 41*(1), 155-164. doi:10.1016/j.jbiomech.2007.07.002

De Silva, T., Punnoose, J., Uneri, A., Goerres, J., Jacobson, M., Ketcha, M., . . . Siewerdsen, J. (2017). C-arm Positioning Using Virtual Fluoroscopy for Image-Guided Surgery. *Proceedings of SPIE*.

Dougherty, G. (2009). *Digital Image Processing for Medical Applications.* Cambridge University Press. doi:978-0-511-53343-3

G. Webb, A. (2003). *Introduction to Biomedical Imaging.* Urbana: John Wiley & Sons.

Gammuto, M., Martelli, S., Trozzi, C., Bragonzoni, L., & Russo, A. (2008). A simulation environment for estimation of the performance of RSA cages. *38*(9), 1000-1006. doi:10.1016/j.compbiomed.2008.07.007

García Ruesgas, L. (2014). *Modelo Geométrico Proyectivo para la Determinación Precisa del Foco Emisor de Sistemas Radiológicos a Partir de una Imagen Radiográfica Estándar con Marcadores de Referencia.* PhD Thesis, Universidad de Sevilla, Sevilla.

Garling, E. H., Kaptein, B. L., Nelissen, R. G., & Valstar, E. R. (2005). Marker Configurationi Model-Based Roentgen Fluoroscopic Analysis. *Journal of Biomechanics, 28,* 893-901.

Gustke, K. (2005). Preoperative planning for revision total knee arthoplasty: avoiding chaos. (E. BV, Ed.) *Journal of Arthoplasty*, 37-40. doi:10.1016/j.arth.2005.03.026

Hoppe, S., Noo, F., Dennerlein, F., & Lauritsch, G. (2007). Geometric Calibration of the Circle Plus arc Trajectory. *Physics in Medicine and Biology, 52*(23), 6943-6960. doi:10.1088/0031-9155/52/23/012

Hsu, C.-P., Lin, S.-C., Shih, K.-S., Huang, C.-H., & Lee, C.-H. (2014). Predicting 3D pose in partially overlapped X-ray images of knee prostheses using model-based Roentgen stereophotogrammetric analysis (RSA). *Medical & Biological Engineering & Computing, 52*(12), 1061-1071. doi:10.1007/s11517-014-1206-2

Imai, S., Higashijima, K., Ishida, A. F., & Hoshino, A. M. (2003). Determination of the position and orientation of artificial knee implants using markers embedded in a bone: preliminary in vitro experiments. *Medical Engineering & Physics, 25*(5), 419-424. doi:10.1016/s1350-4533(03)00037-7

Ioppolo, J., Börlin, N., Bragdon, C., Li, M., Price, R., & Wood, D. M. (2007). Validation of a low-dose hybrid RSA and fluoroscopy technique: Determination of accuracy, bias and precision. *Journal of Biomechanics, 40*(3), 686-692. doi:10.1016/j.jbiomech.2006.01.012

Kaptein, B., E.R., V., Stoel B.C., R. P., & Reiber, J. (2007). A new type of model-based Roentgen stereophotogrammetric analysis for solving the occluded marker problem. *Journal of Biomechanics, 38*(11), 2330-2334. doi:10.1016/j.jbiomech.2004.09.018

Kaptein, B., Valstar, E., & Stoel, B. R. (2003). A new model-based RSA method validated using CAD models and models from reversed engineering. *Jounal of Biomechanics, 36*(6), 873-882. doi:10.1016/s0021-9290(03)00002-2

Kärrholm, J. (1989). Roentgen Stereophotogrammetry. Review of Orthopaedic Applications. *Acta Orthopaedica Scandinavica*.

Kärrholm, J., Gill, R. H., & Valstar, E. R. (2006, July). The history and future of radiostereometric analysis. *Clinical Orthopaedics and Related Research, 448*, 10-21. doi:10.1097/01.blo.0000224001.95141.fe

Lança, L., & Silva, A. (2009). Digital radiography detectors – A technical overview: Part 2. *Radiography, 15*(2), 134-138. doi:10.1016/j.radi.2008.02.005

Lin, P., Shueler, B., Balter, S., Strauss, K., Wunderle, K., LaFrance, M., . . . Bercha, I. (2015). Accuracy and calibration of integrated radiation output indicators in diagnostic radioglogy: Areport of the AAPM Imaging Phsics Committee Task Group 190. *Medical Physics, 52*(12), 6815-6829. doi:10.1118/104934831

Liu, W. P., Otake, Y., Azizian, M., Wagner, O. J., Sorger, J. M., Armand, M., & Taylor, R. H. (2015). 2D-3D radiograph to cone-beam computed tomography (CBCT) registration for C-arm image-guided robotic surgery. *International Journal of Computer Assisted Radiology and Surgery, 10*(8), 1239-1252. doi:10.1007/s11548-014-1132-7

Liu, X., Thometz, J., Marquez-Barrientos, C., & Tassone, C. (2013). Correlation between stereoradiography and 3D topographic measurements. *Scoliosis, 8*(Suppl 2), O22. doi:10.1186/1748-7161-8-s2-o22

M. Levi, D., M. Wolfe, J., Lkuender, K. R., Bartoshuk, L., & Herz, R. S. (2018). *Sensation and Perception* (4 ed.). Sinauer Associates.

Madanat, R., Moritz, N., Vedel, E., Svedström, E., & Aro, H. T. (2009). Radio-opaque bioactive glass markers for radiostereometric analysis. *Acta Biomaterialia, 5*(9), 3497-3505. doi:10.1016/j.actbio.2009.05.038

Montagna, L., Bragonzoni, L., Zampagni, M., Russo, A., Motta, M., Albisinni, U., & Marcacci, M. (2005). Investigation into the detection of marker movement by biplanar RSA. *Medical Engineering & Physics*, 641-648. doi:10.1016/j.medengphy.2004.12.004

Muharemovic, O., Gosvig, K. K., Troelsen, A., Thomsen, M. G., & Kallemose, T. (2018). A pilot study to determine the effect of radiographer training on radiostereometric analysis imaging technique. *Radiography, 24*(2), e37-e43. doi:10.1016/j.radi.2017.12.003

Muharemovic, O., Troelsen, A., Thomsen, M., Kallemose, T., & Gosvig, K. (2018). The effect of personalized versus standard patient protocols for radiostereometric analysis (RSA). *Radiography, 24*(2), e31-e36. doi:10.1016/j.radi.2017.11.006

Ohl, X., Stanchina, C., Billuart, F., & Skalli, W. (2009). Shoulder bony landmarks location using the EOS® low-dose stereoradiography system: a reproducibility study. *Surgical and Radiologic Anatomy, 32*(2), 153-158. doi:10.1007/s00276-009-0566-z

Rowlands, J. (2003). The physics of computed radiography.

S., A. (2012). MATLAB: a practical introduction to programming and problem solving, second edition. In A. S., *MATLAB.* Elsevier.

Selvik, G. (1989). Roentgen Stereophotogrammetry. *Acta Orthopaedica Scandinavica*. doi:10.3109/1745367890915484

Syu, C.-B., Lai, J.-Y., Chang, R.-Y., Shih, K.-S., Chen, K.-J., & Lin, S.-C. (2012). Automatic model-based roentgen stereophotogrammetric analysis (RSA) of total knee prostheses. *Journal of Biomechanics, 45*(1), 164-171. doi:10.1016/j.jbiomech.2011.09.011

Talukdar, A., & Wilson, D. (1999). Modeling and optimization of rotational C-arm stereoscopic X-ray angiography. *IEEE Transactions on Medical Imaging, 18*(7), 604-616. doi:10.1109/42.790460

Thürauf, S., Hornung, O., Korner, M., Vorgt, F., Nasseri, M. A., & Knoll, A. (2018). Model-Based Calibration of a Robotic C-Arm System Using X-Ray Imaging. *Journal of Medical Robotics Research*. doi:10.1142/S2424928X18410027

Trozzi, C., Kaptein, B., Garling, E., Shelyakova, T., Russo, A., Bragonzoni, L., & Martelli, S. (2008). Precision assessment of model-based RSA for a total knee prosthesis in a biplanar set-up. *The Knee*, 396-402.

Valstar, E. R. (2001). *Digital Roentgen Stereophotogrammetry: Development, Validation, and Clinical Application.*

Valstar, E. R., Gill, R., Ryd, L., Flivik, G., Börlin, N., & Kärrholm, J. (2005). Guidelines for standardization of radiostereometry (RSA) of implants. *Acta Orthopaedica, 76*(4), 563-572. doi:10.1080/1745367010041574

Whitley, A., Sloane, C., Hoadley, G., Moore, A., & Alsop, C. (2005). *Clark's Positioning In Radiography.* (12 ed.). Arnold, Hodder Headline Group.

Xunhua, Y., & Leif, R. (2000). Accuracy analysis for RSA: a computer simulation study on 3D marker reconstruction. *Journal of Biomechanics*, 493-498.

Yuan, X., Ryd, L., & Tanner, I. L. (2002). Roentgen single-plane photogrammetric analysis (RSPA). A new approach to the study of musculoskeletal movement. *The Journal of Bone and Joint Surgery., British volume, 84-B*(6), 90-914. doi:10.1302/0301-620x.84b6.0840908